SUMMARY

In the past studies, the evaluation of natural disasters usually analyzed by deterministic theory. Therefore, the result of the analysis dichotomy, safe or failure. However, it is difficult to explain the reality of the real environment. Generally, the uncertainty would have two possible types, the limitation of observation or experiment and the error of data. The uncertainties come from three possible sources. First is an intrinsic quality of social, economic or natural phenomena. Second is a limitation of the knowledge. Final is from decision making. For the evaluation of reliability design, there are two operations, one is the calculation of failure probability, and the other is decision making. For the failure probability, it's the purely mechanical problem with considering the basic mechanical properties. Therefore, the necessary work is the investigation and statistic of parameters. For the decision making, the best option should be select among all the solutions.

In the thesis, the main aim is the reliability analysis of the levee safety. Therefore, it is mainly analyzing of natural disasters with considering the uncertainty of the observation/experiment data. The external force of the levee safety is the water level, and the resistance force of the levee is the stability of the levee. Through the stochastic process of the Fokker-Planck equation and probability density function, the probable distributions of the external force and the resistance force can be estimated. For example, through the reliability analysis of the levee safety, it can be known that even if the soil material is not very good to construct the levee, but through improving the geometry of the levee, the failure probability can also effective to reduce. The failure probability of the levee can understand and help the decision makings of the disaster presentation and reduction in the future.

CONTENTS

CONTENTS I

FIGURE LIST III

TABLE LIST VII

CHAPTER 1 INTRODUCTION 1

1.1 The status of levee 4

1.2 The disaster types of levee 8

1.3 Existing problems 21

1.4 Research aim and category 24

1.5 Thesis scope 27

Reference 31

CHAPTER 2 HYDROLOGY MODEL BASED ON STOCHASTIC PROCESS THEOTY 33

2.1 Basic equation of rainfall-runoff in the single slope 33

2.2 Uncertainty of hydrology 36

2.3 The development of stochastic process theory 42

2.4 Uncertainty of water level based on stochastic process theory 51

Reference 56

CHAPTER 3 STABILITY ANALYSIS OF LEVEE 59

3.1 Slope stability method 62

3.2 Infiltration 66

3.3 Uncertainty of soil parameters 74

3.4 Infiltration failure probability of levee 82

Reference 86

CHAPTER 4 RELIABILITY ANALYSIS 87

4.1 The development of the reiliability analysis 87

4.2 Literature review 90

4.3 Failure probability analysis of levee 103

4.4 Probability of multi-failure 108

Reference 113

CHAPTER 5 SCENARIO TEST **115**

5.1 Calculation conditions and assumptions 118

5.2 Results 123

5.3 Discussion 137

Reference 141

CHAPTER 6 CONCLUSION **143**

FIGURE LIST

Figure 1-1 the trend analysis of the rainfall from 1976 to 2015 in Japan 3
Figure 1-2 the structure of levee 6
Figure 1-3 the construction history of levee of Yodogawa River [3] 6
Figure 1-4 the inhomogeneous materials of the levee [4] 6
Figure 1-5 grain size distribution curve [2] 7
Figure 1-6 the three types of the levee failure induced by flooding 12
Figure 1-7 the locations of the levee failure along Ishikarigawa River, 1981 [7] 14
Figure 1-8 the levee failure in Sendaigawa River in Kagosima, 1993 [8] 15
Figure 1-9 the levee failure process in Abukumagawa River in Fukushima, 1998 [8] 16
Figure 1-10 the infiltration failure in Shounaigawa River in Aichi, 2000 [9] 16
Figure 1-11 the failure situation in Shinanogawa River in Nigata, 2004 [7] 17
Figure 1-12 the inundation and levee failure in Maruyamagawa River in Hyogo, 2004 [11] ... 17
Figure 1-13 the failure process of the levee in Yabegawa River in Fukuoka, 2012 [12] 18
Figure 1-14 the maximum water level record at Ishii station by year 19
Figure 1-15 the aerial photo after typhoon No. 18 19
Figure 1-16 the current status of safety assessments 23
Figure 1-17 the safety assessments with considering the uncertainty of the environment 23
Figure 1-18 the research category of external force of water level 26
Figure 1-19 the research category of resistance force of levee 26
Figure 1-20 the flow chart of the thesis 30
Figure 2-1 the schematic diagram of the rainfall-runoff 35
Figure 2-2 The schematic diagram of temporal of rainfall [7] 38
Figure 2-3 The schematic diagram of spatial of rainfall 38
Figure 2-4 the rainfall data by different observation method 39
Figure 2-5 the comparison of the radar and ground data in Kanto area 40
Figure 2-6 the difference between radar and ground data 41

Figure 2-7 the standard deviation of rainfall data 41
Figure 2-8 A single realization of a one-dimensional Wiener process 47
Figure 2-9 the development of the stochastic process theory 48
Figure 2-10 the stochastic processes of SDE and PDF 49
Figure 2-11 the observation data of hydrology 50
Figure 2-12 Probability distribution of water level from uncertainty rainfall 54
Figure 2-13 Probability distribution of the discharge from uncertainty rainfall 55
Figure 2-14 Probability distribution of the water level from uncertainty rainfall 55
Figure 3-1 the failure occurrence side of the levee 61
Figure 3-2 Division of potential sliding mass into slices 65
Figure 3-3 Casagrande's method 71
Figure 3-4 The conduction process of the practical solution 71
Figure 3-5 the schematic diagram of infiltration process 72
Figure 3-6 the relation between $F(\eta)$ and η 72
Figure 3-7 the comparison between numerical solution and practical solution 73
Figure 3-8 Main components contributing to the total uncertainty in the determination of a geotechnical property [6] 77
Figure 3-9 the uncertainty of soil parameters [8] 77
Figure 3-10 Scatter diagrams with different values of correlation coefficient(0 ~ 1) 79
Figure 3-11 Scatter diagrams with different values of correlation coefficient (0 ~ -1) 80
Figure 3-12 Correlation between cohesion c' and friction angle ϕ' in Japan[8] 81
Figure 3-13 Correlation between cohesion c' and friction angle ϕ' [11] 81
Figure 3-14 the correlation coefficient of the cohesion and the friction angle 84
Figure 3-15 the safety distribution in different water level 84
Figure 3-16 The PDF of safety factor with different water level 85
Figure 3-17 the probability of infiltration failure 85
Figure 4-1 the basic model of the reliability analysis [3] 97
Figure 4-2 the concept of the probability of failure [3] 97
Figure 4-3 the distribution shapes of Z and G 98
Figure 4-4 the circular slip 98
Figure 4-5 the probability of failure (one variable of the probability) 99
Figure 4-6 Nominal probability of failure versus computed factor safety [14] 99

Figure 4-7 A simple event tree for discharge and stage of a river [14] 100
Figure 4-8 Influence diagram for levee failure [14] 100
Figure 4-9 Event tree for levee failure during extreme storm [14] 101
Figure 4-10 failure probability of a dike section 101
Figure 4-11 the study flowchart by TABATA 102
Figure 5-1 The underlying material under levee is assumed impermeable layer 121
Figure 5-2 The assumed slip surface 121
Figure 5-3 the conditions of levee 122
Figure 5-4 the analysis result of S-1 (c'=1 kN/m^2; ϕ'=20°; the grade of levee= 1:3) 124
Figure 5-5 the analysis result of S-1 (c'=1 kN/m^2; ϕ'=20°; the grade of levee= 1:4) 124
Figure 5-6 the analysis result of S-1 (c'=1 kN/m^2; ϕ'=20°; the grade of levee= 1:5) 125
Figure 5-7 the analysis result of S-1 (c'=1 kN/m^2; ϕ'=20°; the grade of levee= 1:6) 125
Figure 5-8 the analysis result of S-2 (c'=1 kN/m^2; ϕ'=27.5°; the grade of levee= 1:3) 126
Figure 5-9 the analysis result of S-2 (c'=1 kN/m^2; ϕ'=27.5°; the grade of levee= 1:4) 126
Figure 5-10 the analysis result of S-2 (c'=1 kN/m^2; ϕ'=27.5°; the grade of levee= 1:5) 127
Figure 5-11 the analysis result of S-2 (c'=1 kN/m^2; ϕ'=27.5°; the grade of levee= 1:6) 127
Figure 5-12 the analysis result of S-3 (c'=1 kN/m^2; ϕ'=35°; the grade of levee= 1:3) 128
Figure 5-13 the analysis result of S-3 (c'=1 kN/m^2; ϕ'=35°; the grade of levee= 1:4) 128
Figure 5-14 the analysis result of S-3 (c'=1 *kN/m2*; ϕ'=35°; the grade of levee= 1:5) 129
Figure 5-15 the analysis result of C-1 (c'=10 kN/m^2; ϕ'=1°; the grade of levee= 1:3) 129
Figure 5-16 the analysis result of C-1 (c'=10 kN/m^2; ϕ'=1°; the grade of levee= 1:4) 130
Figure 5-17 the analysis result of C-1 (c'=10 kN/m^2; ϕ'=1°; the grade of levee= 1:5) 130
Figure 5-18 the analysis result of C-1 (c'=10 kN/m^2; ϕ'=1°; the grade of levee= 1:6) 131
Figure 5-19 the analysis result of C-2 (c'=35 kN/m^2; ϕ'=1°; the grade of levee= 1:3) 131
Figure 5-20 the analysis result of C-2 (c'=35 kN/m^2; ϕ'=1°; the grade of levee= 1:4) 132
Figure 5-21 the analysis result of C-2 (c'=35 kN/m^2; ϕ'=1°; the grade of levee= 1:5) 132
Figure 5-22 the analysis result of C-2 (c'=35 kN/m^2; ϕ'=1°; the grade of levee= 1:6) 133
Figure 5-23 the analysis result of C-3 (c'=60 kN/m^2; ϕ'=1°; the grade of levee= 1:3) 133
Figure 5-24 the analysis result of C-3 (c'=60 kN/m^2; ϕ'=1°; the grade of levee= 1:4) 134
Figure 5-25 the analysis result of C-3 (c'=60 kN/m^2; ϕ'=1°; the grade of levee= 1:5) 134
Figure 5-26 the analysis result of C-3 (c'=60 kN/m^2; ϕ'=1°; the grade of levee= 1:6) 135
Figure 5-27 the effective of different soil materials (1:3) 135

Figure 5-28 the effective of different soil materials (1:4) 136

Figure 5-29 the effective of different soil materials (1:5) 136

Figure 5-30 the effective of the levee freeboard(S-1) 139

Figure 5-31 the effective of the levee grade (S-1)..... 139

Figure 5-32 the effective of the levee grade (C-1) 140

TABLE LIST

Table 1-1 the design standard of the levee 7

Table 1-2 the water level record in Ishikarigawa River in Hokkaido, 1981 [6] 13

Table 1-3 the failure type in Ishikarigawa River, 1981 [7] 13

Table 1-4 the infiltration failure cases [10] 20

Table 3-1 characteristics of commonly used methods of limit equilibrium analysis for slope stability 65

Table 3-2 Values of coefficient of variation for geotechnical properties [9] 78

Table 5-1 the soil parameters of sandy soil [1] 116

Table 5-2 the soil parameters of clay soil [1] 117

Table 5-3 the deviation of soil parameters 120

Table 5-4 the scenario conditions 120

CHAPTER 1 INTRODUCTION

Due to the global climate change, the scale and frequency of natural disasters are more difficult to predict and measure. Extreme rainfall often brings an astonishing amount of water and causes very serious damage. According to trend analysis of the rainfall from JMA (Japan Meteorological Agency), the hourly rainfall of larger than 50 mm shows the increasing tendency. [1] As shown in Figure 1-1, the occurrence times of the hourly rainfall of 50 *mm* and 80 *mm* is increasing in recent 10 years. It means that the occurrence times of the flood are also raising with more and more large rainfall events. Furthermore, the disaster prevention becomes more important for protecting the people life and property. Therefore, the levee as the prevention of inundation is a very important construction.

Nowadays, the safety evaluation of the levee is based on the deterministic theory, it means that the analyses are only two results, safe or failure. It's not enough to illustrate the real environment because there are some problems existing as followings. First is the result of the dichotomy, safe or failure, no transition from safe to fail. It can't explain the transition process of the failure. Second is the uncertainty of parameters that are usually decided by observation or laboratory experiment. It's not enough to explain the realistic environment. Final is without considering the risk tolerance, or just by the design of the safety coefficient like the freeboard of the levee. Therefore, in the following, the existing problems of the safety evaluation of the levee will be discussed,

including the levee status, the types of damage, the evaluation problems and considering all these issues the new risk analysis method will be suggested.

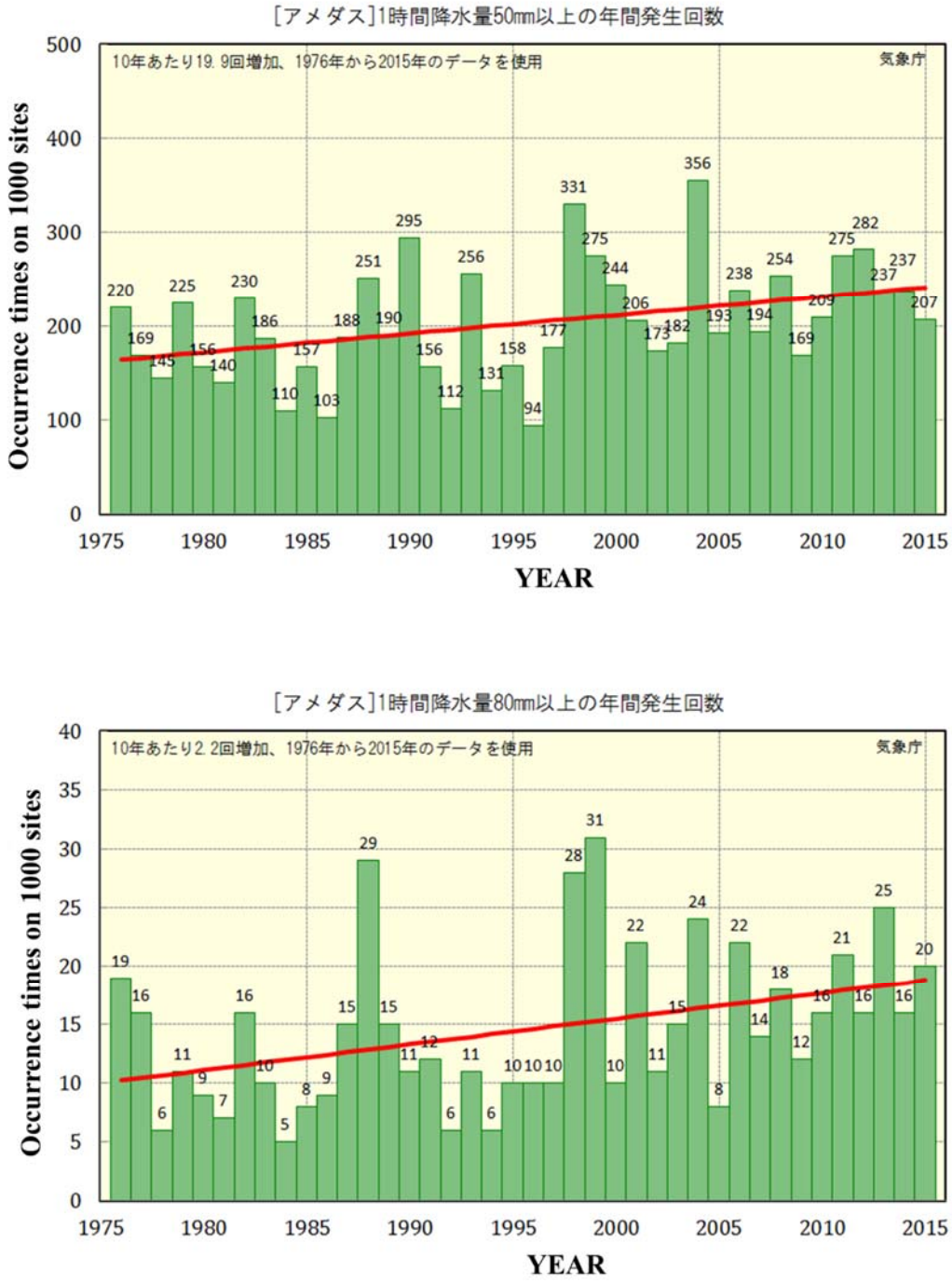

Figure 1-1 the trend analysis of the rainfall from 1976 to 2015 in Japan

1.1 The status of levee

According to the statistical data of MILT (Ministry of Land, Infrastructure, Transport and Tourism) in March, 2015, the total levee length of the government-administered rivers is 13393.8 km (one side). The basic structure of levee is including of design high-water level (H.W.L.), freeboard, crown and the slope of the levee. The height of the levee is design high-water level plus the freeboard, that is according to the "Government Ordinance for Structural Standard for River Administration Facilities" (as shown in Figure 1-2).

The main role of the levee is to prevent river flooding. Therefore, there is a lot of factors like river terrain, geology, hydrology and flood pattern that will affect the construction of the levee. As the levee construction, it has the following characteristics [2]:

(1) People can't decide the position of the levee because it is always built along the river. Therefore, the plane alignment and geology can't be chosen.
(2) According to the natural situations, the types and materials will also change. The design of levee is by the terrain, geology, location and hydrology conditions.
(3) The foundation of levee can't choose from people. The levee is built on the natural foundations.
(4) The scale of the levee will change. The levee is built to prevent the flooding therefore it will change with disaster prevention standards.

The Figure 1-2 shows the characteristics above of the levee. It was firstly built in 1594, and until now it has through four times of the additional constructions. [3]

The soil material of the levee is inhomogeneous. From microscopic terms, according to the soil particle, the soil can be divided into gravel, sand, silt and clay.

Even if the same soil type, the soil particle and shape may be different. It means the soil nature is inhomogeneous. On the other hand, because of the continuous additional construction of the levee with different ages, construction methods, the levee materials are macroscopic inhomogeneous. Figure 1-4 shows inhomogeneous materials because of the continuous construction levee. For example, the construction history of Yodogawa levee, the earliest construction is in 1594 by Toyotomi Hideyoshi, and then continuous reinforced are in 1896, 1918, and 1939. Moreover, Figure 1-5 shows the grain size distribution of the levee in Japan. It shows a very wide range of the distribution of the material. For example, the range of D_{50} is from 0.005 *mm* to 60 *mm* and 1/3 of the range is about the potential danger of the levee damage. It explains that the material of the levee is not only good material, but also the weak soil material used.

According to the "Government Ordinance for Structural Standard for River Administration Facilities" and "Technical Criteria for River Works; Manual for River Works in Japan", the freeboard and the crown of the levee are different by the design high-water discharge. The Table 1-1 is the design standard of the levee. The freeboard is like a safety coefficient of the levee. The freeboard is considering with the effect of the possible wave (wind waves, swell), hydraulic jump, flood control, driftwood, the water level difference between the right-left bank etc.

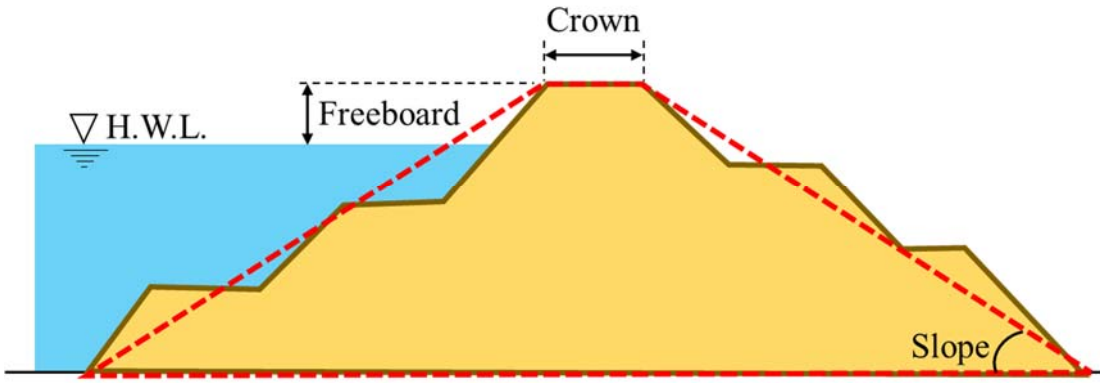

Figure 1-2 the structure of levee

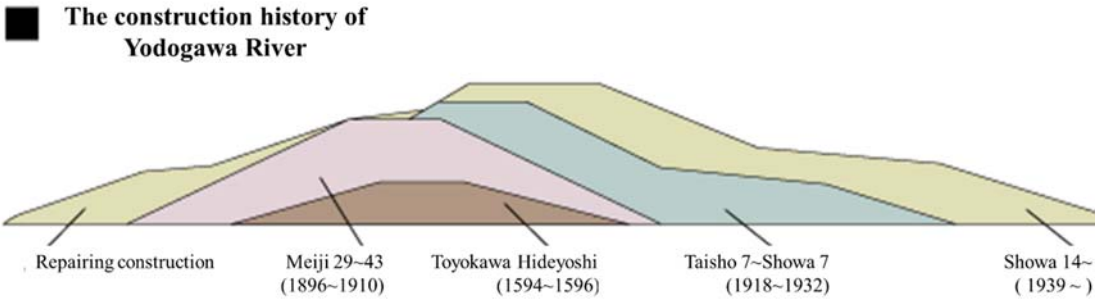

Figure 1-3 the construction history of levee of Yodogawa River [3]

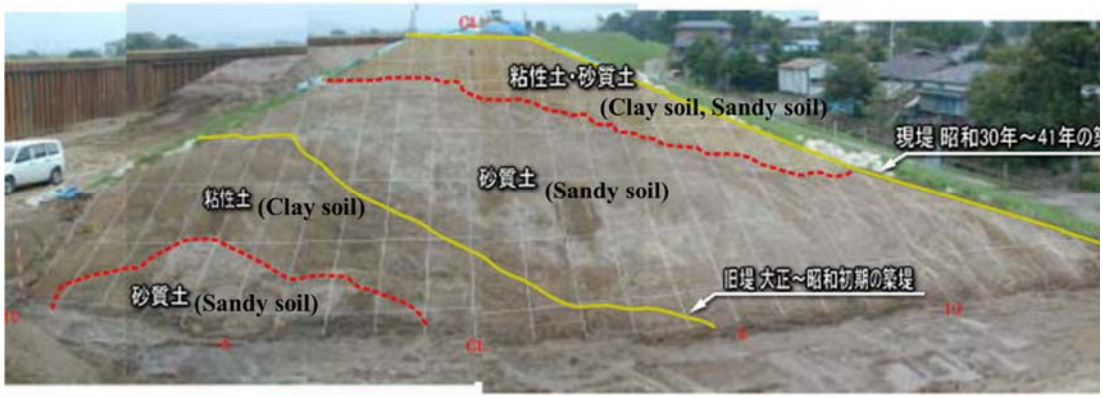

Figure 1-4 the inhomogeneous materials of the levee [4]

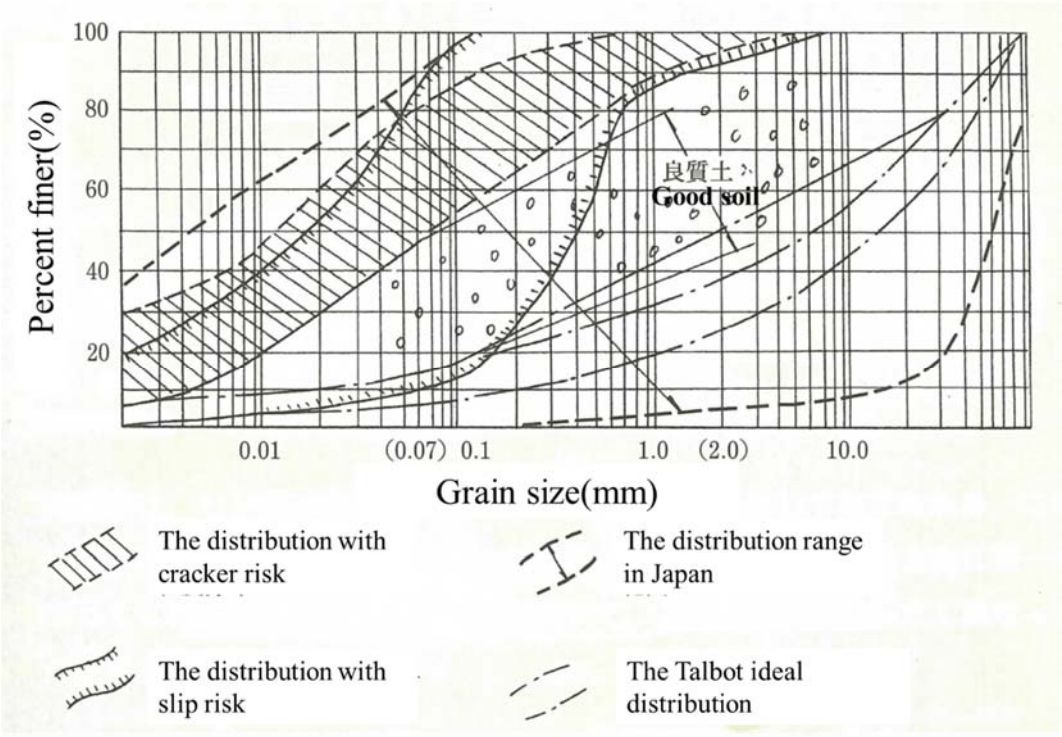

Figure 1-5 grain size distribution curve [2]

Table 1-1 the design standard of the levee

The design high water discharge [m^3/s]	The height of the freeboard [m]	The width of the crown [m]
< 200	0.6	3
200 ~ 500	0.8	
500 ~ 2,000	1	4
2,000 ~ 5,000	1.2	5
5,000 ~ 10,000	1.5	6
> 10,000	2	7

1.2 The disaster types of levee

In general, the common failure types of levee can be subdivided into three types, overflow/overtopping, erosion and infiltration failure. The overflow/overtopping occurs when the water level exceeds the crown of the levee. The continuous overflow water may begin erosion to the surface of the inboard of the levee. Finally, the levee will failure. [5] The erosion failure generally occurs on the outboard side of the levee and is the result of water flowing past the levee face. If the imposed shear stress from the water abrading against the soil levee face is high enough, soil scours occur and the integrity of the overall levee is significantly reduced. [5] The infiltration failure is that infiltration water causes slope failures by saturating the slope material, thereby weakening the adhesive properties of the soil and its stability. The mechanism of the three failure types is shown in Figure 1-6. The following is some disaster cases of levee failure by different failure types.

1. Ishikarigawa River in Hokkaido, 1981（石狩川）

In August 1981, the extreme rainfall caused a very serious disaster along Ishikarigawa River in Hokkaido. There were 11 sites that levee broke along the river, and among these sites, there are 9 sites that were overtopping failure. The record of the water level is shown in Table 1-2 [6], the failure type is shown in Table 1-3 [7] and the disaster locations are shown in Figure 1-7 [7].

2. Sendaigawa River in Kagosima, 1993(川内川)

In August 1993, in Sendaigawa the infiltration failure of the levee occurred. (as shown in Figure 1-8)

3. Shinanogawa River in Nagano, 1995(信濃川)

In 1995, there was a levee failure about 60 m occurred along the branch river of Shinanogawa River.

4. Abukumagawa River in Fukushima, 1998(阿武隈川)

Including of one site along the tributary of Abukmagawa, Horikawa, there were totally three sites that levee broken. The failure types were caused by surface erosion. The figure 1-9 shows the failure process.

5. Shounaigawa River in Aichi, 2000(庄内川)

There were three sites of levee failure along Shunaigawa River in 2000. Because of the increasing infiltration in the levee, the stability was gradually decreasing and the slip of the levee was beginning then finally the levee totally broken. The failure situation is shown in Figure 1-10.

6. Yahagigawa River in Aichi, 2000(矢作川)

There were two sites of levee failure along the branches of Yahagigawa River in 2000. The one failure occurred before overflow, it's caused by the scouring. The other site was caused by an overflow.

7. Kuzuryugawa River in Fukui, 2004(九頭竜川)

There were nine sites of levee failure along the branches of Kuzuryugawa River in 2004, and the failures were caused by overflow.

8. Shinanogawa River in Nigata, 2004(信濃川)

The levee failure occurred in Suwa area on Shinaogawa watershed. The length of failure was about 120 m, and it was caused by overflow then the continuous overflow water scoured the surface of levee, finally the levee was broken. Another four failure

sites were on the other branch of Shinanogawa River. The length of the failure was about 50 m, it was also caused by overflow. The failure situation in Suwa area is shown in Figure 1-11.

9. Maruyamagawa River in Hyogo, 2004(円山川)

There were two sites of the levee failure along the Maruyamagawa River and its branch. One of the failure was caused by infiltration and the other was firstly overflow. The serious inundation situation and the failure levee are shown in Figure 1-12.

10. Tenryugawa River in Nagano, 2006(天竜川)

There was one site of the levee failure along Tenryugawa River in 2006. The failure length was about 100 m. The failure was caused by the erosion and scouring.

11. Igarashigawa River in Nigata, 2011(五十嵐川)

According to the record of the water level of Igarashigawa River, the levee failure was occurred by overflow.

12. Yabegawa River in Fukuoka, 2012(矢部川)

Along the Yabegawa River and its branch, there were total 20 sites of the levee failure. Most of these failures were caused by piping failure because of the continuous high water level over than 5 hours. The Figure 1-13 shows the process of levee failure.

13. Kinugawa River in Tsukaba, 2015(鬼怒川)

The serious flood occurred in Sept. 2015 and its main reason of disaster was because of the levee failure. The type of levee failure was caused by overflow and the overflow water continuous scoured the levee surface, finally the levee was totally

broken and large scale inundation happened. The Figure 1-14 shows the water level record of Kinugawa River, before typhoon No. 18 in 2015, the maximum record was 2.44 m in 1979 however, at 10th Sept the maximum water level was 2.79 m. The Figure 1-15 shows the failure situation of the levee.

The above cases are some large scale levee disasters. On the other hand, NILIM (National Institute for Land and Infrastructure Management) collected the 23 infiltration failure cases of levee of Japan, including their soil parameters and the hydrology conditions during rainfall events as shown in Table 1-4. [10] Among these cases, there are nine cases that the peak water level during the rainfall is lower than high water level. It highlights a very important issue, even if the water level is lower than H.W.L, the failure occurs still possible.

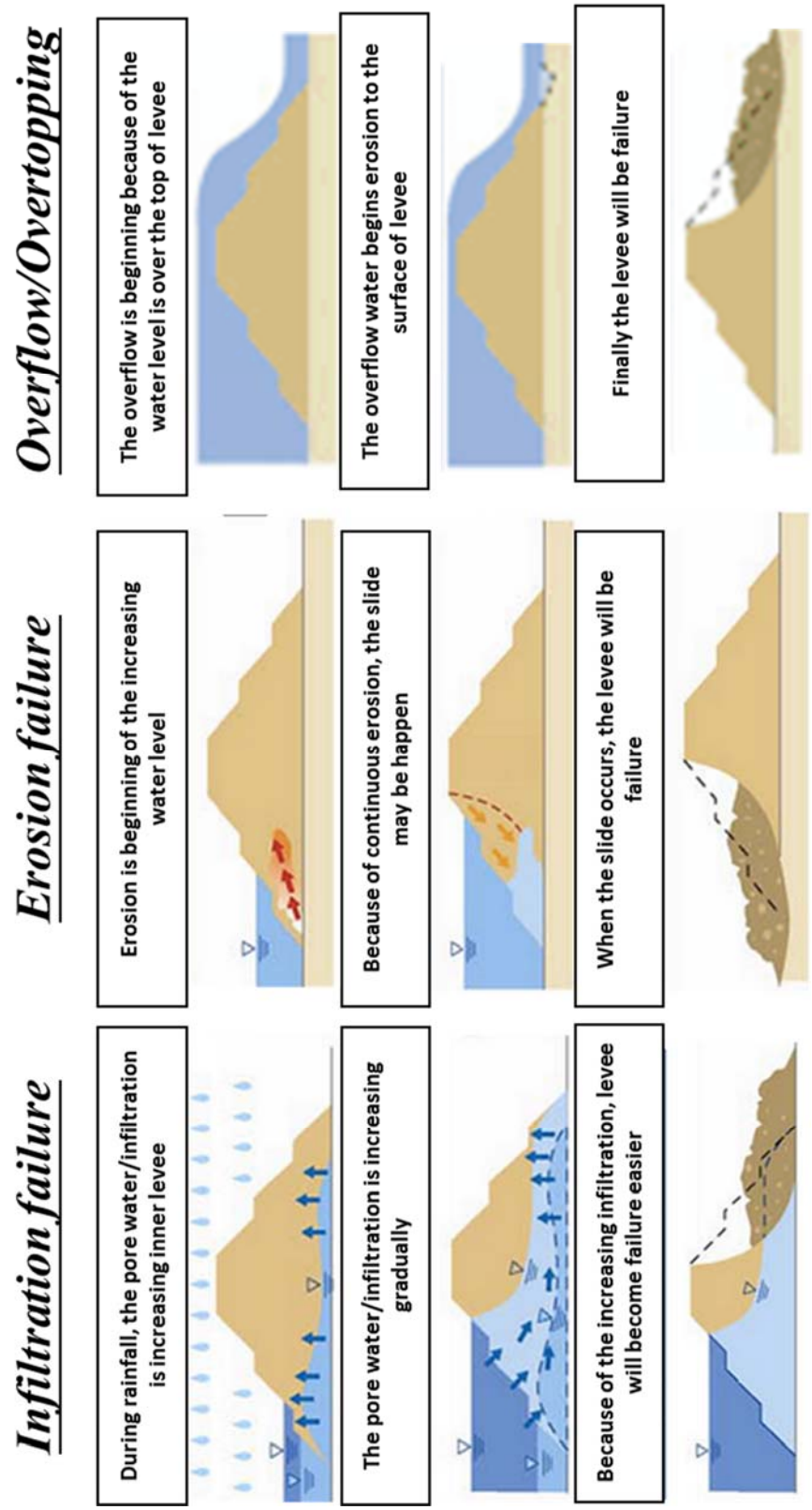

Figure 1-6 the three types of the levee failure induced by flooding

Table 1-2 the water level record in Ishikarigawa River in Hokkaido, 1981 [6]

Station	Ino (伊納)	Osamunai (納内)	Hashimotocho (橋本町)	Tsukigata (月形)	Ishikara Ohashi (石狩大橋)
Design high-water level	95.54	61.55	28.83	16.6	8.75
Warning water level	91.4	58.6	26.1	13.8	5.6
Designated water level	90.7	57	24.8	12	4.7
August, 1981	95.25	62.4	27.02	16.99	9.23

Table 1-3 the failure type in Ishikarigawa River, 1981 [7]

No.	River name	Failure type
①	Makunbetsugawa(真勲別川)	Overtopping
②	Ishikarigawa(石狩川)	Overtopping
③	Ishikarigawa(石狩川)	Overtopping
④	Horomuigawa(幌向川)	Overtopping
⑤	Horomuigawa(幌向川)	Overtopping
⑥	Kenufuchigawa(嶮淵川)	Overtopping
⑦	Shimamatsugawa(島松川)	Leakage
⑧	Sankabibaigawa(産化美唄川)	Overtopping
⑨	Naiegawa(奈井江川)	Overtopping
⑩	Ouhougawa(大鳳川)	Overtopping
⑪	Izarigawa(漁川)	Leakage

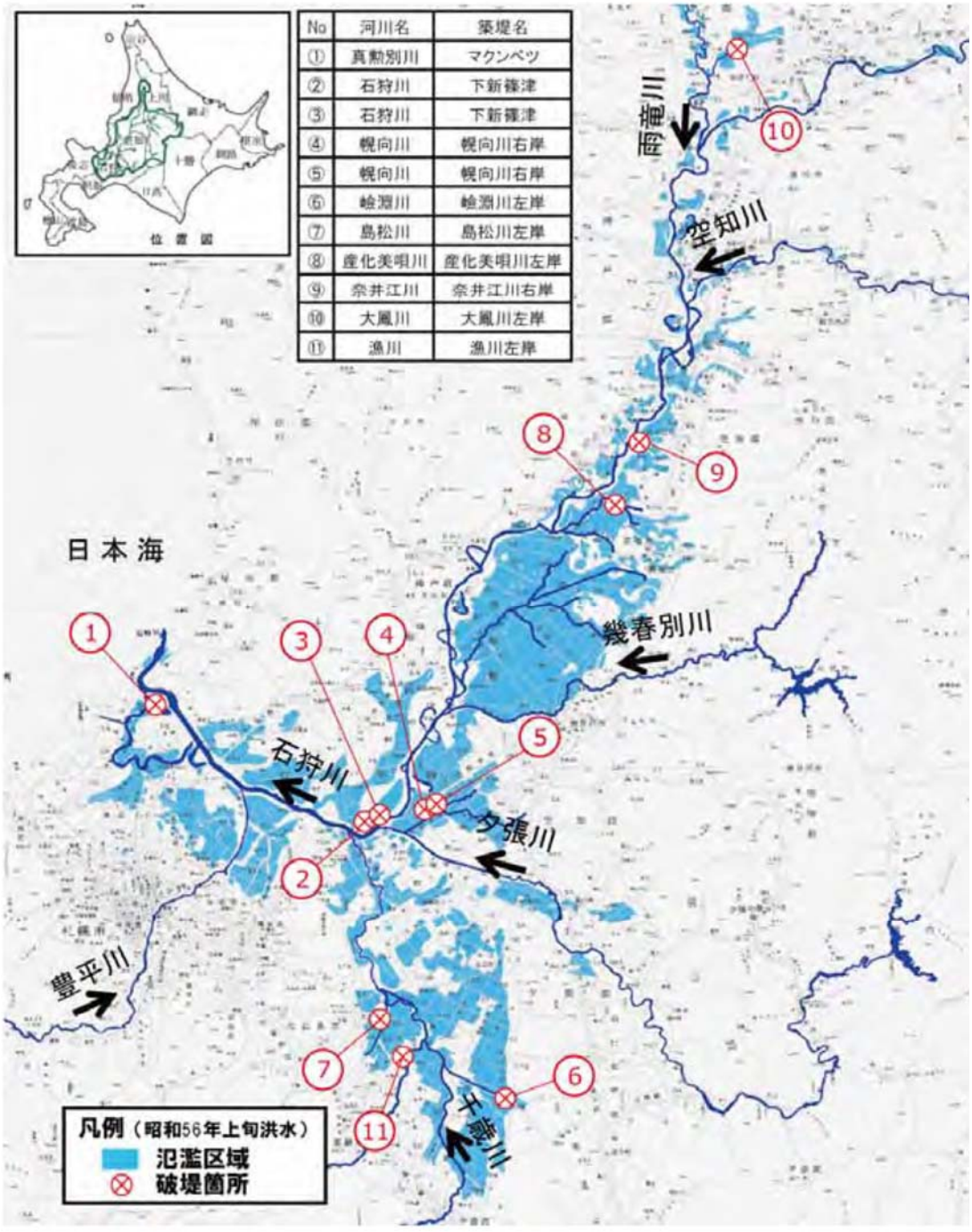

Figure 1-7 the locations of the levee failure along Ishikarigawa River, 1981 [7]

The slip failure induced by infiltration

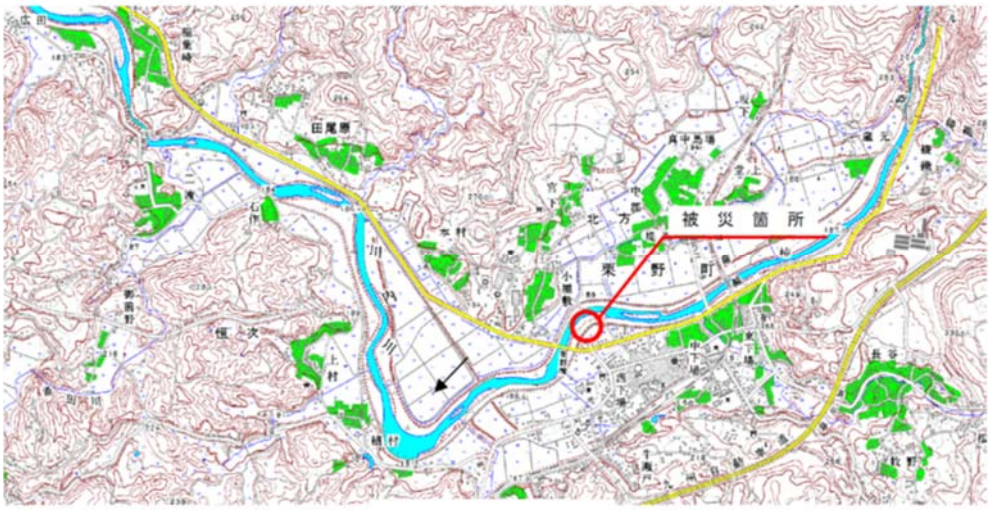

location

Figure 1-8 the levee failure in Sendaigawa River in Kagosima, 1993 [8]

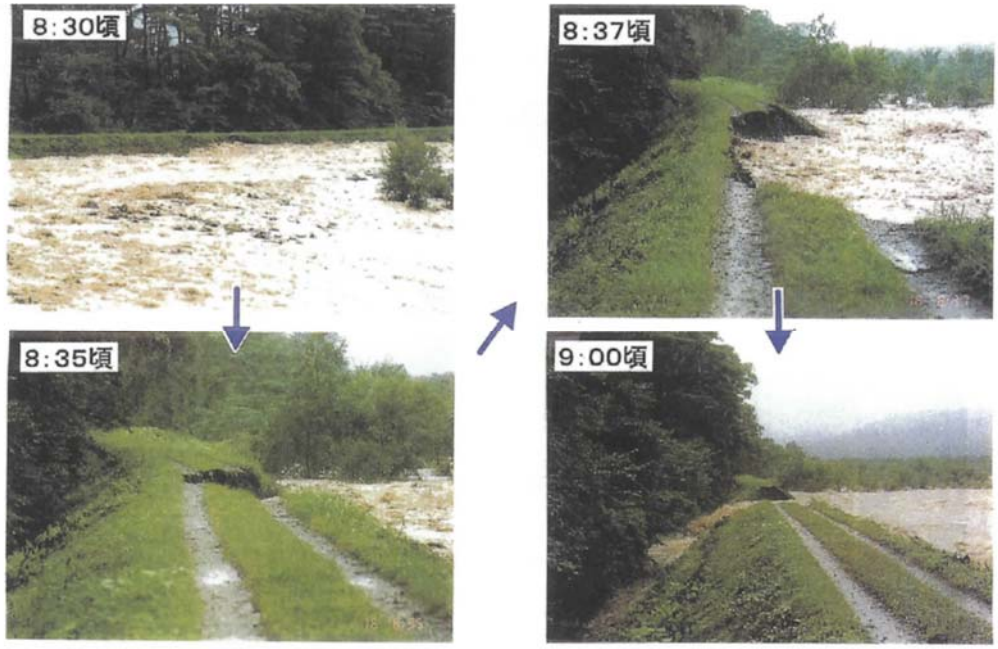

Figure 1-9 the levee failure process in Abukumagawa River in Fukushima, 1998 [8]

Figure 1-10 the infiltration failure in Shounaigawa River in Aichi, 2000 [9]

Figure 1-11 the failure situation in Shinanogawa River in Nigata, 2004 [7]

Figure 1-12 the inundation and levee failure in Maruyamagawa River in Hyogo, 2004 [11]

Figure 1-13 the failure process of the levee in Yabegawa River in Fukuoka, 2012 [12]

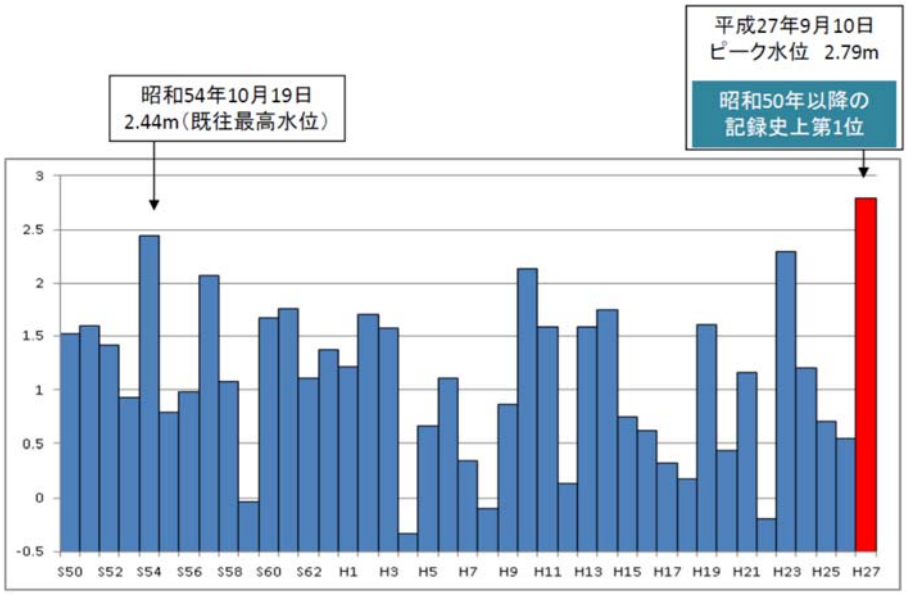

Figure 1-14 the maximum water level record at Ishii station by year

（From: Ministry of Land, Infrastructure, Transport and Tourism. Kanto Regional Development Bureau）

Figure 1-15 the aerial photo after typhoon No. 18

（From: Ministry of Land, Infrastructure, Transport and Tourism. Kanto Regional Development Bureau）

Table 1-4 the infiltration failure cases [10]

No.	Site	Date	Soil of Levee	Peak level > HWL
1	Mogamigawa R_CsNo92~No94)	1958.7.28	Clay	yes
2	Abukumagawa L_4K	1958.9.27	Clay	yes
3	Yoneshirogawa L_5K	1972.7.9	Sandy	yes
4	Ujigawa L_23.8K	1953.8.25	Sandy	yes
5	Hiikawa R_11.4~11.6K	1965.7.23	Sandy	no
6	Edogawa L_24.5K	1982.9.12	Sandy	no
7	Arakawa L_11.3K	1981.10.22	Sandy	no
8	Arakawa L_13.7K	1981.10.22	Clay	no
9	Arakawa R_23K	1982.9.12	Clay	no
10	Arakawa L_28.2K	1982.9.12	Clay	-
11	Arakawa L_64K	1982.9.12	Sandy	-
12	Arakawa L_67.6K	1982.9.12	Clay	-
13	Arakawa L_69.6K	1982.9.12	Sandy	-
14	Arakawa L_70K	1982.9.12	Sandy	-
15	Arakawa L_70.4K	1982.9.12	Clay	-
16	Arakawa L_71.2K	1982.9.12	Clay	-
17	Arakawa L_72K	1982.9.12	Sandy	-
18	Arakawa R_72K	1982.9.12	Sandy	-
19	Shounaigawa L_25K	2000.9.11	Sandy	no
20	Shounaigawa R_23.8K	2000.9.11	Sandy	no
21	Shounaigawa L_24.4K	2000.9.11	Sandy	no
22	Aganogawa L_19.2K	2004.7.1	Clay	no
23	Yoneshirogawa L_7.8K	2007.9.17	Sandy	yes

L: Left bank; R: Right bank

1.3 Existing problems

The safety standard of a levee usually uses the water level as the reference basis. Especially for the high water level, it is the critical condition for the safety to danger. As shown in Figure 1-16, when the water level is lower than the high water level, the levee is safe. On the contrary, when the water level is higher than the high water level, it is dangerous. The results of the safety assessments of a levee are only two outcomes, safety and safe and dangerous. The assessment method is the deterministic method with all deterministic parameters or coefficients. However above-mentioned Table 1-4 shows the cases that levee broken occurred when the water level is lower than high water level.

Furthermore, the rainfall intensity is increasing gradually year by year, and it means the occurrence frequency of the large scale floods perhaps increases. The floods may cause serious losses, including of the people lives and property. However, the current assessment is not enough to explain the exceptional cases of the levee failure before the water level is lower than high water level and it can't explain the transition process of the failure occurrence. The main reason is that the uncertainty of the environment is not considered in the safety assessment.

"Certainty" refers to a situation in which the outcome of an event or the value of a parameter is known with unit probability. Conversely, uncertainty occurs when a collection of values associated with respective uncertain "states of nature" occur with strictly non-negative probabilities for at least different possible values. [13] Generally, the uncertainty would have two possible types, one is the limitation of observation or experiment and the other is an error of data. The uncertainties come from three possible sources. The first is an intrinsic quality of social, economic or natural phenomena. The

second is a limitation of the knowledge. Final is from decision making. (Matsuo Minoru, 1984) [14] For the evaluation of reliability design, there is two operations, one is the calculation of failure probability, and the other is decision making. For the failure probability, it's the purely mechanical problem with considering the basic mechanical properties. Therefore, the necessary work is the investigation and statistic of parameters. For the decision making, the best option should be selected among all the solutions. This study is main analyzes of natural disasters and therefore the content of this chapter will discuss the uncertainty of the basic mechanical properties.

If the safety assessment considers the uncertainty of the environment, the evaluation result will like Figure 1-17. The schematic diagram shows the probable result of the safety evaluation. By considering the variation of the parameters, figure (a) shows the evaluation results of the probability and the average safety factor is 1.5. For the deterministic method, the result is safety for the levee because the average or expectation value of the parameters is used. However, with considering the variation of the parameters of the uncertainty, the real probability distribution of the safety factor will be shown as the figure (a), even if the average is safe, there is still 3 % failure existing. Moreover, the failure transition will be as the figure (b) because the failure probability will increase with the water level rising.

In conclusion, the current safety assessment can't explain the realistic failure transition. A new method with considering the uncertainty is necessary. Therefore, in the thesis, I will suggest a new evaluation method to understand the probability of the levee failure for the water level rising.

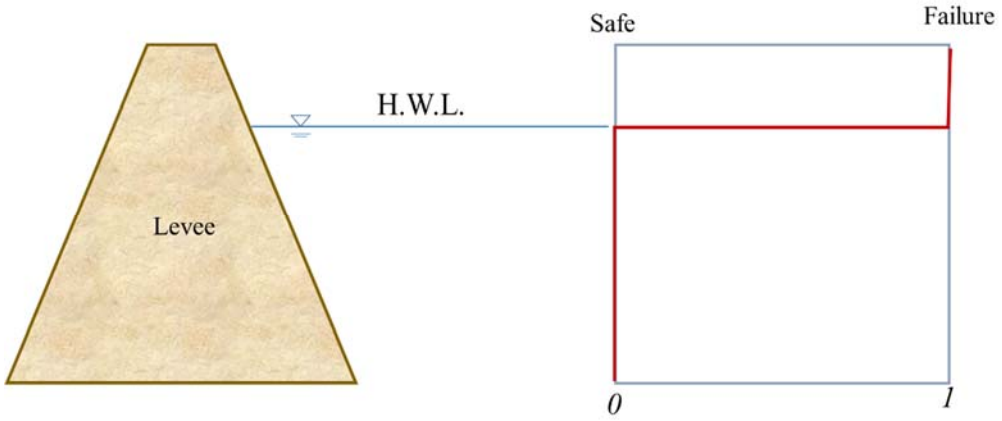

Figure 1-16 the current status of safety assessments

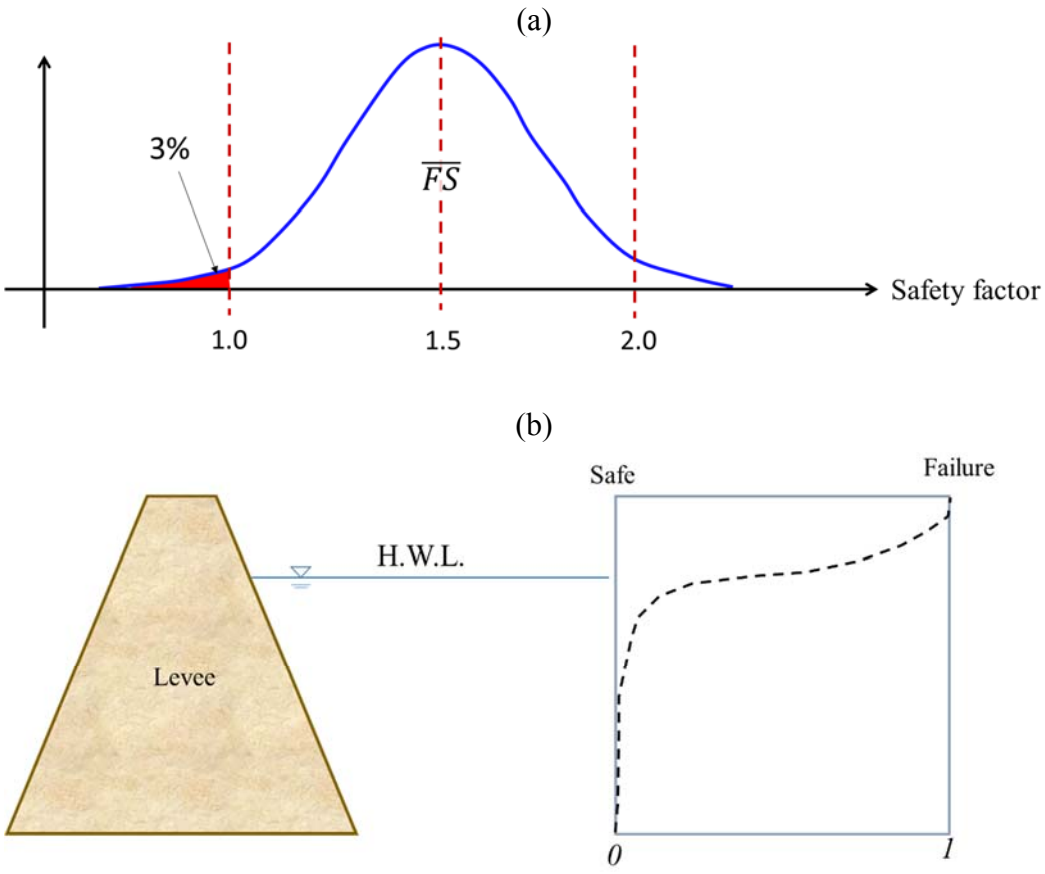

Figure 1-17 the safety assessments with considering the uncertainty of the environment

1.4 Research aim and category

The existing problem is very complex because of many uncertainties of the real environment as previously mentioned. Therefore, the possible influence elements should be dismantled and analysis. The safety of the levee will be considered by the relationship between the resistance force and the external force of the levee. The external force is from the effects of the water level; the resistance force is from the levee its own condition. Figure 1-18 and Figure 1-19 are the structure dismantling results of the resistance and external forces.

For the external force, the water level, it usually calculates by the rainfall data, so-called rainfall-runoff model. The parameters and the coefficients of the model are calculated or decided by the geology, the terrain, the observation method of the rainfall and so on. However, it is very complex because of many uncertainties of the real environment. Therefore, the thesis will first simplify the uncertainty of the environment, and the uncertainty of the rainfall will be considered in the evaluation of the rainfall-runoff model to assess the probable distribution of the water level (as shown in Figure 1-18).

On the other hand, for the resistance force, the status of the reality levee is also very complex. It can be divided to two respects, one is the construction materials of the levee, and the other is the geometric conditions of the levee. The soil material is inhomogeneous from the soil characteristics, construction and others because of the continuous constructed and reinforced by different years. The geometry conditions like the levee slope, the height of the levee and the width of the levee are also effected the stability or safety of the levee. Therefore, the first is the simplification of the levee conditions, including of the materials and spatial conditions. The uncertainty of the soil

material focuses on the variation of the soil parameters, not the spatial uncertainty of the material distributed. Therefore, the levee is considered by the one cross section, not the continuous construction. By considering the uncertainty of the soil parameters, the failure probability of the levee can be calculated (as shown in Figure 1-19).

In the thesis, the new method to assess the reliability of the levee safety is according to the external force from the water level and the resistance force from the stability of the levee.

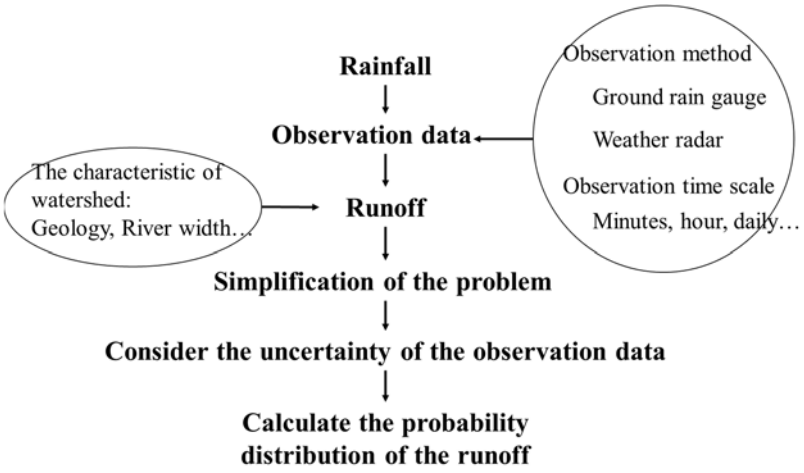

Figure 1-18 the research category of external force of water level

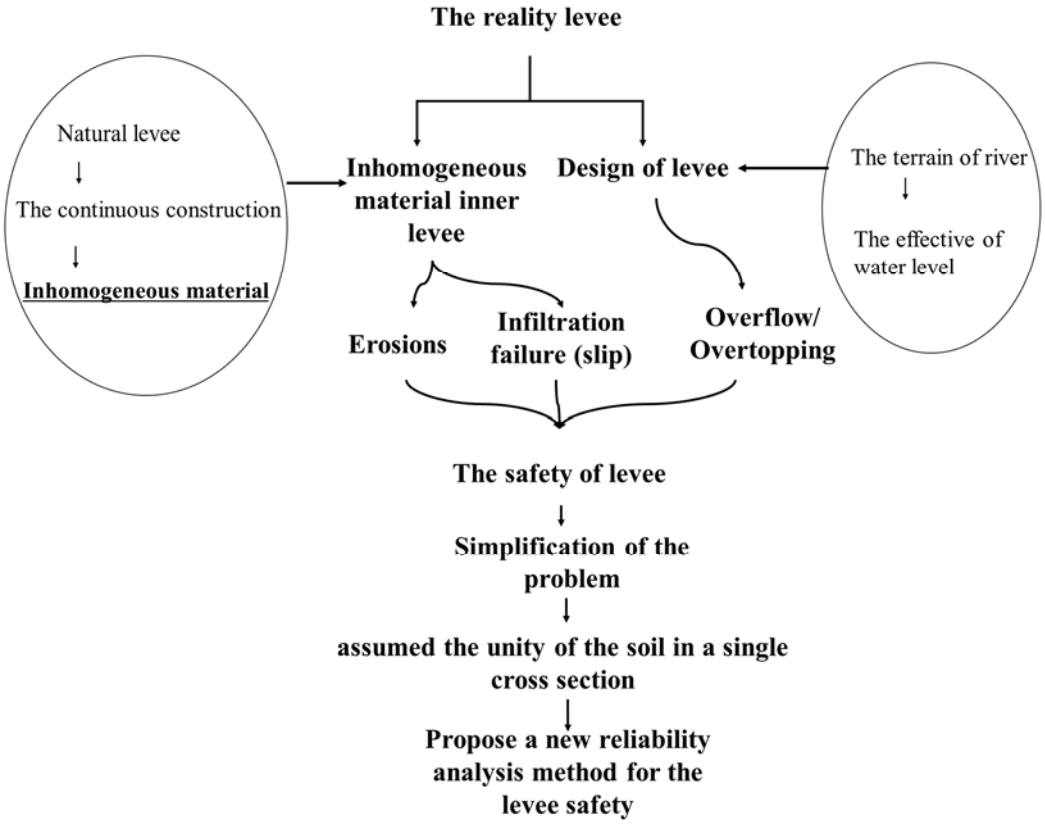

Figure 1-19 the research category of resistance force of levee

1.5 Thesis scope

According to the section 1.4, the research aim and the category, the thesis can be subdivided into three parts, the external force, the resistance force and reliability analysis. Therefore, in the thesis, there are six main chapters, and the flow chart is as shown as Figure 1-20. The following will explain the contents of each chapter.

Chapter 1 is the introduction of the thesis. First is the background information, including of the levee of Japan and the disaster types of the levee. Second is the explanation of uncertainty, occurs when a collection of values associated with respective uncertain "states of nature" occur with strictly non-negative probabilities for a least different possible values. Final is the research aim, the category and thesis scope.

Chapter 2 is the hydrology model based on the stochastic process theory. There are a lot of probability methods to calculate the water level of flood and herein the authors would use the method, which based on the relation between the runoff heights of stochastic differential equation and the mathematic equation of Fokker-Planck to obtain the uncertainty of rainfall and runoff. First is the basic equation of a generalized rainfall-runoff model by mathematics. The equation applied to the single slope plays a very important role in the thesis. Second is the definition of the uncertainty of hydrology. Uncertainty in rainfall observation and estimation also can be categorized into natural inherent variability (aleatory) and knowledge uncertainty (epistemic). The data of rainfall are gotten from the several methods like rainfall gauge on the ground or weather radar. With different method, it exists the following uncertainty. Aleatory uncertainty of rainfall consists of physical uncertainty with temporal and spatial. Third is the stochastic process theory, including of its development to be the basis for the stochastic process of the hydrological model. It is subdivided into the two parts: the developments

of the stochastic differential equation theory and the probability density function. Final is according to the above sections, herein the uncertainty of water level will base on the relation between the runoff heights of stochastic differential equation and the mathematic equation of Fokker-Planck to obtain the uncertainty of rainfall and runoff.

Chapter 3 is the stability analysis of the levee. The types of levee failure can be classified to infiltration failure, erosion failure and overflow/overtopping failure because of the increasing water level during rainfall. In the chapter, the infiltration failure will be discussed by the slope stability method. The safety factor of slope is defined as the ratio of the shear strength divided by the shear stress required for equilibrium slope. Second is the uncertainty of soil parameters. The uncertainty of soil parameters comes both from the spatial variability and from errors in testing. Final is the infiltration failure probability of levee. For the infiltration failure evaluation of the levee, the thesis uses the circular slip method of slope stability to calculate the safety factor of the levee slope. According to the above section, the modified Fellenius method is used. In the equation, the main parameters of the equation are soil cohesion, the soil friction angle, the weight of the soil block, the pore water pressure and the geometric conditions of the circular slip. Among these parameters, the geometric conditions are according to the slip surface to decide, the pore water pressure and the weight are changing with the water level change, and the soil cohesion and the friction angle are usually decided by the lab test or in situ test. Traditionally, the cohesion and the friction angle are the unique value. Herein in order to consider the uncertainty of soil parameters, the variation/ deviation of the parameters will be conducted to evaluate the failure probability of the levee slope.

Chapter 4 is the reliability analysis. Reliability is probabilities or statistics in mathematics. Therefore, the performance of phenomenon or decision must display by probability. Traditionally in civil engineering assessments of the risk of failure are made

on the basis of allowable factors of safety, learned from previous experiences for the considered system in its anticipated environment. In the chapter, the failure of levee can be classified two types, one is overflow and the other is infiltration failure calculated by a circular slide method. The overflow failure probability is calculated from the distribution of water level. The infiltration failure is combined the probability of slip with considering the uncertainty of soil parameters in the certain water level h. Furthermore, there are main failure types considered, overflow and infiltration failure. Therefore, the detail probability calculated is including the following types: the only overflow failure; the only infiltration failure; when one of the two failures occurs; when both overflow and infiltration failure occur.

Chapter 5 is the scenario test. The chapter assumes some scenario conditions to simulate the failure probability of levee. The geometry of the levee is: the height of levee is7. 5 m, H.W.L. is 6.5 m (freeboard is 1.0 m) and the grade is 1:2~1:5. The conditions of soil parameters are different according to the soil materials. Finally, the four results can be got: the only overflow failure, P_{fo}; the only infiltration failure, P_{f1}; when both overflow and infiltration failure occur, P_{f2};, when one of the two failures occurs P_{f3}. Furthermore, the effectiveness of the freeboard is also calculated.

Chapter 6 is the conclusion. In the thesis, the main concept is considered the uncertainty of external force- water level and resistance force- stability of levee to evaluate the reliability of the levee. The chapter is the conclusion of the thesis. The achievement and result are summarized here.

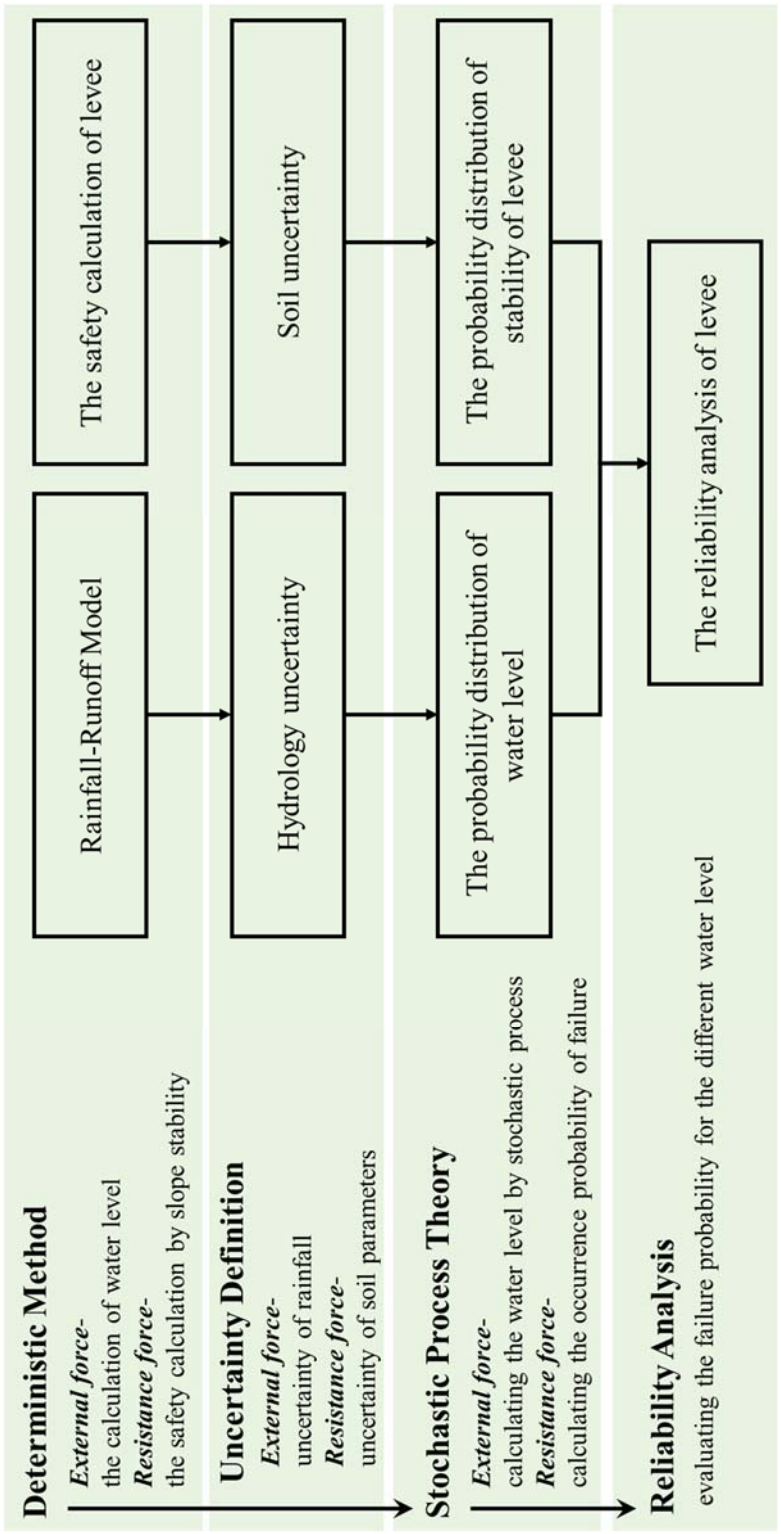

Figure 1-20 the flow chart of the thesis

Reference

[1] http://www.jma.go.jp/jma/kishou/info/heavyraintrend.html

[2] Hideo Nakajima, 2003, "Illustration- River Levee", Gihodo Shuppan Co., Ltd. (in Japanese)

[3] http://www.yodogawa.kkr.mlit.go.jp/activity/maintenance/renforcement/

[4] http://www.thr.mlit.go.jp/karyuu/_update/whatsnew/h15/2003_7_26_jishin_sokuhou/teiboukaisaku.htm

[5] Investigation of the Performance of the New Orleans Flood Protection Systems in Hurricane Katrina on August 29, 2005. "Final Report- Volume I : Main Text and Executive Summary". 2006.

[6] Natl. Res. Center for Disaster Prevention, 1982. "The Investigation Report of the Front and No. 12 Typhoon in Ishikaragawa River Flood from August 3th to 6th in 1982" (in Japanese)

[7] Public Works Research Institute CERI, Ministry of Land, Infrastructure and Transport Hokkaido Development Bureau, 2011. "Experimental report on the levee break widening mechanism of the overtopping levee break behavior of the river levee" (in Japanese)

[8] http://www.skr.mlit.go.jp/tokushima/river/yoriyoi/yoriyoikawa/teibou/teibou040823/160823-1-2.pdf

[9] Foundation of Hokkaido River Disaster Prevention Research Center,2004. "Countermeasures Against Leakage of Levees"

[10] Yoshito Kikumori, 2008. "Study on Accuracy Improvement of Safety Evaluation for Seppage Failure Levees". Technical Note of NILIM No. 4410 January 2008.

[11] http://www.mlit.go.jp/river/pamphlet_jirei/bousai/saigai/2005/30.pdf

[12] http://www.cee.ehime-u.ac.jp/~gm/session.pdf

[13] Allen L. Jones, Steven. Kramer, Pedro Arduino, (2000), "Estimation of Uncertainty in Geotechnical Properties for Performace-Based Earthquake Engineering." Peer Report.

[14] Matsuo Minaru, (1984). “Geotechnology-With the idea of the reliability design and reality.” Gihodo Shuppan Co., Ltd.

CHAPTER 2 HYDROLOGY MODEL BASED ON STOCHASTIC PROCESS THEOTY

There are a lot of probability methods to calculate the water level of flood and in this research, the authors would use the method that Yoshimi et al. (2015) proposed [1]. It's based on the relation between the runoff heights of stochastic differential equation and the mathematic equation of Fokker-Planck to obtain the uncertainty of rainfall and runoff.

2.1 Basic equation of rainfall-runoff in the single slope

According to many approaches like an experiment, observation or numerical analysis, Yamada [1][2] proposed basic equation of a generalized rainfall-runoff model by mathematics. The equation applied to the single slope plays a very important role in the thesis. The following content is the summary of the rainfall-runoff model.

The continuity equation is according to the relation between the submerged depth and the unit discharge of the single slope supposing a rectangular cross section as shown in Eq. 2-1. Furthermore, for the various runoff pattern the motion law is shown as Eq. 2-2, the average flow velocity of the cross section (the unit discharge) is shown as the multiplication ratio of the submerged depth. By combing Eq. 2-1 and Eq.

2-2, the unit discharge can be re-written as Eq. 2-3. Eq. 2-4~ Eq. 2-5 are the parameters of Eq. 2-3. The parameters α and m refer to the unsaturated soil from Shimura [3], Suzuki [4][5] and Kubota [6].

$$\frac{\partial h}{\partial t}+\frac{\partial q}{\partial x}=r(t) \qquad \text{Eq. 2-1}$$

$$v=\alpha h^{m}, q=vh=\alpha h^{m+1} \qquad \text{Eq. 2-2}$$

$$\frac{\partial q}{\partial t}+aq^{\beta}\frac{\partial q}{\partial x}=aq^{\beta}r(t) \qquad \text{Eq. 2-3}$$

$$a=(m+1)\alpha^{\frac{1}{m+1}}, \qquad \beta=\frac{m}{m+1} \qquad \text{Eq. 2-4}$$

$$\alpha=\frac{k_s i}{D^{\gamma-1}w^{\gamma}}, \mathrm{m}=\gamma-1 \qquad \text{Eq. 2-5}$$

Here, v is the mean velocity of the cross section [mm/h]; h is the submerged depth [mm]; q is the unit discharge [mm^2/h]; $r(t)$ is the effective rainfall intensity [mm/h]; and α and m are the parameters of the watershed. About α and m, i is the gradient of slope; D is the depth of surface soil layer; γ is the non-dimensional of soil permeability; ks is the permeation coefficient of soil; w is the effective void ratio.

Here the assumption is the rainfall would be directly flow out to the river, thus the possible affected area near the river is considered that the length of the slope surface is assumed to be very shorter than the length of real slope. Therefore, the q can be shown as Eq. 2-6 by the separation of variables method. The q (unit discharge) and $q*$ (the height of runoff [mm/h]) will be shown as Eq. 2-7. Eq. 2-3 will be written like Eq. 2-8. The Figure 2-1 is the result of the rainfall-runoff model.

$$q(x,t)\cong xq_{*}(t) \qquad \text{Eq. 2-6}$$

$$\frac{\partial q(x,t)}{\partial x}=q_{*}(t) \qquad \text{Eq. 2-7}$$

$$\frac{dq_{*}}{dt}=a_0 q_{*}^{\beta}(r(t)-q_{*}), a_0=aL^{\beta-1} \qquad \text{Eq. 2-8}$$

r=50 *mm/h*; t=6 *h* (rainfall duration)

ks=0.02 *cms*; *L*=30000 *mm*; m=4 ; i=15^o

D=200 *mm* ;*w*=0.42

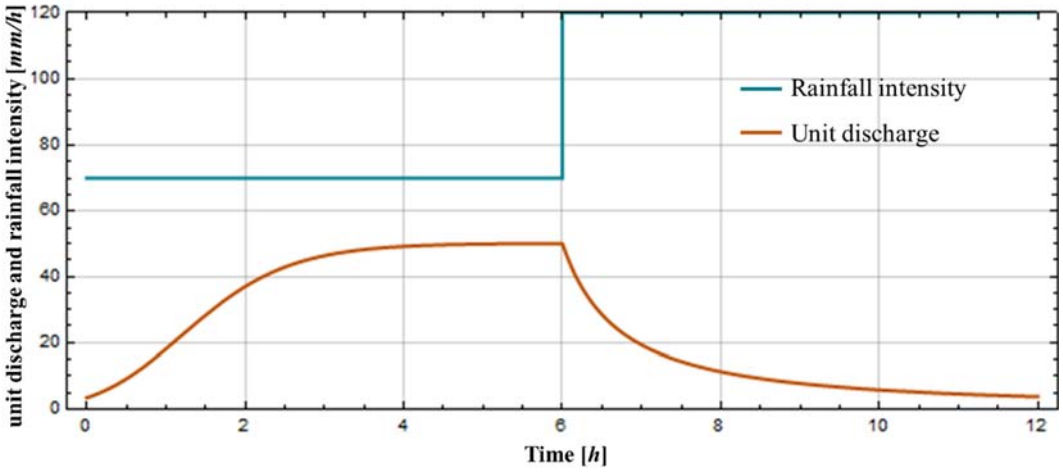

Figure 2-1 the schematic diagram of the rainfall-runoff

2.2 Uncertainty of hydrology

Uncertainty in rainfall observation and estimation also can be categorized into natural inherent variability (aleatory) and knowledge uncertainty (epistemic). The data of rainfall are gotten from the several methods like rainfall gauge on the ground or weather radar. With different method, it exists the following uncertainty. Aleatory uncertainty of rainfall consists of physical uncertainty with temporal and spatial. The temporal is like the observation time scale of rainfall (as shown in Figure 2-2). As Figure 2-2, it shows the difference of hourly rainfall and 10-minute rainfall with a different time scale of observation rainfall. The spatial is like Figure 2-3, it shows the difference distribution date from rainfall gauge, radar and real rainfall. Epistemic uncertainty of rainfall consists of characterizing uncertainty, model uncertainty, transformation uncertainty, which can be related to incomplete knowledge.

The Figure 2-4 shows the rainfall data of the different time scale, minute and hour, and the different methods, including the ground rain gauges and the weather radar- X Band Radar in the upstream of Kinugawa watershed during No. 18 typhoon in 2015. The figure shows the temporal uncertainty and spatial uncertainty. Figure 2-4 (a) shows the obvious features between the minute rainfall and the hour rainfall of the observation data by X-Band Radar. Figure 2-4 (b) shows the rainfall data by the different observation method, the ground rain gauge and X-Band Radar, and it shows the different values between these two methods.

According to the comparison rainfall data on the weather radar and the ground rainfall gauge, the possible uncertainty can be quantitated by the different observation methods. Figure 2-5 shows the comparison data on the weather radar and the ground gauge in Kanto area. It shows the difference existing by the difference observation methods. Figure 2-6 is the difference (the radar data – the ground data). Figure 2-7 is

the standard deviation of the observation rainfall data. As Figure 2-7, the standard deviation of rainfall will increase by the rainfall intensity increasing.

On the other hand, the uncertainties in hydrology model stem mainly from the three important sources, observational uncertainty, model uncertainty, and parameter uncertainty. [8]

Observational uncertainty is related to the observation used for rainfall-runoff modelling. The observation is the measurement of the input rainfall and output discharge of the hydrological systems and sometimes of its states (like water content, ground water or others). The observational uncertainty usually consists of two components: measurement deviation due to instrumental and human error; deviation due to inadequate representation of a data sample due to scale incompatibility or difference in time and space.

Model uncertainty means a model is a simplified representation of the real environment. The real processes are greatly simplified while deriving the basic concepts and equations of the model with inappropriate approximations. Model deviations can also arise from the mathematical implementation that transforms a conceptual model into a numerical model.

Parameter uncertainty is in the model parameters results from an inability to accurately quantify the input parameters of a model. The parameters of the model may not have direct physical meaning. Furthermore, those parameters that have a physical meaning cannot be directly measured or it is too costly to measure them in the field. The values of such parameters are generally estimated by indirect means.

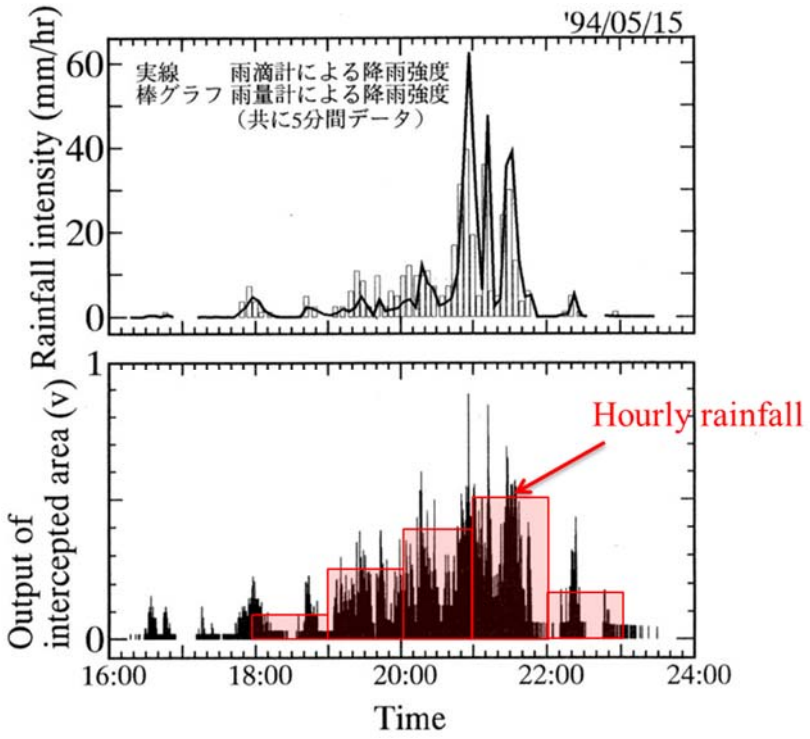

Figure 2-2 The schematic diagram of temporal of rainfall [7]

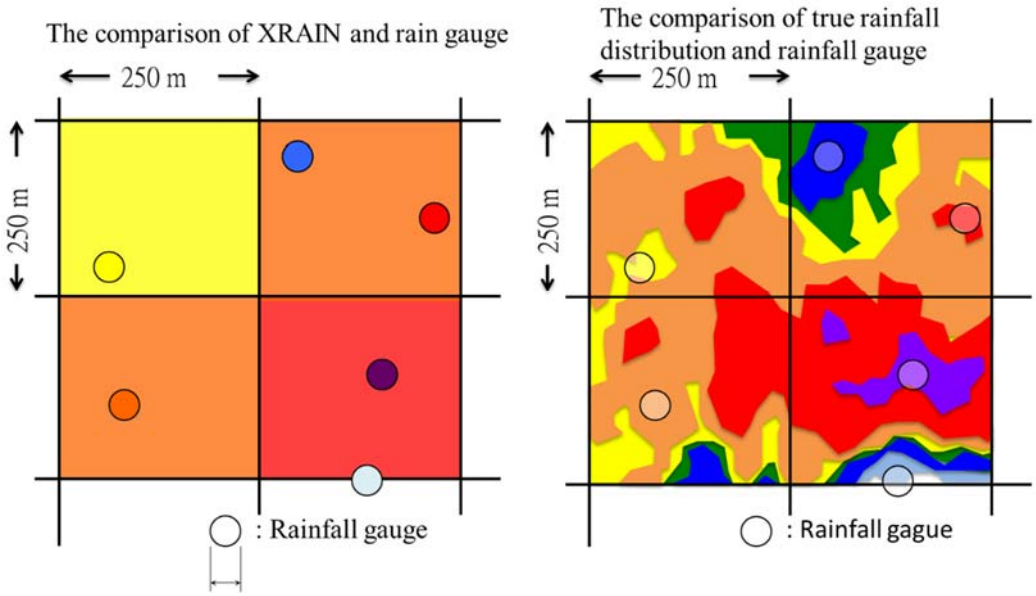

Figure 2-3 The schematic diagram of spatial of rainfall

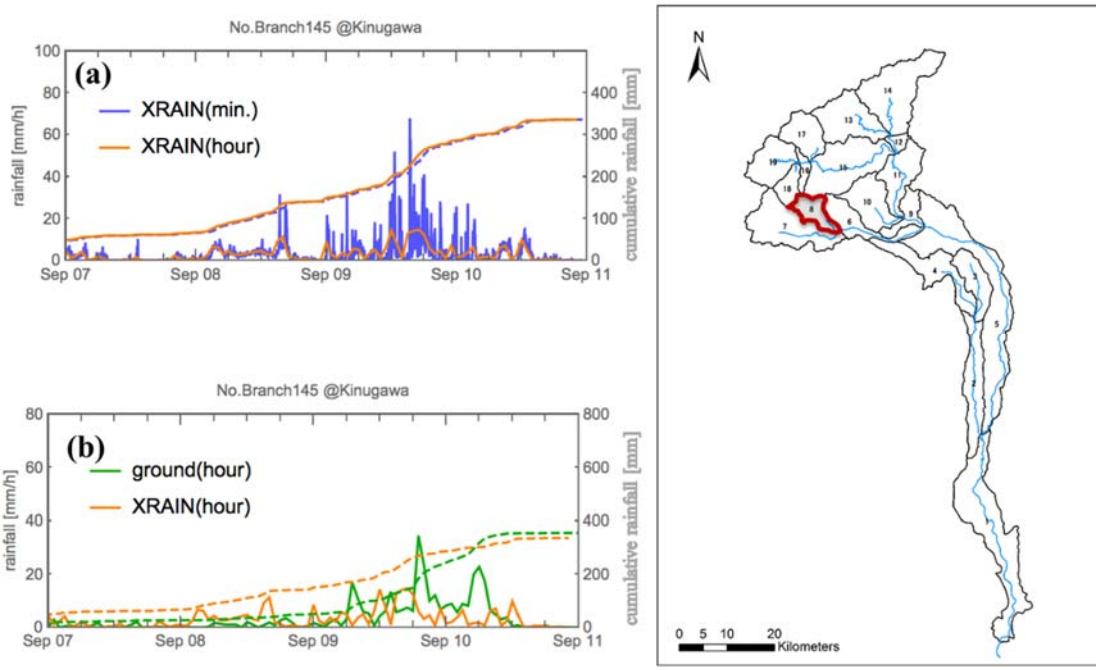

Figure 2-4 the rainfall data by different observation method

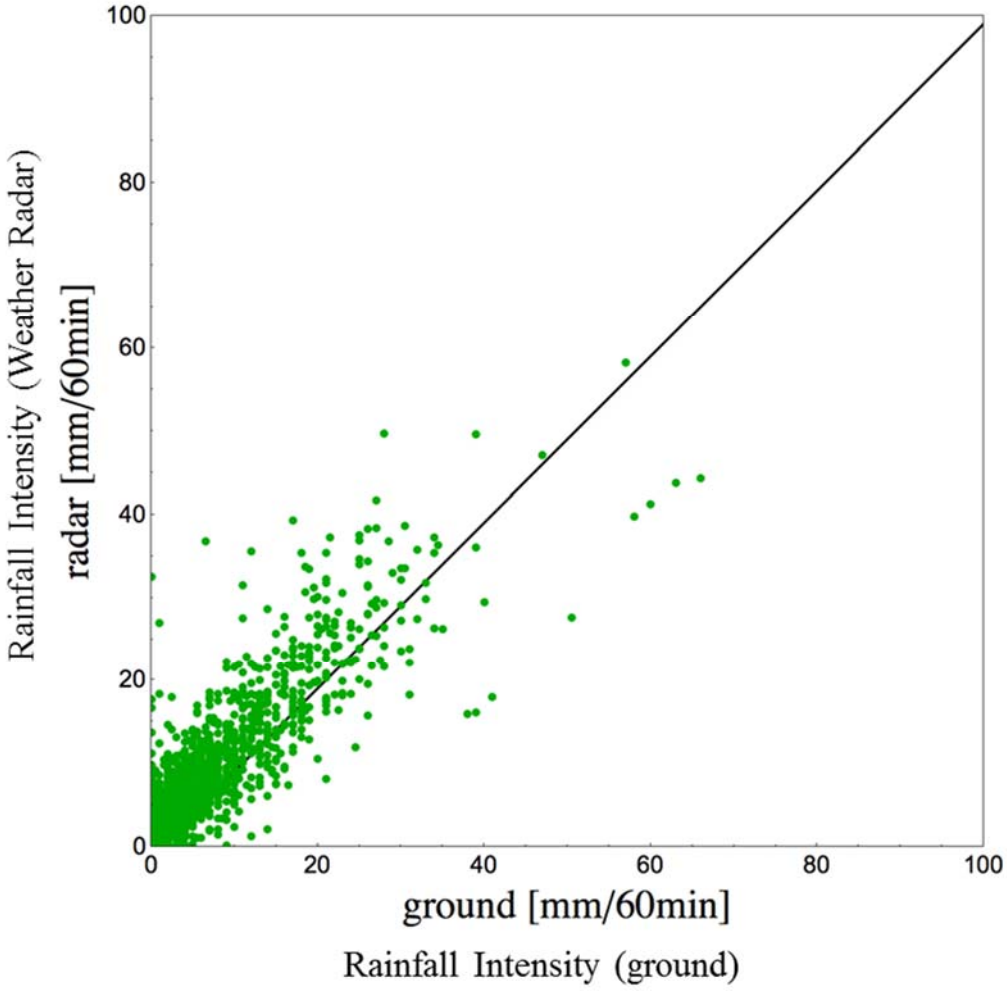

Figure 2-5 the comparison of the radar and ground data in Kanto area

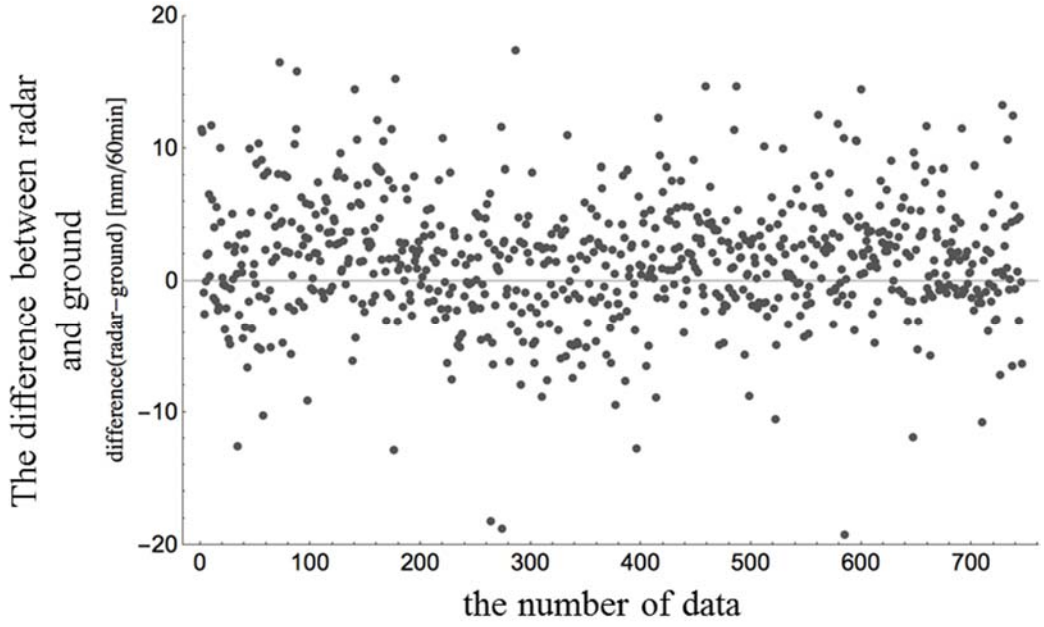

Figure 2-6 the difference between radar and ground data

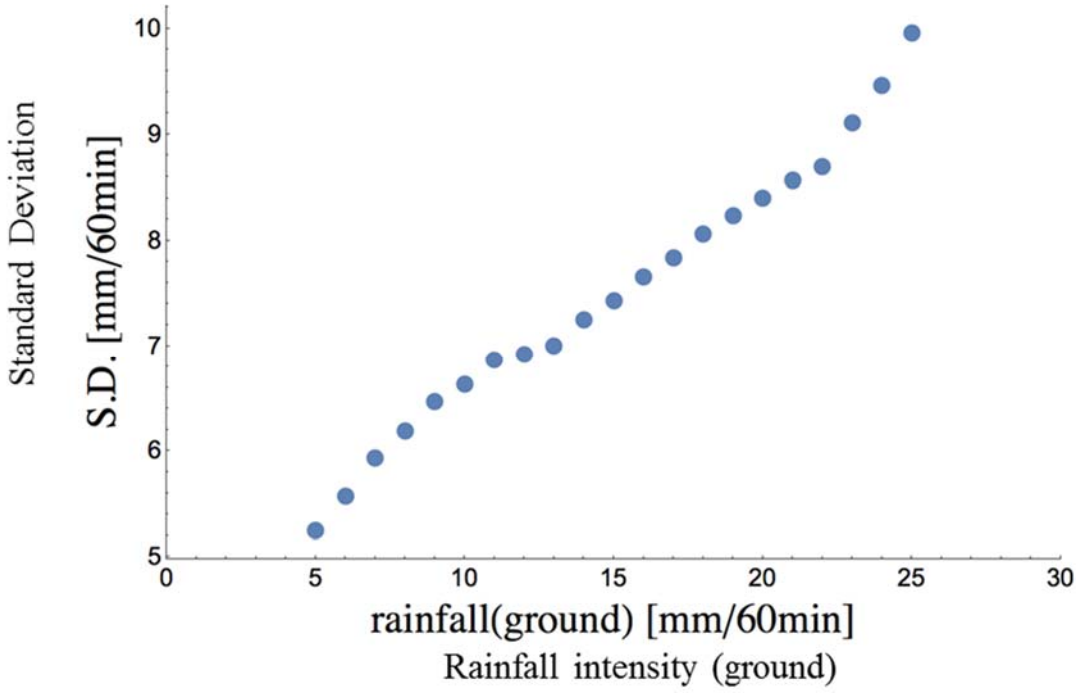

Figure 2-7 the standard deviation of rainfall data

2.3 The development of stochastic process theory

As discussed in section 2.2, how to conduct the uncertainties into the hydrological modelling is a very important issue. Therefore, the section will discuss the stochastic process theory, including of its development to be the basis for the stochastic process of the hydrological model. The following will subdivide into the two parts: the developments of the stochastic differential equation theory and the probability density function.

2.3.1 The stochastic differential equation (SDE)

Robert Brown in 1827 was studying the North American angiosperm species Clarkia pulchella. He looked with particular care at the structure of the pollen-grains. These he took, not from already opened anthers, but from fully-formed pollen sacs that were yet to open and which he dissected at the bench. He suspended some of the pollen grains in water and examined them closely, only to see them 'filled with particles' that were 'very evidently in motion'. There is no question of Brown confusing his observations with other movements caused, perhaps, by evaporation currents. He made sure that the movement 'arose neither from currents in the fluid, nor from its gradual evaporation, but belonged to the particle itself. He carried out careful experiments to disprove these alternative explanations. In later years, it was in the observation of the incessant agitation of minute suspended particles that Brown's name became inextricably linked. The effect, which was to become known as Brownian Movement, was first noticed by him in 1827 (Brown, 1827). The analysis of Brownian movement by Albert Einstein in 1905 led to the formulation of the Boltzmann Constant. [9]

There are two parts of Einstein's theory: the first part consists in the formulation of a diffusion equation for Brownian particles, in which the diffusion coefficient is related to the mean squared displacement of a Brownian particle, while the second part

consists in Einstein's argument was to determine how far a Brownian particle travels in a given time interval. He proposed the famous Einstein relation (also called Einstein-Smoluchowski relation). The relation combines a macroscopic thermodynamic quantity (the temperature, T) and a "mechanical" quantity (the drag coefficient, b) to give the diffusion coefficient. For a sphere of radius a in a fluid of viscosity η, the drag coefficient $b = 6\pi\eta a$ and k_B is the Boltzmann constant. Therefore, the Einstein relation can be written in Eq. 2-9: [10]

$$\mathrm{D} = \frac{k_B T}{6\pi\eta a} \qquad \text{Eq. 2-9}$$

As Einstein wrote in 1905: "The coefficient of diffusion of the suspended substance therefore depends (except for universal constants and the absolute temperature) only on the coefficient of viscosity of the liquid and on the size of the suspended particles." The equation describing Brownian motion was subsequently verified by the experimental work of Jean Baptiste Perrin in 1908. At the same time, the original Langevin equation describes Brownian motion (Paul Langevin, 1908), the apparently random movement of a particle in a fluid due to collisions with the molecules of the fluid. It is a stochastic differential equation describing the time evolution of a subset of the degrees of freedom.

In 1921, Norbert Wiener proposed the Wiener process described Brownian motion as a continuous-time stochastic process. The Wiener process plays an important role both in pure and applied mathematics. In pure mathematics, the Wiener process gave rise to the study of continuous time martingales. Figure 2-8 is a simple example of a Wiener process. A zoomed plot of a subinterval showing than the curve does not get smoother when it is zoomed in. It is a key process in terms of which more complicated stochastic processes can be described. [11]

In 1945, Kiyosi Ito developed the ideas for stochastic analysis with many important papers on the topic. Among them were On a stochastic integral equation (1946), On the stochastic integral (1948), Stochastic differential equations in a differentiable manifold (1950), Brownian motions in a Lie group (1950), and On stochastic differential equations (1951). Itô calculus extends the methods of calculus to stochastic processes such as Brownian motion (Wiener process). It has important applications in mathematical finance and stochastic differential equations. The central concept is the Itô stochastic integral, a stochastic generalization of the Riemann–Stieltjes integral in the analysis. [12] [13]

2.3.2 The probability density function (PDF)

In physics, Liouville's theorem is a key theorem in classical statistical and Hamiltonian mechanics. It asserts that the phase-space distribution function is constant along the trajectories of the system — that is the density of system points in the vicinity of a given system point traveling through phase-space is constant with time. The Liouville equation describes the time evolution of the phase space distribution function. Although the equation is usually referred to as the "Liouville equation", Josiah Willard Gibbs was the first to recognize the importance of this equation as the fundamental equation of statistical mechanics. It is referred to as the Liouville equation because its derivation from non-canonical systems utilize an identical first derived by Liouville in 1838. [14]

The Boltzmann equation describes the statistical behavior of a thermodynamic system and it was devised by Ludwig Boltzmann in 1872. The equation arises not by statistical analysis of all the individual positions and momenta of each particle in the fluid; rather by considering the probability that a number of particles all occupy a very small region of space centered at the tip of the position vector, and have very nearly equal small changes in momenta from a momentum vector, in an instant of time. [15]

In 1906, independently of Albert Einstein, Marian Smoluchowski described Brownian motion. Smoluchowski presented an equation which became an important basis of the theory of stochastic processes. Later the equation was arrived at independently by both the British mathematician Sydney Chapman and the Russian mathematician Andrey Kolmogorov. Therefore, it was also called the Chapman–Kolmogorov equation. It is an identity relating the joint probability distributions of different sets of coordinates on a stochastic process. [16]

The Fokker–Planck equation is a partial differential equation that describes the time evolution of the probability density function of the velocity of a particle under the influence of drag forces and random forces, as in Brownian motion in the 1910s. The equation can be generalized to other observers as well. It is named after Adriaan Fokker (1914) and Max Planck (1917) and is also known as the Kolmogorov forward equation (diffusion), named after Andrey Kolmogorov, who first introduced it in a 1931 paper. When applied to particle position distributions, it is better known as the Smoluchowski equation. The case with zero diffusion is known in statistical mechanics as Liouville equation. [17][18] Every Fokker–Planck equation is equivalent to a path integral. The path integral formulation is an excellent starting point for the application of field theory methods.

2.3.3 The stochastic process of SDE and PDF

The above two sections summarized the development history of the stochastic process theory, including both of the stochastic difference equation (SDE) and the probability density function (PDF). (as shown in Figure 2-9) The difference of the SDE and PDF is shown in Figure 2-10. The result of SDE is the path by random variables and the result of PDF are the integral path like a distribution.

The Figure 2-11 shows the observation hydrological data like atmosphere pressure and flow velocity. The hydrological phenomenon is similar to the Brownian motion and Wiener process, therefore herein the uncertainty hydrology will conduct the stochastic process theory.

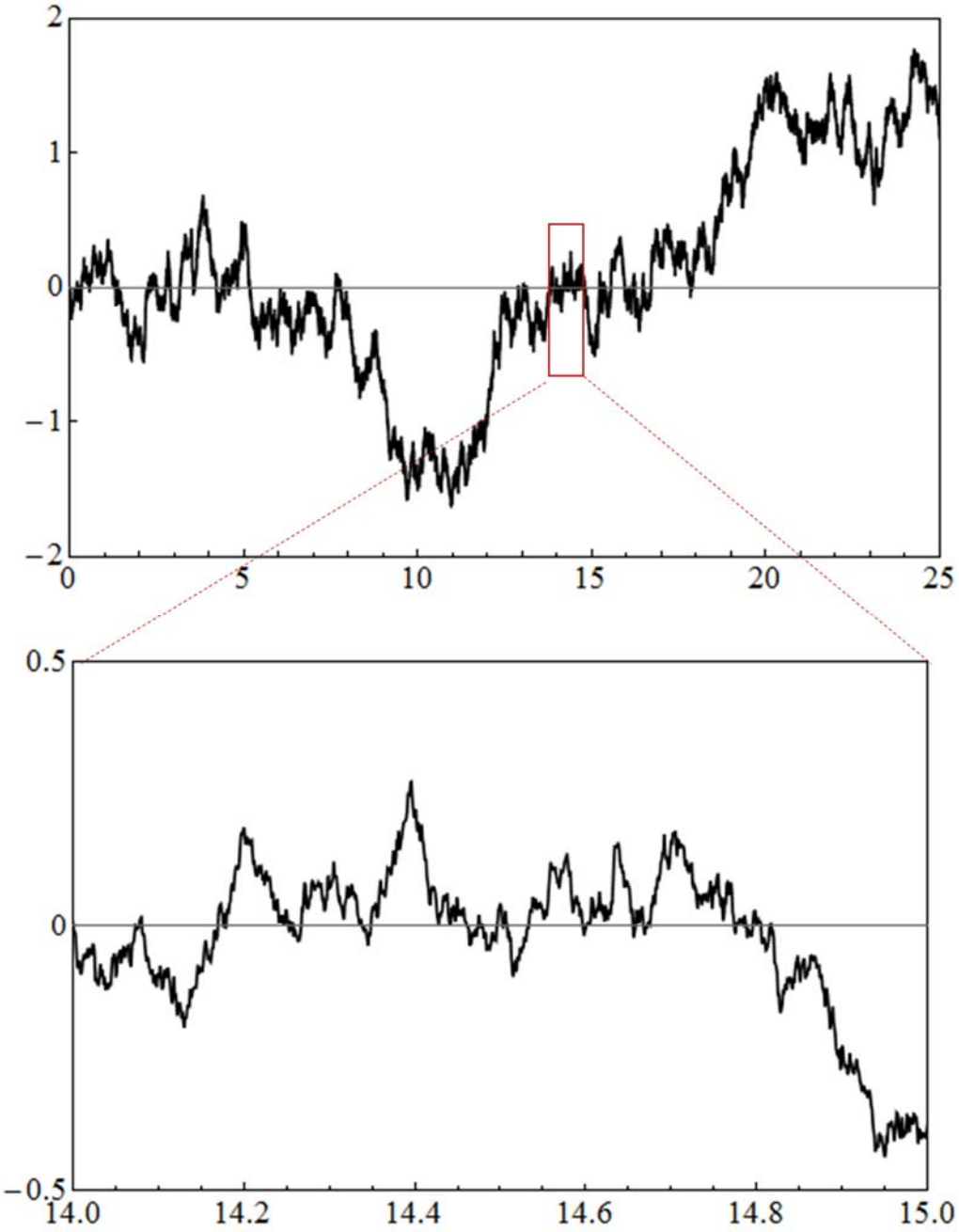

Figure 2-8 A single realization of a one-dimensional Wiener process

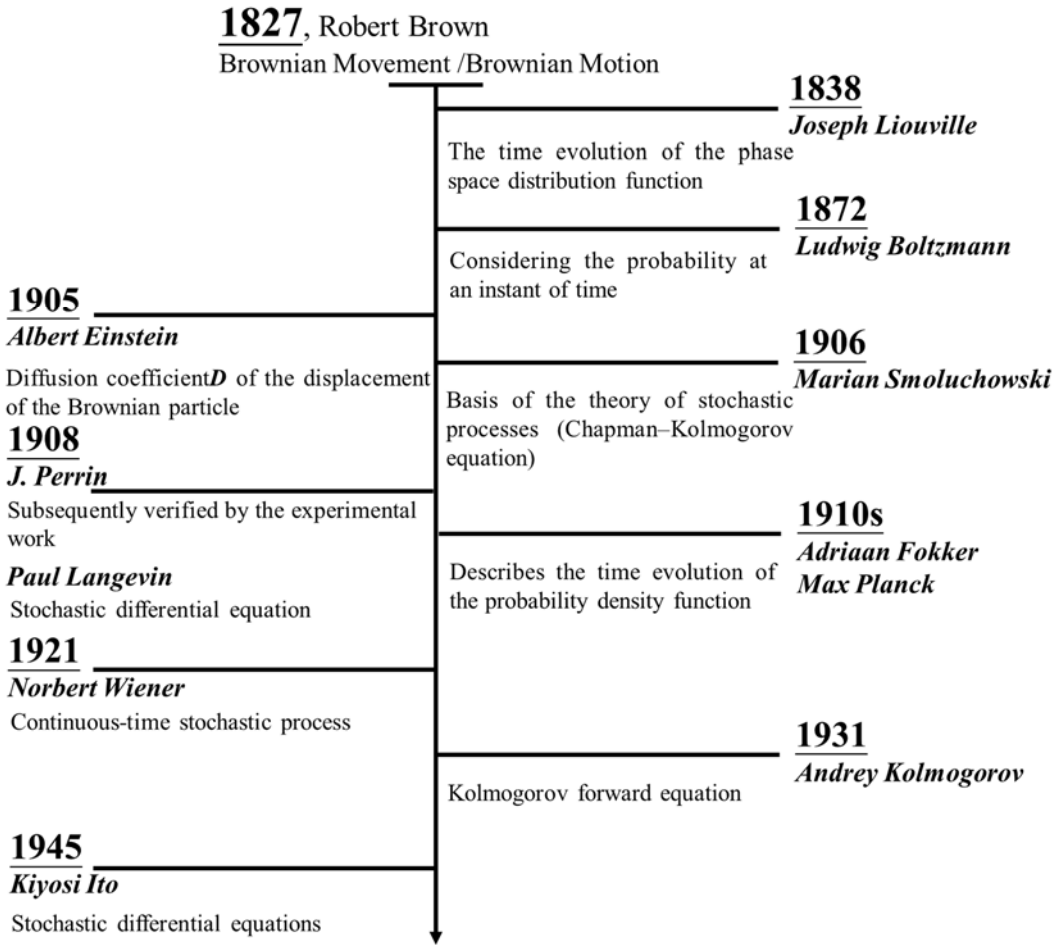

Figure 2-9 the development of the stochastic process theory

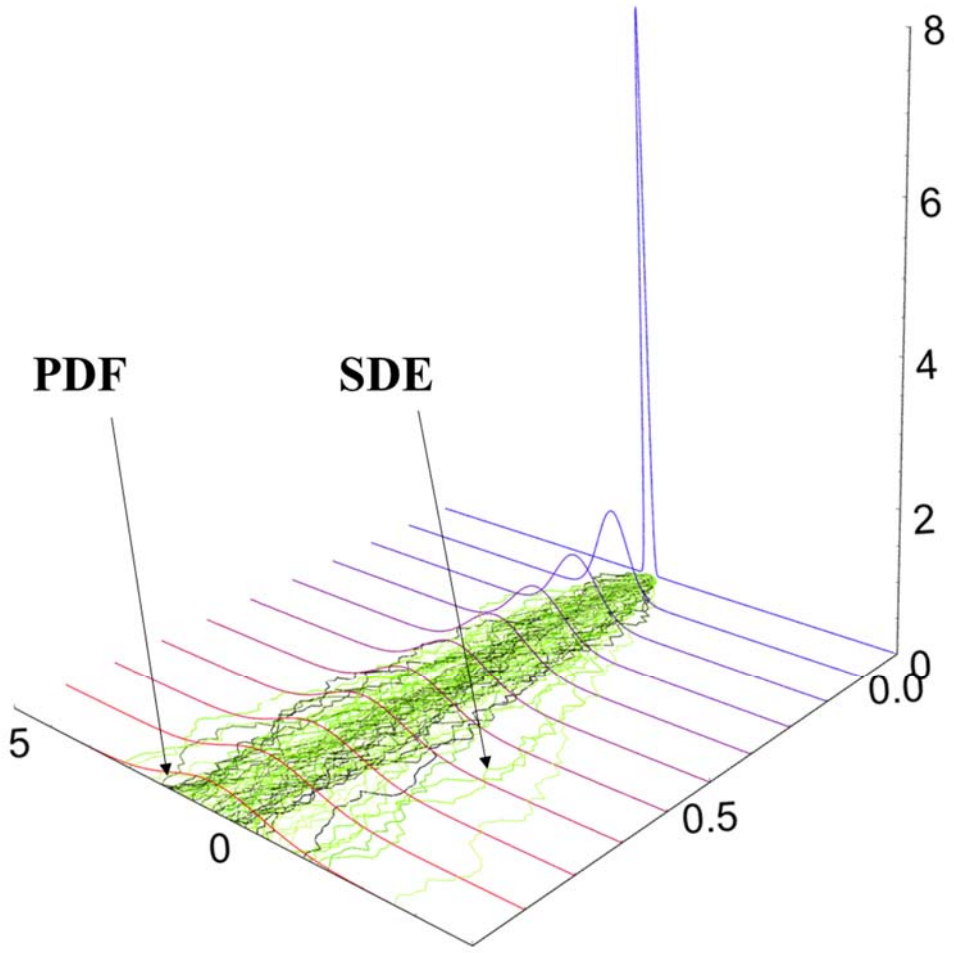

Figure 2-10 the stochastic processes of SDE and PDF

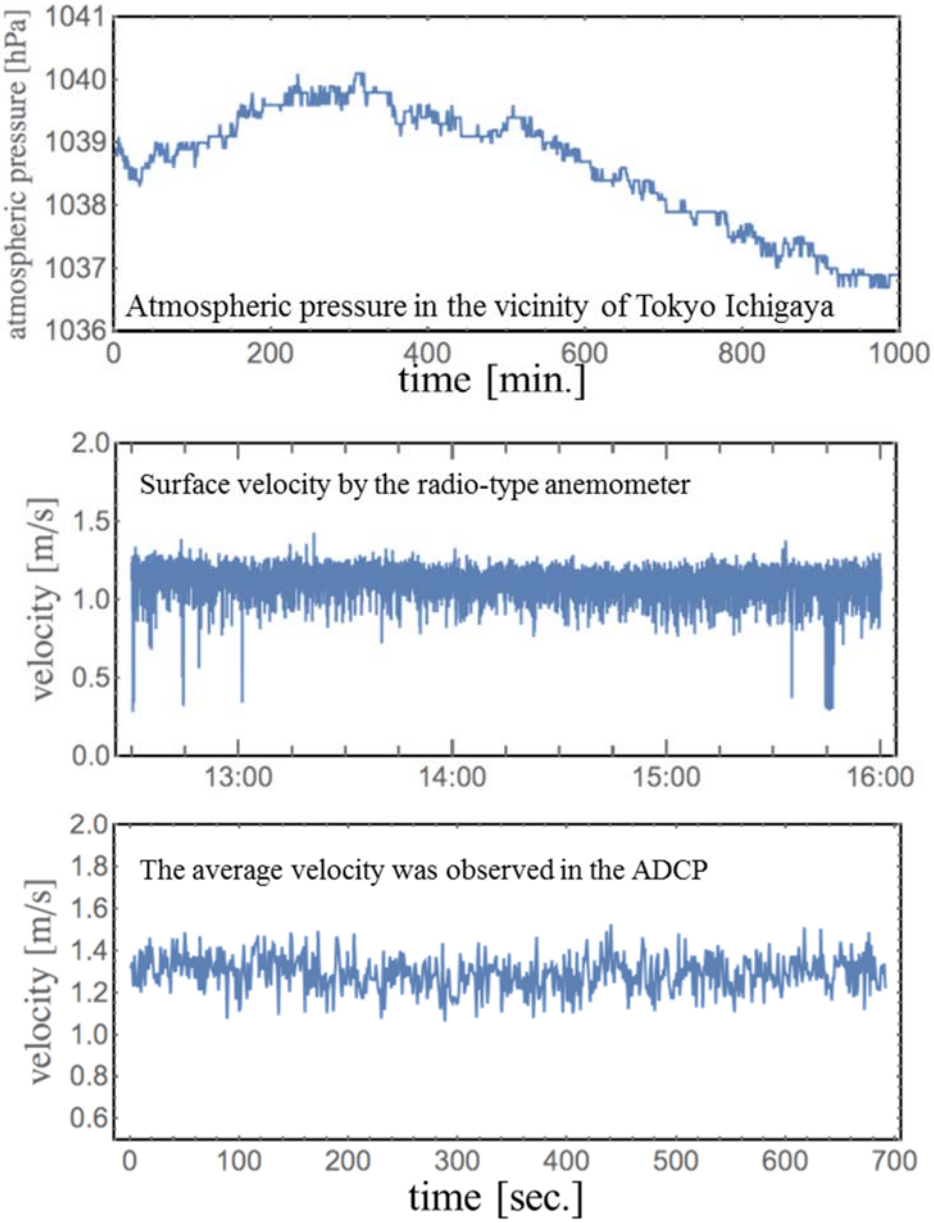

Figure 2-11 the observation data of hydrology

2.4 Uncertainty of water level based on stochastic process theory

According to the above section 2.2 and 2.3 sections, herein the uncertainty of water level will base on the relation between the runoff heights of stochastic differential equation and the mathematic equation of Fokker-Planck to obtain the uncertainty of rainfall and runoff. [19]

The input of rainfall intensity is $r(t) = \bar{r}(t) + r'(t)$, and it shows the mean value $\bar{r}(t)$ of rainfall with dispersion $r'(t)$. After difference, Eq. 2-8 can be written to give a new equation like Eq. 2-10.

$$dq_* = a_0 q_*^{\beta}(\bar{r} - q_*)dt + a_0 q_*^{\beta} r' dt \qquad \text{Eq.2-10}$$

Here the $r'(t)dt$ is assumed to the $\sigma\sqrt{T_L}dw$. Here dw is the microtime amount of change according to normal distribution $N\left(0, \sqrt{dt}\right)$ that is based on Wiener process. It shows that the uncertainty of rainfall is the normal distribution. $\sigma\sqrt{T_L}dw$ is used from the diffusion theory of G.I. Taylor, σ is the standard deviation of rainfall time series, and T_L is time constant. The Eq. 2-10 can be rewritten like Eq. 2-11.

$$dq_* = a_0 q_*^{\beta}(\bar{r} - q_*)dt + a_0 q_*^{\beta} \sigma\sqrt{T_L}dw \qquad \text{Eq.2-11}$$

The first term of right side (Eq. 2-11) is determinate and the second term is stochastic. In addition, Fokker-Planck equation is known to describe the development at the time of the existence density function of the specimen with the phenomena with the probability differential equation. For an Ito process driven by the standard Wiener process and described by the SDE (Eq. 2-12):

$$dx = y(x,t)dt + z(x,t)dw \qquad \text{Eq.2-12}$$

With drift $y(x,t) = a_0 q_*^{\beta}(\bar{r} - q_*)$ and diffusion coefficient $z(x,t) = a_0 q_*^{\beta}\sigma\sqrt{T_L}$, the Fokker-Planck equation, Eq. 2-13, for the probability density p of the random variable is as the Eq. 2-14.

$$\frac{\partial p(x,t)}{\partial t} = -\frac{\partial y(x,t)p(x,t)}{\partial x} + \frac{1}{2}\frac{\partial^2[z(x,t)]^2 p(x,t)}{\partial x^2} \qquad \text{Eq. 2-13}$$

$$\frac{\partial p(q_*(t),t)}{\partial t} = -\frac{\partial a_0 q_*^{\beta}(\bar{r} - q_*)p(q_*(t),t)}{\partial q} + \frac{1}{2}\frac{\partial^2\left[a_0 q_*^{\beta} r'(t)\right]^2 p(q_*(t),t)}{\partial q_*^2} \qquad \text{Eq. 2-14}$$

Eq. 2-14 is the probability distribution of runoff height with time by Fokker-Planck equation. Then, if the constant is assumed, the Eq. 2-14 can be written to Eq. 2-15 with the analytical solution of probability distribution of runoff height.

$$P(q_*) = P_0 \frac{1}{\left(a_0 q_*^{\beta}\sigma\sqrt{T_L}\right)^2} exp\left[\frac{2}{a_0\sigma^2\sqrt{T_L}}\left(\bar{r}\frac{q_*^{1-\beta}}{1-\beta} - \frac{q_*^{2-\beta}}{2-\beta}\right)\right] \qquad \text{Eq. 2-15}$$

Here P_0 is an integration constant. It is a probability density function (PDF) about runoff height q_* of steady flow and it assumed Eq. 2-15 the basic expression equation. Figure 2-14 shows the result of the probability density function.

Also the PDF of discharge and water level could be transformed as follows description. First a stochastic variable *X* is assumed then the PDF would be transferred to $f_X(x)$. At the same time, the function of *X*, $Y = g(X)$, and the PDF of *Y*, $f_y(y)$, as following equation (Eq. 2-16).

$$f_y(y) = f_x(g^{-1}(y))\frac{dg^{-1}(y)}{dy} \qquad \text{Eq. 2-16}$$

In brief, the relation of runoff height and discharge, the relation of runoff height and water level or the relation of discharge and water level may be easy to transform to

the PDF with discharge and water level. For example, the relation equation of the watershed area A [km^2], runoff height of watershed q_* [mm/h] and the discharge on the concentration point of watershed Q [m^3/s] is as following equation.

$$\mathrm{Q} = \frac{1}{3.6} A q_* = g(q_*) \qquad \text{Eq. 2-17}$$

Then Eq. 2-16 may be transformed as Eq. 2-18. From the PDF of runoff height to the PDF of discharge, the equation can be shown as Eq. 2-19 and its' deformation Eq. 2-20. Finally, the Eq. 2-21 is the probability density function of the water level.

$$P_Q(Q) = P_{q_*}(g^{-1}(Q)) \frac{dg^{-1}(Q)}{dQ} \qquad \text{Eq. 2-18}$$

$$h = CQ^{\frac{3}{5}} = g(Q), \quad C = \left(B \frac{1}{n} \sqrt{i}\right)^{-\frac{3}{5}} \qquad \text{Eq. 2-19}$$

$$p_h(h) = P_Q(g^{-1}(h)) \frac{dg^{-1}(h)}{dh} \qquad \text{Eq. 2-20}$$

$$p_h(h) = P_Q((\frac{h}{C})^{\frac{5}{3}}) \frac{5}{3} C^{-\frac{3}{5}} h^{\frac{2}{3}} \qquad \text{Eq. 2-21}$$

Here B is the width of river channel [m], n is the roughness coefficient of the river and i is the grade of the river. However, the width B, the roughness coefficient n and the grade I may affect the calculation results because of the scale of watersheds. Kura, Yamada et al. proposed that when the area of the watershed is 100 ~ 200 km^2, the effect may be ignored. Figure 2-13 is the probability distribution of the discharge by Eq. 2-18 and Figure 2-14 is the probability distribution of the water level by transforming equation, Eq. 2-21.

r=50 *mm/h*; *t*=6 *h* (rainfall duration)

ks=0.02 *cms*; *L*=30000 *mm*; m=4 ; i=15°

D=200 *mm* ;*w*=0.42

A=100 km^2; σ =4 *mm/h*

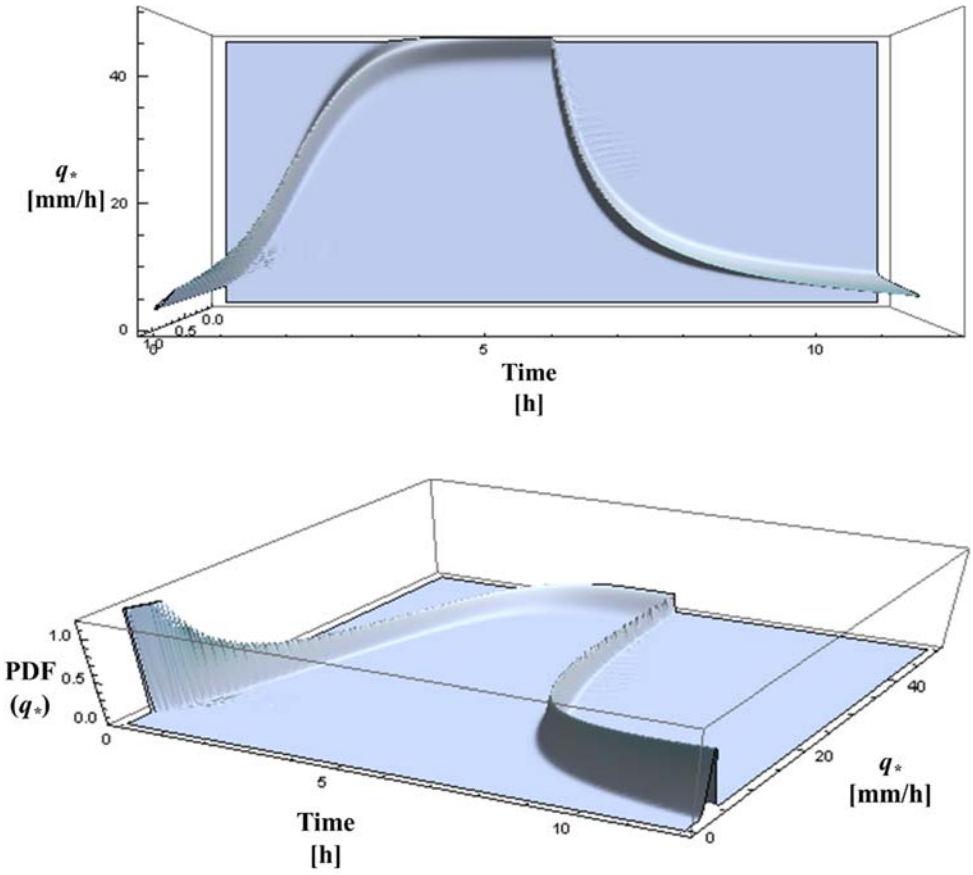

Figure 2-12 Probability distribution of water level from uncertainty rainfall

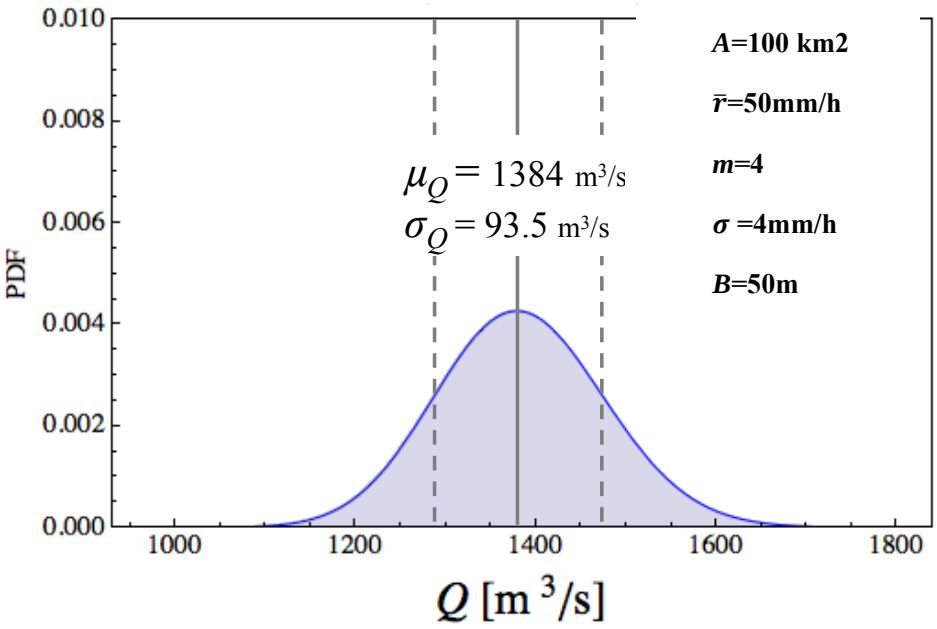

Figure 2-13 Probability distribution of the discharge from uncertainty rainfall

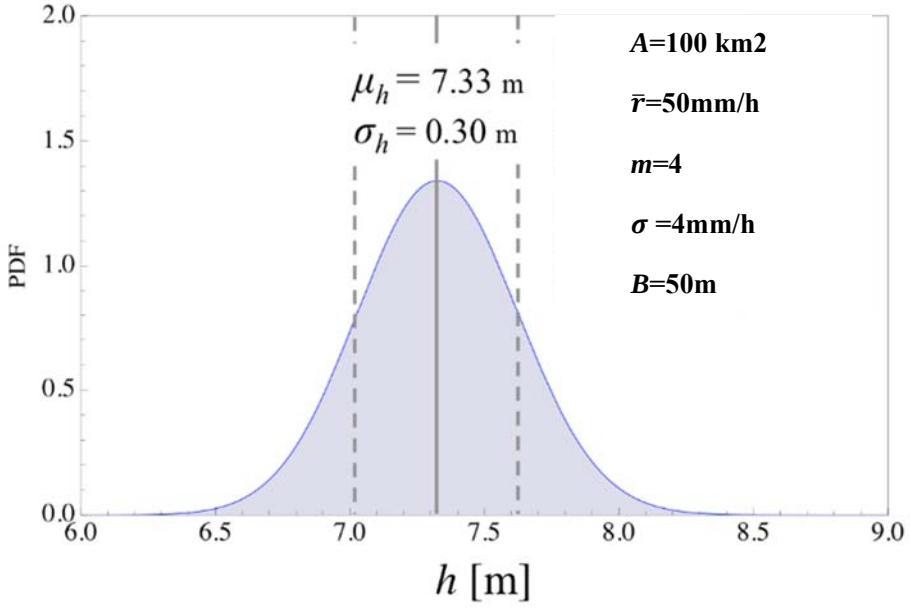

Figure 2-14 Probability distribution of the water level from uncertainty rainfall

Reference

[1] Shuichi KURE, Tadashi YAMADA: A STUDY ON THE EFFECTS OF SLOPE AND RIVER IN RUNOFF, Annual Journal of Hydraulic Engineering, JSCE, Vol.50, pp.337-342, 2006.

[2] Tadashi YAMADA, (2003). "STUDIES ON NONLINEAR RUNOFF IN MOUNTAINOUS BASINS", Annual Journal of Hydraulic Engineering, JSCE, Vol.47, pp.259-264, 2003.

[3] Koichi Shimura, Noriaki Ohara, Hiroshi Matsuki, Tadashi Yamada, (2001). "Studies on Runoff Characteristics of the Large-scale Channel Network Using a Physically Based Model" J. Japan Soc. Hydrol. & Water Rescor. Vo. 14, No. 3, pp. 217-288.

[4] SUZUKI, Masakazu, (1984). "The properties of a base-flow recession on small mountainous watersheds (I) Numerical analysis using the saturated unsaturated flow model" J. Jap. For. Soc. 66, pp. 174-182.

[5] SUZUKI, Masakazu, (1984). "The properties of a base-flow recession on small mountainous watersheds (II) Influence of evapotranspiration on recession hydrographs" J. Jap. For. Soc. 66, pp. 211-218.

[6] KUBOTA, Jumpei, FUKUSHIMA, Yoshihiro, SUZUKI, Masakazu, (1988) "Observation and modeling of the runoff process on a hillslope (H) Water budget and location of the groundwater table and its rising" J. Jpn. For. Soc. 70, pp. 381-389.

[7] Yamada Tadashi et.al. (1996), "Observation of The Raindrop Size Distribution with a Newly-Developed Laser Raindrop Gauge", Proceedings of JSCE Vol.539, pp.15-30 [in Japanese]

[8] Durga Lal SHRESTHA, 2009. "Uncertainty Analysis in Rainfall-Runoff Modelling: Application of Machine Learning Techniques" Doctorates thesis.

[9] Brian J Ford. (1996), "Confirming Robert Brown's Observations of Brownian Movement." Confirming Robert Brown's Observations of Brownian Movement, Proceedings of the Royal Microscopical Society, 31 (4): 316-321, 1996.

[10] Princeton University Press. (1989), "The Collected Papers of: Albert Einstein, Volume 2, The Swiss Years: Writings, 1900-1909"

[11] Norbert Wiener. (1921), “The Average of an Analytic Functional and the Brownian Movement”, Proceedings of the National Academy of Sciences of the United States of America, Vol. 7, No. 10, pp. 294-298.

[12] Kiyosi Itô (1944). “Stochastic Integral”. Proc. Imp. Acad. Volume 20, Number 8 (1944), 519-524.

[13] Kiyosi Itô (1951). “On stochastic differential equations”. Memoirs, American Mathematical Society 4, 1–51

[14] Liouville, J. (1838). “Note sur la Théorie de la Variation des constantes arbitraries”. Journal de mathématiques pures et appliquées 1re série, tome 3, p. 342-349.

[15] Harris, Stewart. (1971). “An introduction to the theory of the Boltzmann equation.” Dover Books. p. 221.

[16] Smoluchowski, M. (1906), "Zur kinetischen Theorie der Brownschen Molekularbewegung und der Suspensionen", Annalen der Physik 21 (14): 756–780,

[17] A. D. Fokker. (1914), “Die mittlere Energie rotierender elektrischer Dipole im Strahlungsfeld “. Ann d. Physik 43: 810-820.

[18] M. Planck. (1917), “Über einen Satz der Statistischen Dynamik und seine Erweiterung in der Quantentheorie”. Sitzung der physikalisch-mathematischen Klasse vom.

[19] Kazuhiro YOSHIMI, Tadashi YAMADA and Tomohito J. YAMADA, (2015). “Assessment of Uncertainty in Rainfall-runoff Analysis Incorporating Stochastic Differential Equation”, Annual Journal of Hydraulic Engineering, JSCE, Vol.59, pp.259-264, 2015.

CHAPTER 3 STABILITY ANALYSIS OF LEVEE

The types of levee failure can be classified to infiltration failure, erosion failure and overflow/overtopping failure because of the increasing water level during rainfall. In the chapter, the infiltration failure will be discussed by the slope stability method. In general, the analysis method of slope stability categorized into circle slide method and infinite slope method. The safety factor of slope is defined as the ratio of the shear strength divided by the shear stress required for equilibrium slope:

$$FS = \frac{shear\ strength}{shear\ stress\ required\ for\ equilibrium}$$

The factor of safety (FS) is an overall measure of the amount by which the strength of the soil would have to fall short of the values described by cohesion and friction angle in order for the slope to fail. This strength –related definition of FS is well suited for practical purposes because soil strength is usually parameter that is most difficult to evaluate. [1]

Furthermore, the slip side of the levee usually occurs opposite side with the riverside like Figure 3-1. That's because the effect of the hydrostatic pressure of the water level. It means the levee side close to the river is not easy to slip with the "protection" from the water pressure. It's like the tofu under the water, besides the buoyancy effect of the water, the confining pressure also protects the tofu keep the shape completely. However, it will easily fail because of the levee toe scouring.

Therefore, in the thesis, the infiltration failure is calculated on the opposite site of the levee with the riverside.

The following sections will introduce the slope stability and stability in considering with uncertainty of soil parameters. The following sections will first introduce analytical methods with circular slip method. Second is the uncertainty of the soil parameters, and final is the probability of the levee failure.

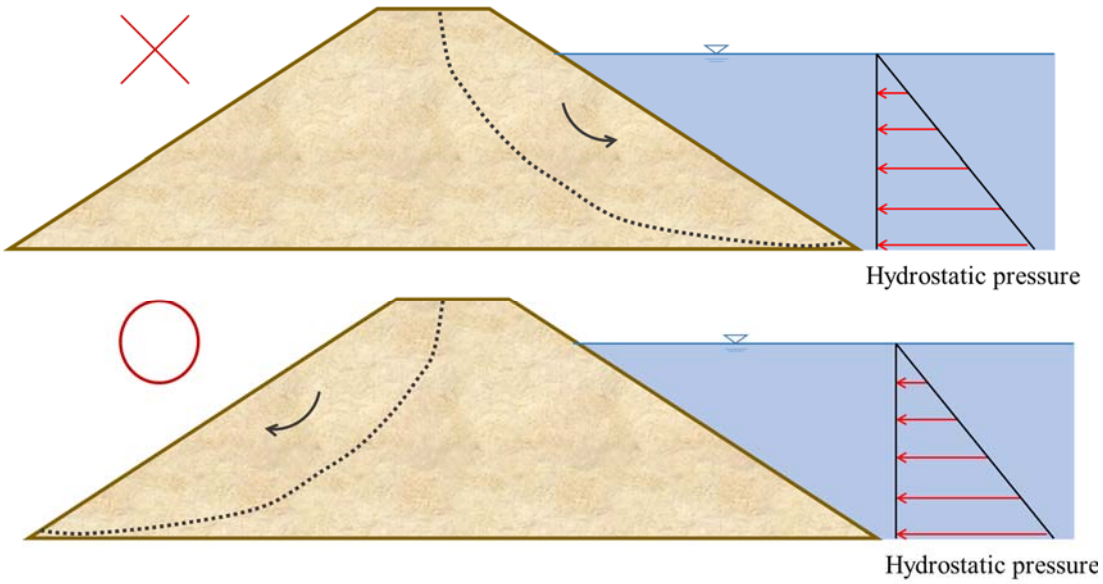

Figure 3-1 the failure occurrence side of the levee

3.1 Slope stability method

Most stability analyses of slopes have been made by assumption that the curve of potential sliding is an arc of a circle. Slip circle method of circular failure analysis uses the theory of limit equilibrium. This method is used to investigate the equilibrium of a soil mass tending to move down the slope under influence of gravity. The trial slip circle is drawn and the material above the assumed slip surface is divided into a number of vertical slices (as shown in Figure 3-2). In the ordinary slip circle the forces between slices are neglected and each slice is assumed to act independently as a column of soil of unit thickness and width. The weight of each slice is assumed to act at its center. The factor of safety is assumed to be the same at all points along the slip surface. The surface with the minimum factor of safety is termed the critical slip surface. Such a critical surface and the corresponding minimum factor of safety represent the most likely sliding surface.

All limit equilibrium methods assume that the shear strengths of the materials along the potential failure surface are governed by linear (Mohr-Coulomb) or non-linear relationships between shear strength and the normal stress on the failure surface. The most commonly used variation is Terzaghi's theory of shear strength which states that

$$\tau = \sigma' \tan\emptyset' + c' \qquad \text{Eq. 3-1}$$

Where τ is the shear strength of the interface, $\sigma' = \sigma - u$ is the effective stress (σ is the total stress normal to the interface and u is the pore water pressure on the interface), $\emptyset'$ is the effective friction angle, and c' is the effective cohesion. The methods of slices are the most popular limit equilibrium technique. In this approach, the soil mass is discretized into vertical slices. Several versions of the method are in use. These variations can produce different results (factor of safety) because of different assumptions and inter-slice boundary conditions. [2]

However, the various methods of limit equilibrium analysis use different assumptions to make up the balance between equations and unknowns. The characteristics of various practically used methods with regard to the conditions of equilibrium that they satisfy and they are summarized in Table 3-1. There are five common methods as followings:

1. Ordinary method of slices (Fellenius, 1927)

Applicable to non-homogeneous slopes and c-ø soils where slip surface can be approximated by a circle. Very convenient for calculations.

2. Bishop's Modified Method (Bishop, 1955)

Applicable to non-homogeneous slopes and c-ø soils where slip surface can be approximated by a circle. More accurate than Ordinary Method of slices, especially for analyses with high pore water pressures.

3. Janbu's Generalized Procedure of Slices (Janbu, 1968)

Applicable to non-circular slip surfaces. Also for shallow, long planar failure surfaces that are not parallel to the ground surface.

4. Morgenstern & Price's Method (Morgenstern & Price's, 1965)

An accurate procedure applicable to virtually all slope geometries and soil profiles. Rigorous, well established complete equilibrium procedure.

5. Spencer's Method (Spencer, 1967)

An accurate procedure applicable to virtually all slope geometries and soil profiles. The simplest complete equilibrium procedure for computing factor of safety.

In japan, the method most commonly used is the Ordinary method of slices (Fellenius, 1927), and second is Bishop's Modified Method (Bishop, 1955). However, the pore water pressure in Fellenius method are treated as acting perpendicular to the sliding surface. When the slip surface gradient becomes large, the pore water pressure will be excessively calculated. In order to solve the such problem, the Modified Fellenius method has be suggested. In the thesis, the used main method is the Modified Fellenius method like Eq. 3-2.

$$FS = \frac{\sum[c' \cdot l + (W - u \cdot b)cos\alpha \cdot tan\emptyset']}{\sum W \cdot sin\alpha} \quad \text{Eq. 3-2}$$

Here *FS* is the safety factor of slope stability, *c*' is cohesion [kN/m^2], $\emptyset'$ is friction angle of soil [^{o}], *l* is the length of the slice [m], *W* is the weight of the slice [kN/m], *u* is the pore water pressure [kN/m^2] and α is the inclination of the slip surface within the slice to the horizontal plane [^{o}].

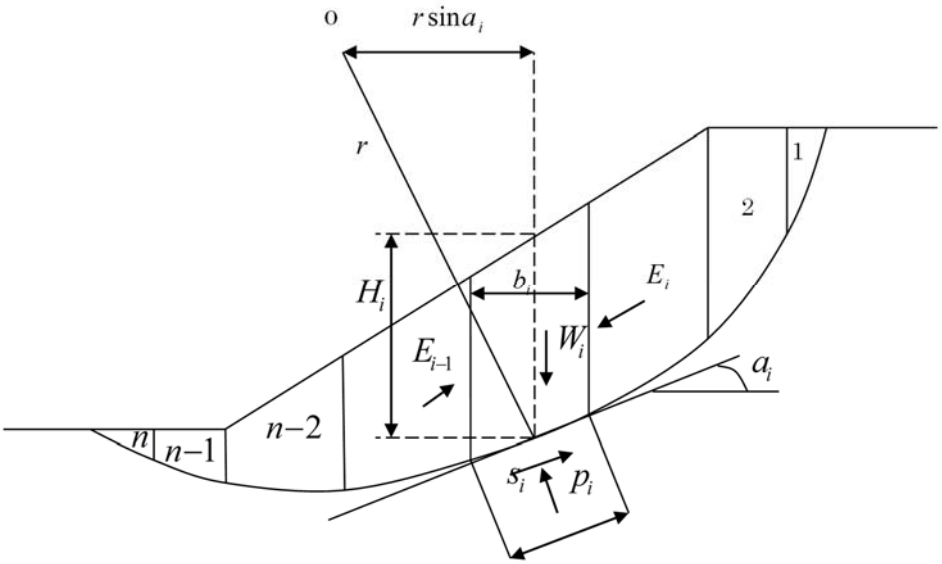

Figure 3-2 Division of potential sliding mass into slices

Table 3-1 characteristics of commonly used methods of limit equilibrium analysis for slope stability

Method	Equilibrium conditions satisfied	Slip surface
Ordinary Method of Slices (Fellenius, 1927)	Moment equilibrium about center of circle	Circular slip surface
Bishop's Modified Method (Bishop, 1955)	Vertical equilibrium and overall moment equilibrium	Circular
Janbu's Generalized Procedure of Slices (Janbu, 1968)	Force equilibrium (vertical and horizontal)	Any shape
Morgenstern & Price's Method (Morgenstern & Price's, 1965)	All conditions of equilibrium	Any shape
Spencer's Method (Spencer, 1967)	All conditions of equilibrium	Any shape

3.2 Infiltration

Failure of soil slopes, both natural and man-made, during or shortly after rainfall is a commonly occurring phenomena. It means that water is the most important factor in most of the slope stability analysis. Pore water in soil can strongly influence the physical interaction among soil grains. Changes in pore water pressure can directly affect the effective stresses, which in turn, affect both the shear strength and consolidation behavior of soil. Therefore, analysis of pore fluid seepage plays an important role in the solution of many geotechnical problems, especially those concerning the stability analysis of slopes and man-made structures.

Thus the know-how about the infiltration is very important for the stability analysis of levee. There are a lot of methods that can calculate the seepage face and can be can be categorized into experiments method, analytical method, numerical method, semi-theoretical method and so on. The following will introduce the Casagrande's method (1932, 1937) [3] and Uchida method [4], then propose a new method for the solution of seepage face.

1. Casagrande's method

The method is a very famous semi-theoretical formula in estimating the seepage face on levee by the basic parabola equation (as Eq.3-3) , like shown as Figure 3-3.

$$y = \sqrt{2y_0 x + y_o^2}$$
$$y_0 = \sqrt{d^2 + H^2} - d \qquad \text{Eq. 3-3}$$

2. Uchida method

The Uchida method is an approximate solution of seepage face. It is used commonly to estimate the time arriving the seepage face (as shown in Eq.3-4). Here h is the height of water inner levee[m], H is the water level[m], k is the permeability coefficient, Δt is the time of infiltration and λ is the void ratio of soil.

$$\frac{h(x,t)}{H} = 1 - \left\{ \frac{x/H}{\sqrt{8/3\lambda}\sqrt{k\Delta t/H}} \right\}^{\frac{3}{2}} \quad \text{Eq. 3-4}$$

3. A new method of practical solution for seepage face

A new method is proposed by using the group theoretic (Birkoff, 1950[5]). The conduction process is shown as Figure 3-4. By using the similarity transformation, the non-linear diffusion equation can transform to the non-linear ordinary differential equation. In order to get the analytical solution, the compatible functional form can be obtained. Finally, the new practical solution is established.

The Eq.3-5 is the Darcy's law and in considering the hydrostatic pressure, the basic equation of Eq. 3-6 is used to conduct to Eq. 3-7 and here k is the permeability coefficient [m/s], λ is the ratio of water content. The simple schematic diagram is shown as Figure 3-5,

$$u = -k\frac{\partial h}{\partial x} \quad \text{Eq. 3-5}$$

$$q = vh, \;\; \lambda\frac{\partial h}{\partial t} + \frac{\partial q}{\partial x} = 0 \quad \text{Eq. 3-6}$$

$$\frac{\partial h(x,t)}{\partial t} = k_0\frac{\partial}{\partial x}\left(h\frac{\partial h}{\partial x}\right), \quad k_0 = \frac{k_*}{\lambda}, \; k_* = k \times h_0 \quad \text{Eq. 3-7}$$

According to the Eq. 3-7, the following variables are assumed as Eq. 3-8. After substituting Eq. 3-8 to Eq. 3-7, it can re-write as Eq. 3-9 and Eq. 3-10.

$$\tilde{x} = a^{\alpha}x, \qquad \tilde{t} = a^{\beta}t, \qquad \tilde{h} = a^{r}h$$
$$x = a^{-\alpha}\tilde{x}, \qquad t = a^{-\beta}\tilde{t}, \qquad h = a^{-r}\tilde{h} \qquad \text{Eq. 3-8}$$

$$\frac{\partial h}{\partial t} = a^{\beta-r}\frac{\partial \tilde{h}}{\partial \tilde{t}}, \qquad k_0\frac{\partial}{\partial x}\left(h\frac{\partial h}{\partial x}\right) = a^{2\alpha-2r}k_0\frac{\partial}{\partial \tilde{x}}\left(\tilde{h}\frac{\partial \tilde{h}}{\partial \tilde{x}}\right) \qquad \text{Eq.3 -9}$$

$$\frac{\partial \tilde{h}}{\partial \tilde{t}} - a^{2\alpha-\beta-r}k_0\frac{\partial}{\partial \tilde{x}}\left(\tilde{h}\frac{\partial \tilde{h}}{\partial \tilde{x}}\right) = 0 \qquad \text{Eq. 3-10}$$

Because the group theoretic theory is expected to use, Eq. 3-10 is converted as like the format of Eq. 3-7 therefore Eq. 3-11 is assumed.

$$2\alpha - \beta - r = 0 \qquad \text{Eq. 3-11}$$

By using the Eq. 3-11, the same format equation between Eq. 3-10 and Eq. 3-7 is can observed and then Eq. 3-12 is established. Moreover $\eta = \eta(x,t)$, $g(x,t,h)$ are also considered as the same format as Eq. 3-8 like Eq. 3-13 and Eq. 3-14. Then these two equation can be conducted into Eq. 3-10, the similarity transformation is like Eq. 3-16. Finally, Eq. 3-16 is conducted into Eq. 3-7 like Eq. 3-17, Eq. 3-18 and Eq. 3-19.

$$\emptyset\left(x,t,h,\frac{\partial^k h}{\partial(x)^k},\ldots\frac{\partial^k h}{\partial(t)^k}\right) = \Phi\left(\eta,F,\frac{\partial F}{\partial(\eta)},\ldots\frac{\partial^k F}{\partial(\eta)^k}\right) = 0 \qquad \text{Eq. 3-12}$$

$$\eta = \eta(x,t), \quad F(\eta) = g(x,t,h)$$
$$\eta(x,t) = \eta(\tilde{x},\tilde{t}) = xt^{p} = \tilde{x}\tilde{t}^{p} \qquad \text{Eq. 3-13}$$

$$F(\eta) = (x,t,h) = ht^{q} = \tilde{h}\tilde{t}^{q}$$
$$\eta = xt^{p} = \tilde{x}\tilde{t}^{p} = a^{\alpha}xa^{\beta p}t^{p}$$
$$F(\eta) = ht^{q} = \tilde{h}\tilde{t}^{q} = a^{r}ha^{\beta q}t^{q} \qquad \text{Eq. 3-14}$$

$$p = -\frac{\alpha}{\beta}, \qquad q = -\frac{r}{\beta} \qquad \text{Eq. 3-15}$$

$$\eta = xt^{-\frac{\alpha}{\beta}}, \qquad F(\eta) = ht^{-\frac{r}{\beta}} \qquad \text{Eq. 3-16}$$

$$\frac{\partial h}{\partial t} = -\frac{\alpha}{\beta}\eta\frac{\partial F}{\partial \eta}t^{\frac{r-\beta}{\beta}} + \frac{r}{\beta}Ft^{\frac{r-\beta}{\beta}}, \qquad \frac{\partial}{\partial x}\left(h\frac{\partial h}{\partial x}\right) = t^{\frac{2r-2\alpha}{\beta}}F\frac{\partial^2 F}{\partial \eta^2} \qquad \text{Eq. 3-17}$$

$$-\frac{\alpha}{\beta}\eta\frac{\partial F}{\partial \eta} + \frac{r}{\beta}F = t^{\frac{r-2\alpha+\beta}{\beta}}k_0 F\frac{\partial^2 F}{\partial \eta^2} \qquad \text{Eq. 3-18}$$

$$-\frac{\alpha}{\beta}\eta\frac{\partial F}{\partial \eta} + \frac{r}{\beta}F = k_0 F\frac{\partial^2 F}{\partial \eta^2} \qquad \text{Eq. 3-19}$$

The followings are the initial conditions and boundary conditions for Eq. 3-6.

$I.Cs.\ :\ \ h(x,0) = 0$

$B.Cs.\ :\ \ h(0,t) = 1,\ \ h(\infty,t) \to 0$

By using the similarity transformation, the initial and boundary conditions will be like the followings and the Eq. 3-19 will like Eq. 3-20.

$r = 0, \frac{\alpha}{\beta} = \frac{1}{2}$

$h(0,t) = 1 \Rightarrow x = 0 \Rightarrow \eta = 0 \Rightarrow F(0) = 1 \times t^{-\frac{r}{\beta}}$

$h(\infty,t) \to 0 \Rightarrow x = \infty \Rightarrow F(\infty) = 0$

$$-\frac{1}{2}\eta F'(\eta) = k_0 F(\eta)F''(\eta) \qquad \text{Eq. 3-20}$$

In order to delete k_0, the Eq.3-20 can be transferred like Eq. 3-21. Finally, the non-linear ordinary difference equation can get. It is not the exact solution, therefore the analytical solution is used to solve by function form like Eq. 3-22 (Figure 3-6 show the relation between $F(\eta)$ and η).

$$\eta(x,t) = xt^{-\frac{1}{2}} = \frac{x}{\sqrt{t}} \quad \Rightarrow \quad \eta(x,t) = \frac{1}{\sqrt{4k_0}}\frac{x}{\sqrt{t}} = \frac{x}{\sqrt{4k_0 t}}$$

$$F''(\eta) = -\frac{\eta F'(\eta)}{2k_0 F(\eta)} \qquad F''(\eta) = -\frac{2\eta F'(\eta)}{F(\eta)} \qquad \text{Eq. 3-21}$$

$$F(\eta) = \exp[-0.86\frac{\eta}{\sqrt{0.81-\eta}}] \qquad \text{Eq. 3-22}$$

Figure 3-7 is the comparison between numerical solution (Eq. 3-10) and practical solution (Eq. 3-38). It shows that the two solutions are approximate, however the independent variable of practical solution is less than numerical solution. In practice, practical solution is more convenient to use.

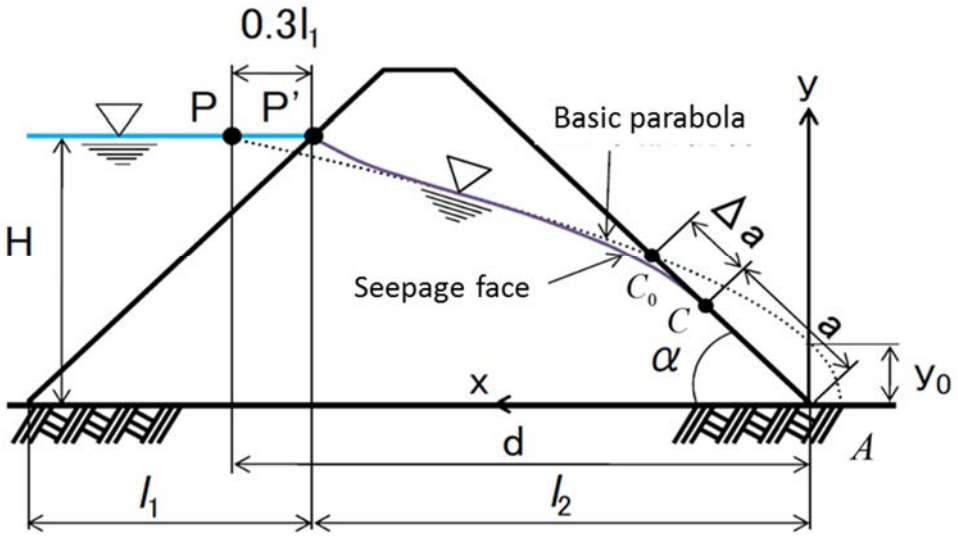

Figure 3-3 Casagrande's method

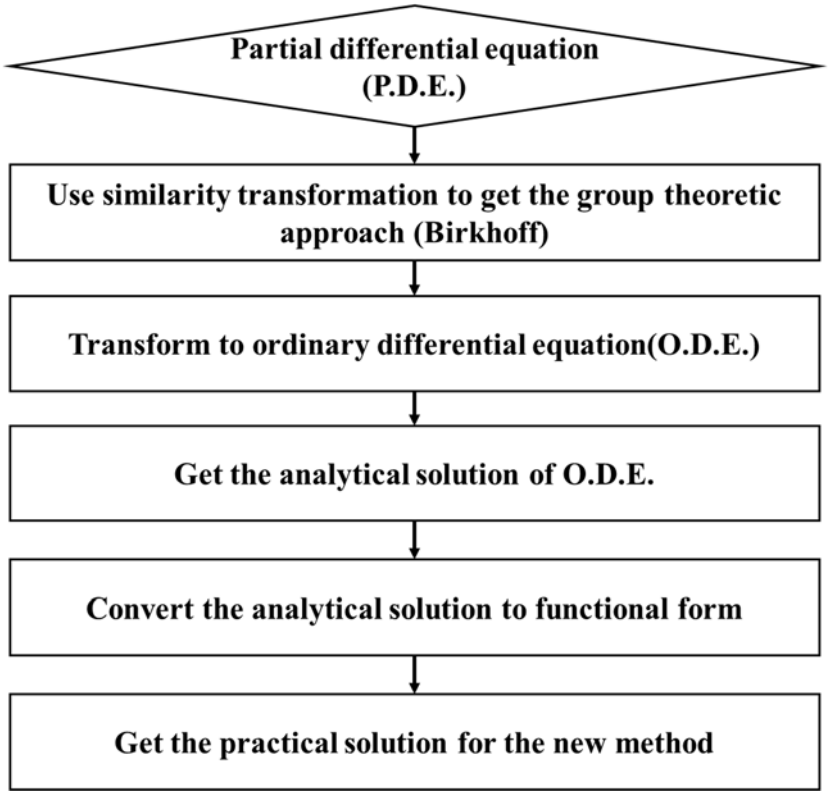

Figure 3-4 The conduction process of the practical solution

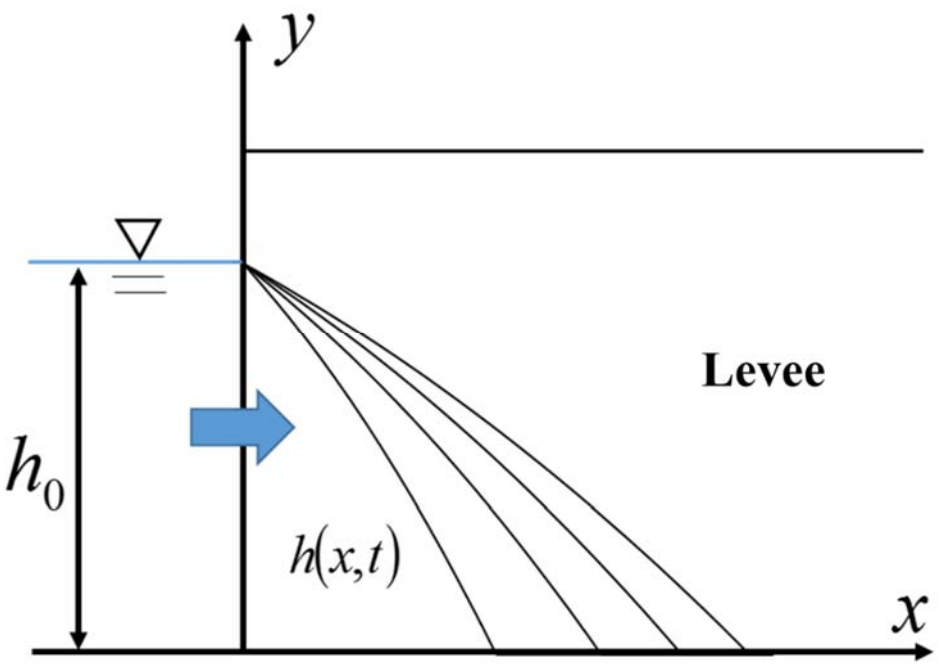

Figure 3-5 the schematic diagram of infiltration process

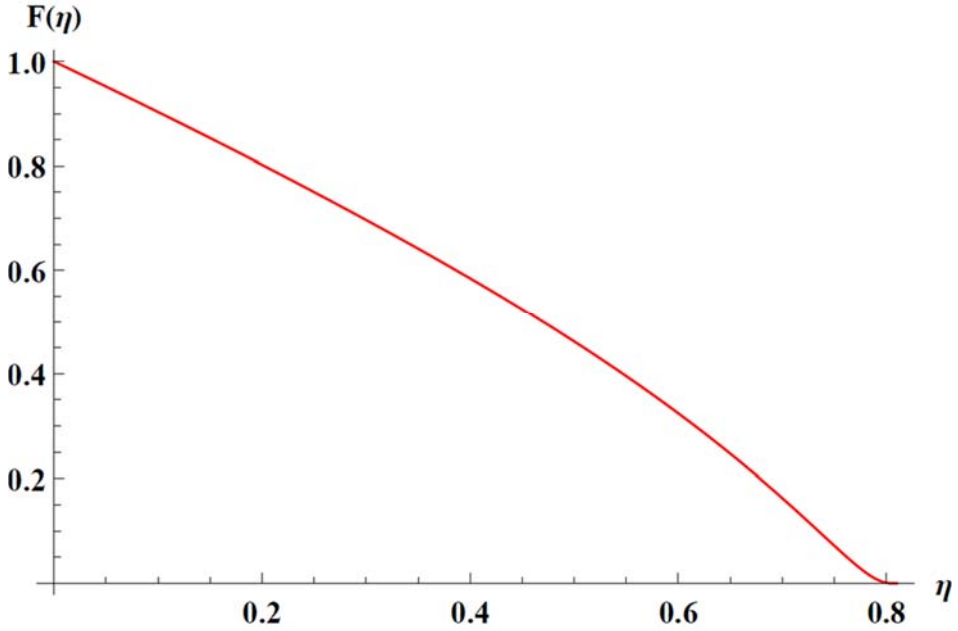

Figure 3-6 the relation between $F(\eta)$ and η

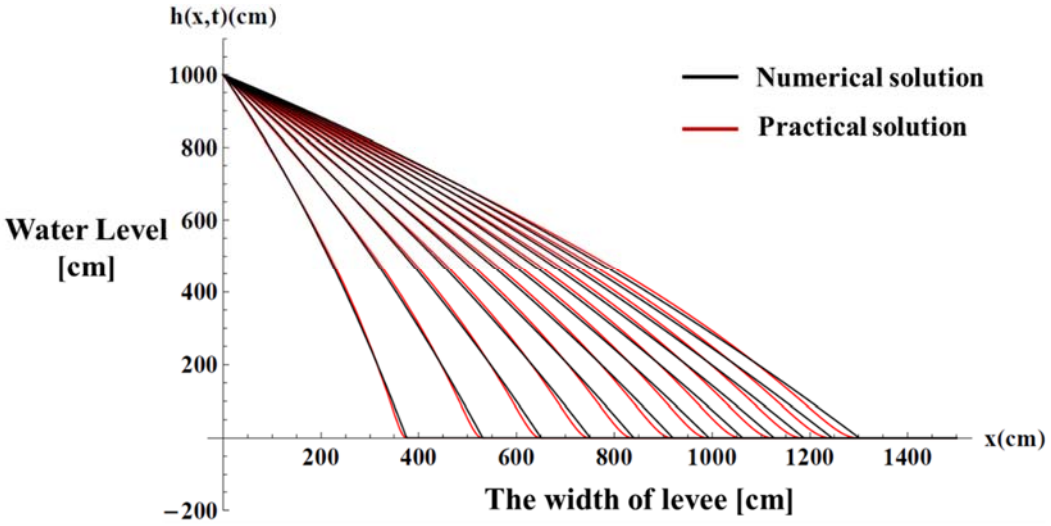

Figure 3-7 the comparison between numerical solution and practical solution

3.3 Uncertainty of soil parameters

Soils are geological materials formed by weathering, erosion and sedimentation processes and so on. They have been subjected to various stresses, pore fluids, and physical and chemical changes. Thus, it is hard to decide by experiments with some specific boring sites. In other words, the uncertainty of soil parameters comes both from the spatial variability and from errors in testing.

3.3.1 Uncertainty source of soil parameters

Uncertainty in soil parameters can be categorized into natural inherent variability (aleatory) and knowledge uncertainty (epistemic) as shown in Figure 3-7. Aleatory uncertainty consists of physical uncertainty with temporal and spatial. It is also known as inherent uncertainty and intrinsic uncertainty and is a natural randomness of a quantity such as the variable in the soil strength from point to point within a soil volume. Epistemic uncertainty consists of characterization uncertainty, model uncertainty, transformation uncertainty, which can be related to incomplete knowledge. [6][7]

In practice, the decision process of soil parameters is like Figure 3-8. The real ground or soil structures are very complex, therefore before design or calculation the ground or soil structures should be simplified by the engineering judgement. According to the idealized ground/ soil structures, the soil sample will be test and get the soil parameters. Finally, the design and construction will according these data. In other words, the soil parameters are through some idealized and simplified process to decide. Furthermore, for the deviation of soil parameters, besides the inhomogeneous environment and water effective, the technology of test is also existing some problems. the problems may be the sample types, sampling technology, operation technology by tester, test methods and so on. [8] Different values of coefficient of variation for

geotechnical properties are summarized in Table 3-2 to provide an overview of the variability of soil parameters. [9]

3.3.2 Correlation of soil parameters

A correlation coefficient is a coefficient that illustrates a quantitative measure of some type of correlation and dependence, meaning statistical relationships between two or more random variables or observed data values.

Pearson's correlation coefficient when applied to a sample is commonly represented by the letter *r* and may be referred to as the sample correlation coefficient or the sample Pearson correlation coefficient. We can obtain a formula for *r* by substituting estimates of the covariance and variances based on a sample into the formula above. So if we have one dataset $\{x_1,...,x_n\}$ containing n values and another dataset $\{y_1,...,y_n\}$ containing *n* values then that formula for *r* is:

$$r = \frac{\sum_{i=1}^{n}(x_i - \bar{x})(y_i - \bar{y})}{\sqrt{\sum_{i=1}^{n}(x_i - \bar{x})^2}\sqrt{\sum_{i=1}^{n}(y_i - \bar{y})^2}} \qquad \text{Eq. 3-23}$$

Where, *n*, x_i, y_i are defined as above, $\bar{x} = \frac{1}{n}\sum_{i=1}^{n} x_i$ (the sample mean); and analogously for $\bar{y}$.

In considering the evaluation method of slope stability, the safety of slope is the relationship between resistance force and driving force. The most important soil parameters are cohesion *c'* and friction angle ϕ '. Moreover, correlation between cohesion *c'* and friction angle ϕ ' may affect the probability distribution of slope stability.

A correlation coefficient is a coefficient that illustrates a quantitative measure of some type of correlation and dependence, meaning statistical relationships between two or more random variables or observed data values. In statistics, the Pearson product-

moment correlation coefficient is the common measure of the linear correlation between two variables X and Y, giving a value between +1 and -1 inclusive, where 1 is total positive correlation, 0 is no correlation, and -1 is total negative correlation (as shown in Figure 3-9 and Figure 3-10). It is widely used in the sciences as a measure of the degree of linear dependence between two variables. [10]

According to the result of soil test in "Geotechnology-With the idea of the reliability design and reality", the correlation between cohesion *c'* and friction angle ϕ ' is shown as Figure 3-11. Moreover, according to the laboratory tests on a wide variety of soils [8], the correlation between cohesion *c'* and friction angle ϕ ' are often negatively correlated with correlation coefficient ranges from -0.72 to 0.35 and Figure 3-12 shows another result. [11]

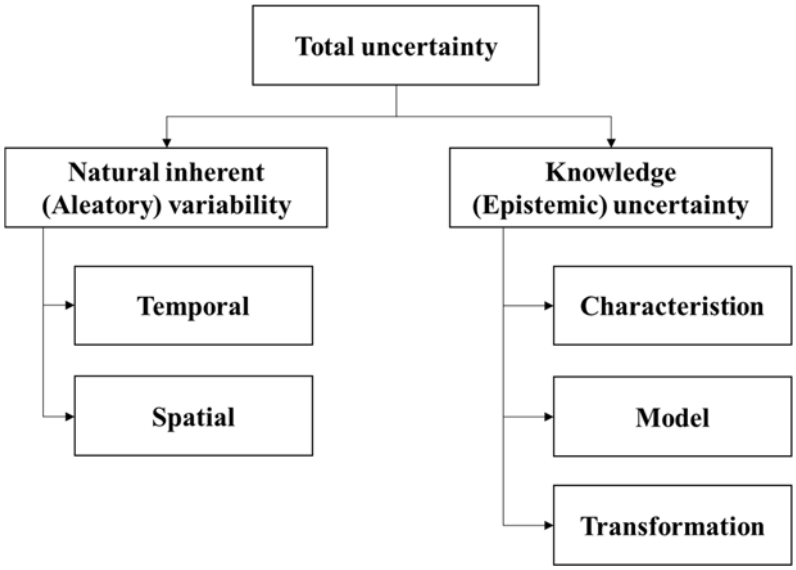

Figure 3-8 Main components contributing to the total uncertainty in the determination of a geotechnical property [6]

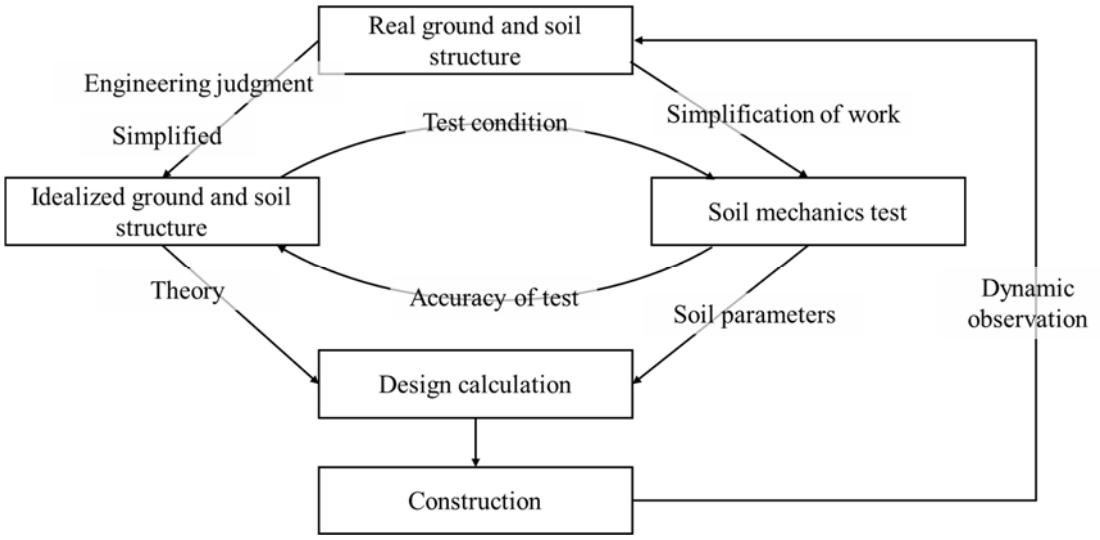

Figure 3-9 the uncertainty of soil parameters [8]

Table 3-2 Values of coefficient of variation for geotechnical properties [9]

Property or in situ test result	Coefficient of variation	Source
Unit weight (γ)	3–7%	Harr (1984), Kulhawy (1992)
Buoyant unit weight (γ_b)	0–10%	Lacasse and Nadim (1997), Duncan (2000)
Effective stress friction angle (ϕ ')	2–13%	Harr (1984), Kulhawy (1992)
Undrained shear strength (*Su*)	13–40%	Harr (1984), Kulhawy (1992), Lacasse and Nadim (1997), Duncan (2000)
Undrained strength ratio (Su / σ_v')	5–15%	Lacasse and Nadim (1997), Duncan (2000)
Compression index (*Cc*)	10–37%	Harr (1984), Kulhawy (1992), Duncan (2000)
Reconsolidation pressure (p_p)	10–35%	Harr (1984), Lacasse and Nadim (1997), Duncan (2000)
Coefficient of permeability of saturated clay (*k*)	68–90%	Harr (1984), Duncan (2000)
Coefficient of permeability of partly saturated clay (*k*)	130–240%	Harr (1984), Benson et al. (1999)
Coefficient of consolidation (c_v)	33–68%	Duncan (2000)
Standard penetration test blow count (*N*)	15–45%	Harr (1984), Kulhawy (1992)
Electric cone penetration test (q_c)	5–15%	Kulhawy (1992)
Mechanical cone penetration test (*qc*)	15–37%	Harr (1984), Kulhawy (1992)
Dilatometer test tip resistance (q_{DMT})	5–15%	Kulhawy (1992)
Vane shear test undrained strength (S_v)	10–20%	Kulhawy (1992)

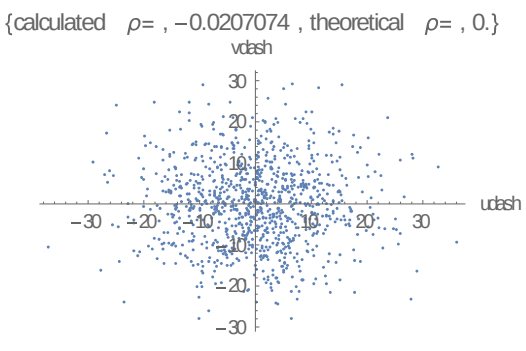

correlation coefficient =0

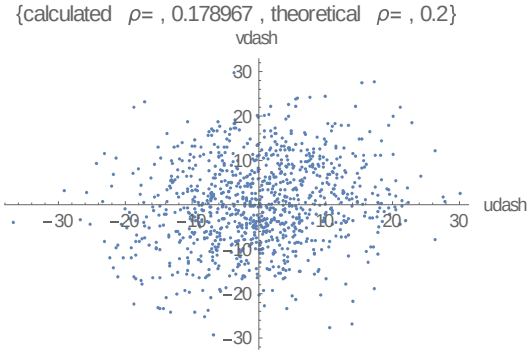

correlation coefficient= 0.2

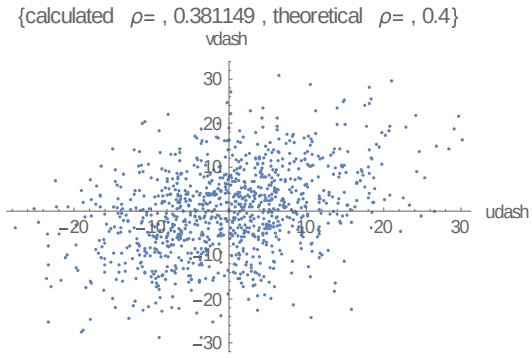

correlation coefficient =0.4

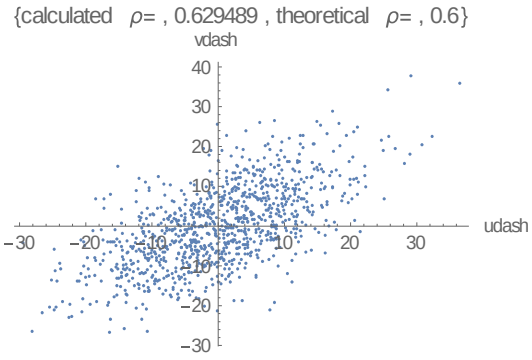

correlation coefficient 0.

6

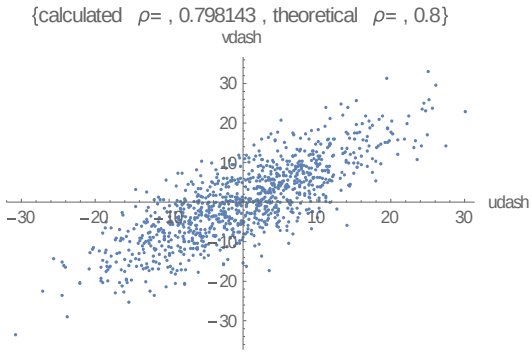

correlation coefficient =0.8

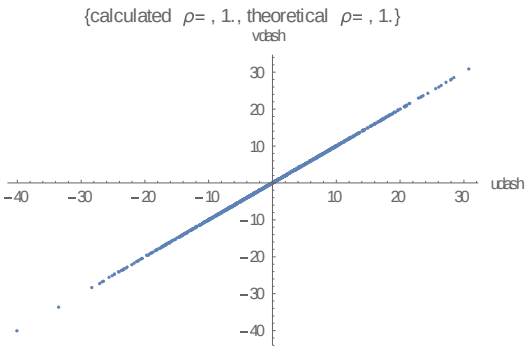

correlation coefficient 1.0

Figure 3-10 Scatter diagrams with different values of correlation coefficient(0 ~ 1)

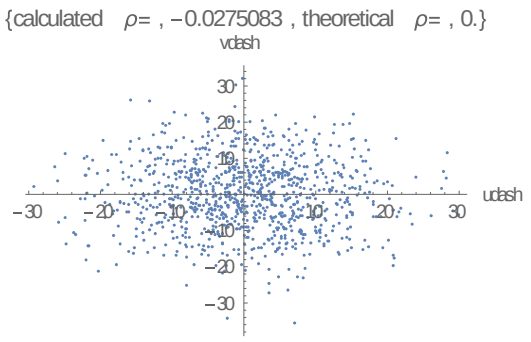

correlation coefficient =0

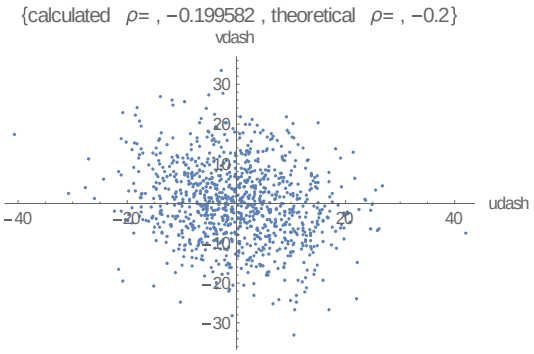

correlation coefficient =-0.2

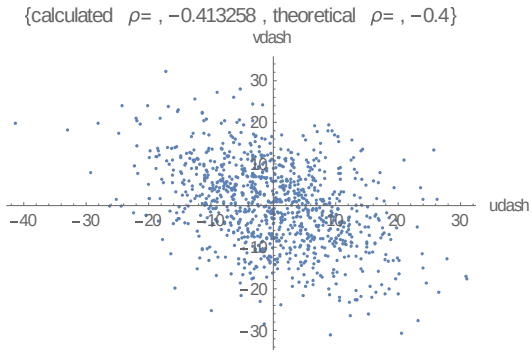

correlation coefficient =-0.4

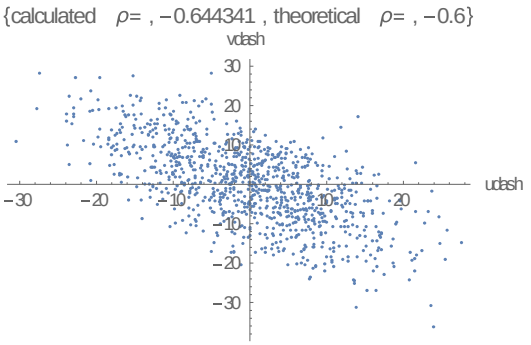

correlation coefficient =-0.6

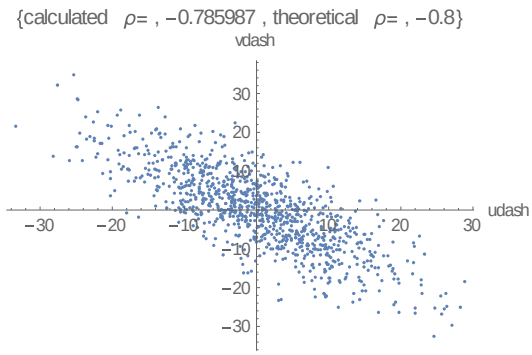

correlation coefficient =-0.8

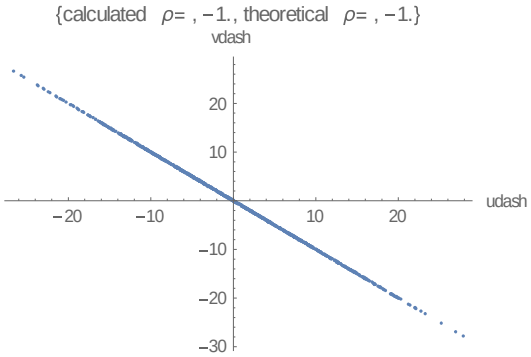

correlation coefficient =-1.0

Figure 3-11 Scatter diagrams with different values of correlation coefficient (0 ~ -1)

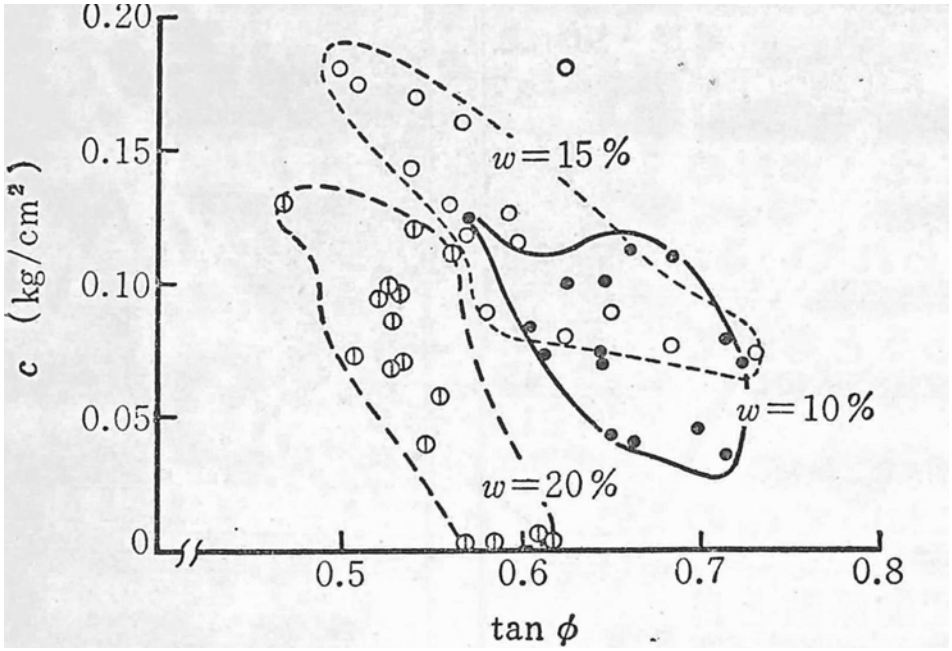

Figure 3-12 Correlation between cohesion c' and friction angle ϕ' in Japan[8]

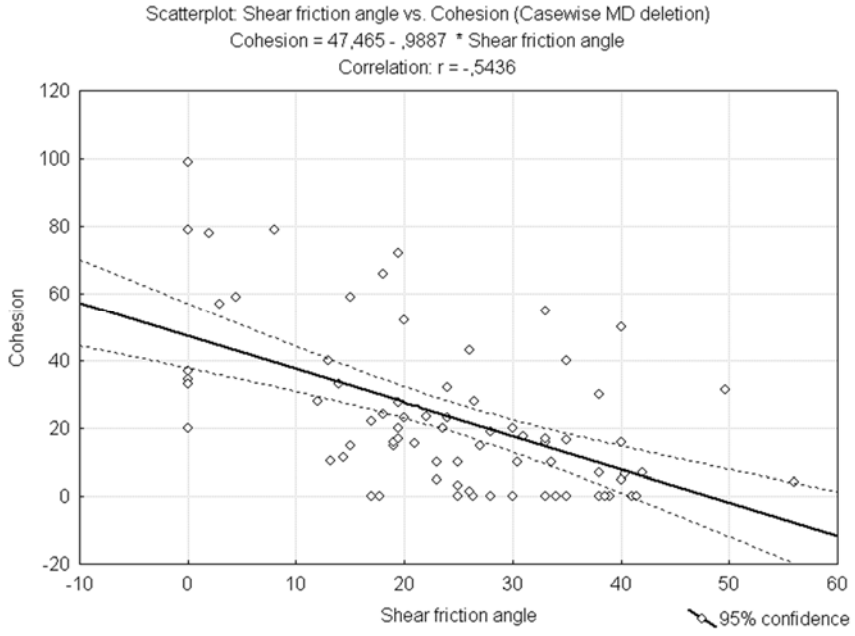

Figure 3-13 Correlation between cohesion c' and friction angle ϕ' [11]

3.4 Infiltration failure probability of levee

For the infiltration failure evaluation of the levee, the thesis uses the circular slip method of slope stability to calculate the safety factor of the levee slope. According to the above section, the modified Fellenius method is be used (as shown in Eq. 3-2). In the Eq. 3-2, the main parameters of the equation are soil cohesion, soil friction angle, the weight of the soil block, the pore water pressure and the geometry conditions of the circular slip. Among these parameters, the geometry conditions are according to the slip surface to decide, the pore water pressure and the weight are change with the water level change, and the soil cohesion and the friction angle are usually decided by the lab test or in situ test.

Traditionally, the cohesion and the friction angle are the unique value. Herein in order to consider the uncertainty of soil parameters, the variation/ deviation of the parameters will be conduct to evaluate the failure probability of the levee slope. In the thesis, the failure probability is calculated by Eq. 3- 24.

$$P_f(h) = \frac{n_h}{N_h} \qquad \text{Eq. 3-24}$$

The $P_f(h)$ is the failure probability of the levee slope in the certain water level h; N_h is the total calculation times; n_h is the failure times of all N_h. Here the failure is defined as the FS (Eq. 3-2) < 1.0.

Figure 3-13 ~ Figure 3-16 are the calculation examples by considering the deviation of the soil parameters with the different water level. The condition of the levee is assumed as followings: the height of the levee is 7.5m, the width of the levee top is 4.0m, the slope of the levee is 1:4; the times of the calculation is 1000 times. The soil parameters are as the followings: the cohesion is 1 kN/m^2 and the variation coefficient is 13 %; the friction angle is 27.5° and the variation coefficient is 40 %; the

correlation coefficient of the cohesion and the friction angle is -0.7. Figure 3-13 is the result of the correlation coefficient with the value -0.7. Figure 3-14 shows the relation among the safety factor (*FS*), the cohesion (*c'*) and the friction angle (∅′) in water level 1.0 m (blue points), 3.5 m (green points) and 6.5 m (red points). The gray plane is the safety factor 1.0. When the result points are location under the plane, they are failure status, and when the points are above the pane, they are safe status. Furthermore, the distribution of the safety factor of the certain water level can be shown as Figure 3-15. It can clearly observe the distribution of the safety factor on the certain water level. By using Eq. 3-24, the failure probability of the levee can be shown as Figure 3-16. The figure shows the probability change with the water level rising.

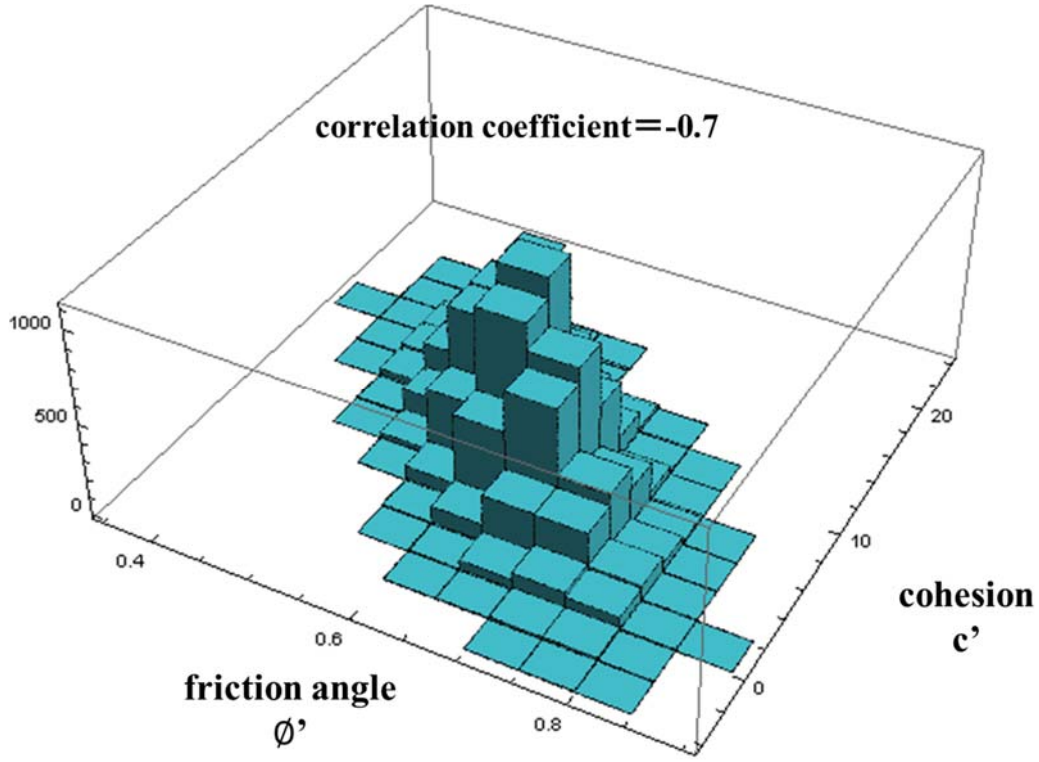

Figure 3-14 the correlation coefficient of the cohesion and the friction angle

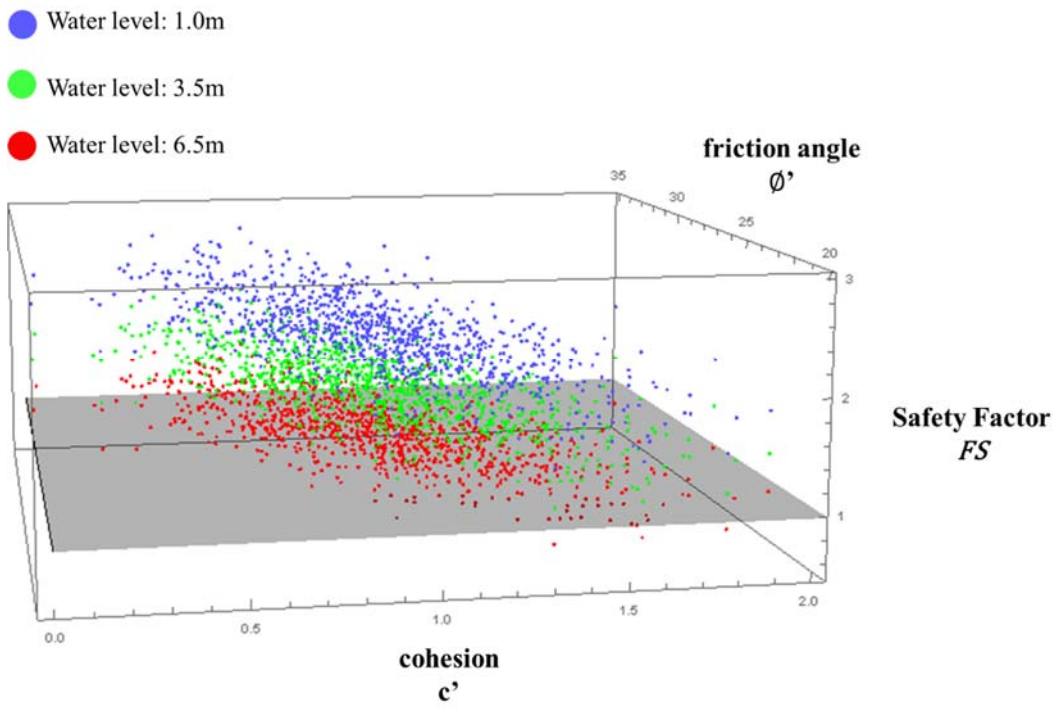

Figure 3-15 the safety distribution in different water level

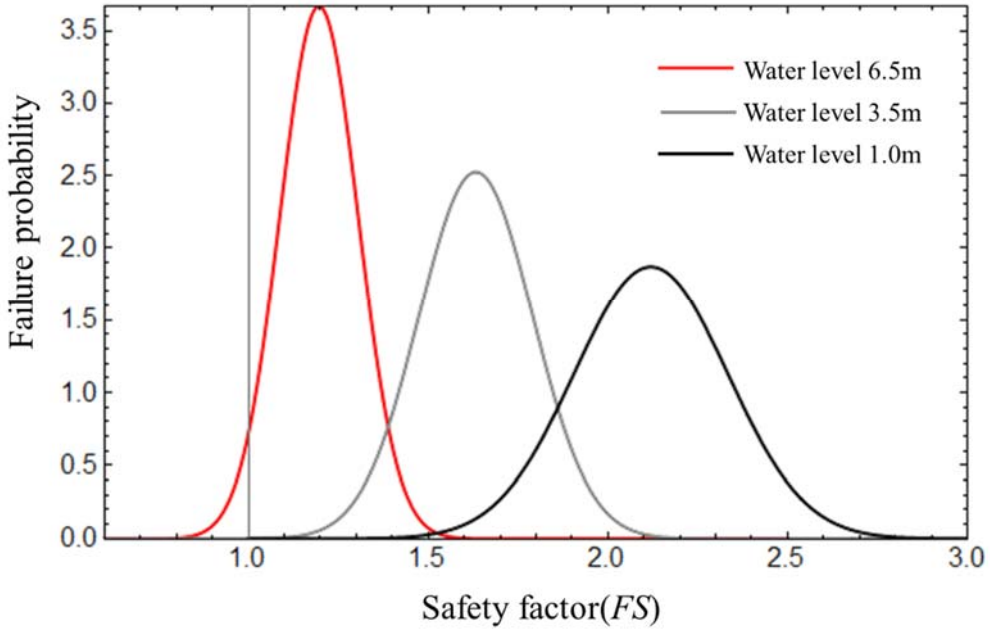

Figure 3-16 The PDF of safety factor with different water level

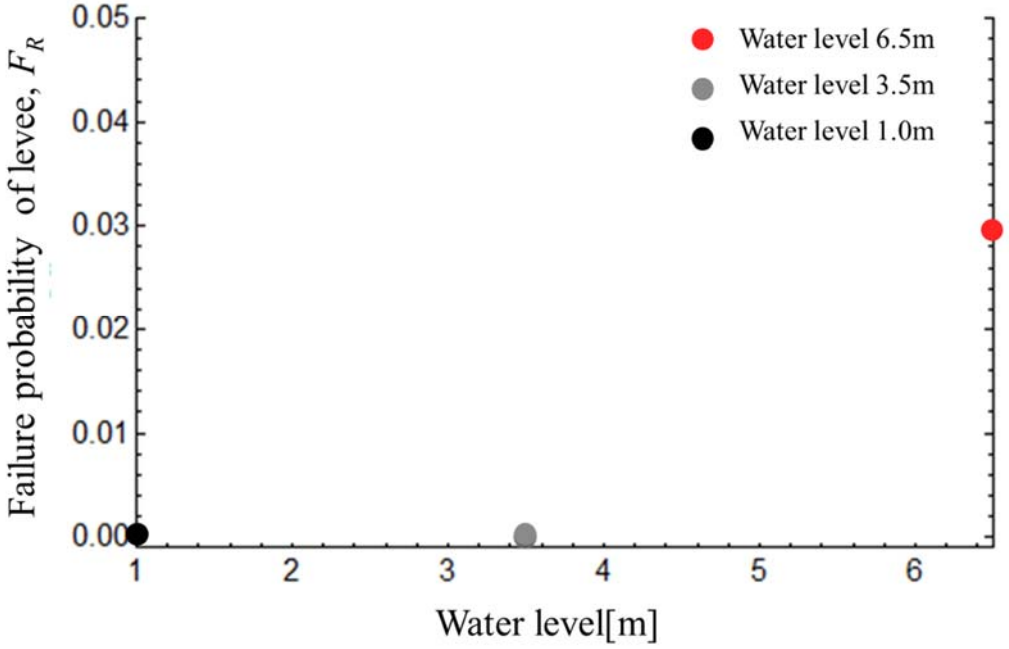

Figure 3-17 the probability of infiltration failure

Reference

[1] A. Keith Turner, Robert L. Schuster, (1996). "Landslides, Investigation and Mitigation- Special Report 247." Transportation Research Board, National Research Council, USA.

[2] https://en.wikipedia.org/wiki/Slope_stability_analysis

[3] Casagrande, A (1937). "Seepage through dams". Journal of the New England Water Works Association, pp.5-12

[4] Shigeo Uchida, (1952). "On the Non-Steady Percolation with a Free Boundary". JSCE Vol.37-2. pp.58-62

[5] Birkhoff. G., (1950). "Hydrodynamics", Princeton University Press

[6] Maximilian Huber, (2013). "Soil variability and its consequences in geotechnical engineering." PHD Thesis.

[7] Rasmus Müller, (2013). "Probabilistic stability analysis of embankments founded on clay." " PHD Thesis.

[8] Matsuno Minaru, (1984). "Geotechnology-With the idea of the reliability design and reality." Gihodo Shuppan Co., Ltd.

[9] J. Michael Duncan, (2000). "Factors of safety and reliability in geotechnical engineering." J. Geotech. and Geoenvir. Engrg., ASCE, 126, 307–316.

[10] GEO-SLOPE International Ltd., (2012) "Stability Modeling with SLOPE/W", An engineering methodology.

[11] I. Petrovic, (2008) "Probabilistic Stability Analysis of Sanitary Landfill Jakusevec", 1st Middle European Conference on Landfill Technology.

CHAPTER 4 RELIABILITY ANALYSIS

Reliability is probabilities or statistics in mathematics. Therefore, the performance of phenomenon or decision must display by probability. For example, the expression of "absolute safe or failure" is impossible and relatively "99% safe" or "99% failure" is used. In other words, in reliability analysis or design, never failure of construction does not exist. In this chapter, the failure probability of levee and its reliability analysis will explain as followings.

4.1 The development of the reiliability analysis

Before World War II, "reliability" has been linked mostly to repeatability. A test (in any type of science) was considered reliable if the same results would be obtained repeatedly. In the 1920s product improvement through the use of statistical process control was promoted by Dr. Walter A. Shewart at Bell Labs. The development of reliability engineering was here on a parallel path with quality. The modern use of the word reliability was defined by the U.S. military in the 1940s and evolved to the present. It initially came to mean that a product would operate when expected and for a specified period of time. In the time around the WWII and later, many reliability issues were due to inherent unreliability of electronics and to fatigue issues.

In 1945, M.A. Miner published the seminal paper titled "Cumulative Damage in Fatigue" in an ASME journal. A main application for reliability engineering in the military was for the vacuum tube as used in radar systems and other electronics, for which reliability has proved to be very problematic and costly. The IEEE formed the Reliability Society in 1948. In 1950, on the military side, a group called the Advisory Group on the Reliability of Electronic Equipment, AGREE, was born. [1]

In Japan, in 1958, United States of America invited Japanese delegation of JUSE (Union of Japanese Scientists and Engineers) to join the conference, the 5th National Conference on Quality Control and Reliability. For the conference, the reliability study committee has been formed by Prof. Takagi (Tokyo University) and Prof. Karatsu (the Institute of Electrical Communication). This is the beginning of reliability study of Japan.

In the 1960s, more emphasis was given to reliability component and system level up for the reliability test. For example, the famous "Military Standard 781" was built at that time.

At the same time, the study of reliability analysis was beginning in the field of civil engineering. In the 1950s and 1960s, Alfred Freudenthal published a series of fundamental papers in which many of precepts of modern risk and reliability theory first appeared. With respect to mechanical engineering and other filed, the development of civil engineering is relatively. The main reason is the database for our field. Civil engineering is a very complex field including of human activities, natural phenomenon and so on, therefore a lot of variables are filled with a variety of problems. The reliability analysis of civil engineering was first starting from the collection and statistical analysis of soil properties by Matsuo, Hopper, Meyerhof and Lumb. [2]

In 1971, the first international conference on "the application of statistics and probability in soil and structural engineering" has been held in Hong Kong. In 1976, MIS held the summer session of "Risk and Decision Problem in Geotechnical Engineering". In 1977, International Conference on Soil Mechanics and Foundation Engineering (9th 1977 Tokyo, Japan) formed a special session of "the stochastic design approach in soil mechanics."

4.2 Literature review

There are many literatures proposing various methods for civil engineering including of structural engineering, geotechnical engineering, river engineering and so on. The following section will introduce some important reliability-based design/ analysis in civil engineering especially for the failure probability and reliability analysis.

4.2.1 Structural engineering

The reliability analysis of the structural engineering was earlier to develop and relatively more mature than other fields in civil engineering. Therefore, many published researches explain the issue very completely as following literatures. JSCE (Japan Society of Civil Engineers) published the "Safety, Reliability of the Structure" in 1976. [3] Nobuyoshi TAKAOKA translated and published the "Theory of Reliability Design of Civil Engineering Structures" of Rzhanitsyn, Aleksei Rukofivich from Russia in 1980. [4] Milton E. Harr published the "Reliability-Based Design in Civil Engineering" in 1987. [5] Motoyuki SUZUKI published the "Reliability-Based Design for Structures" in 2010. [6]

The basic model is shown as Figure 4-1. It shows the distributions of the loading (S) and the resistance (R) for the any component of the structure or the structure. The failure will occur when the status is $S > R$. Therefore, its probability will be called probability of failure (P_f) (the relation equation as Eq. 4-1 shows).

$$P_f = P(S > R) = P\left(\frac{R}{S} < 1\right) = P(S - R > 0) \qquad \text{Eq. 4-1}$$

The distribution functions of S and R are shown as $F_S(x), F_R(y)$ or $f_S(x), f_R(y)$. The joint probability density function of S and R can be shown as $f_{S,R}(x, y)$. Furthermore, within the range, $0 < R < S$, the integral result is the probability of

failure (P_f) as shown in Eq. 4-2. If S and R are independent, the relation will be $f_{S,R}(x,y) = f_S(x) \cdot f_R(y)$, and the probability of failure (P_f) will be shown as Eq. 4-3. (as shown in Figure 4-2)

$$P_f = P(S > R) = \int_0^\infty \int_0^x f_{S,R}(x,y)dydx = \int_0^\infty \int_0^y f_{S,R}(x,y)dxdy \qquad \text{Eq. 4-2}$$

$$\begin{aligned} P_f &= \int_0^\infty f_S(x) \left\{ \int_0^x f_R(y)dy \right\} dx = \int_0^\infty f_S(x)\, F_R(x)dx \\ &= \int_0^\infty f_R(y) \left\{ \int_y^\infty f_S(x)dx \right\} dy = \int_0^\infty f_R(y)\,\{1 - F_S(y)\}dy \end{aligned} \qquad \text{Eq. 4-3}$$

On the other hand, the consideration of the possible distributions of S and R is very important. The uncertainty of loading S is usually from the evaluation. One is the unpredictability of the external force; second is the transformation error from the loading to the design loading model; third is the multi-loading that is neglected. The resistance uncertainty is usually from the strength of the materials. For example, the quality management of the materials will affect the variation of the strength. Furthermore, the analysis method of the material strength is existing some uncertainty. All these uncertainties will cause the distributions of S and R.

4.2.2 Geotechnical engineering

Applications of probabilistic methods in geotechnical problems have increased in recent years. However, because of the unique site characteristics, the uncertainty is difficult to quantize. Respect with other fields in civil engineering, the construction types will also affect the evaluate methods. For example, tunnels, ground deep-excavation, levee and other constructions are very different with their construction sites, types, methods and purpose. In 1984 and 1985, Minoru MATSUO and Japanese Committee of Soil Mechanics and Foundation Engineering (JCSMFE) (now is Japanese Geotechnical Society) published the reliability analysis for geotechnical engineering.

[2][7] In 1997 ,1998 and 2004, USACE (U.S. Army Corps of Engineers) proposed the technical letter and books of the probability and reliability methods for geotechnical engineering. [8][9][10] Besides these important literatures, in the recent years, some publication papers also referred to the reliability design/ analysis including of the uncertainty of the geotechnical engineering. K. Michael Duncan (2000) [11], F. H. Kulhawy, K.K. Phoon (2002) [12], and I. Petrovic (2008) [13], proposed the variation of the soil parameters, and the correlation among the parameters. Herein, the stability of slopes will be the example to explain the application of the probability and reliability analysis.

First is the calculation method of the failure probability. Matsuo defined the probability as the following equation (Eq. 4-4). JCSMFE defined the probability is the same to Matsuo. Here *G* is the safety factor, M_R is the moment of resistance, M_0 is the moment of driving, and Z is $M_R - M_0$. The distribution of *Z* and *G* is shown as Figure 4-3, the distribution shapes of Z and G are almost the same.

$$P_f = \text{Prob}[\text{G} = \frac{M_R}{M_0} \leq 1.0] \text{ or}$$
$$P_f = \text{Prob}[M_R \leq M_0] = \text{Prob}[Z = M_R - M_0 \leq 0] \quad \text{Eq.4-4}$$

Figure 4-4 shows the circular slip and the M_R and M_0 are defined as Eq. 4-5. r_t is the wet unit weight of soil, R is the radius of the circular of the slip surface, A_i is the volume of each slices and τ_i is the shear stress strength (the calculation equation as Eq. 4-6). u_i is the pore water pressure, c' is the cohesion of soil, and $\emptyset'$ is the friction angle. P_i is the vertical stress to the slip surface.

$$M_R = r_t R \sum_i A_i sin\alpha_i$$
$$M_0 = R \sum_i \tau_i l_i \quad \text{Eq.4-5}$$

$$\tau_i = c' + \left(\frac{P_i}{l_i} - u_i\right) \times \tan\emptyset' \qquad \text{Eq. 4-6}$$

Therefore, the failure probability of slope can be shown as Eq. 4-7, r_u is the ratio of the pore water pressure.

$$P_F = Prob[c'/r_t \leq g(tan\emptyset', r_u)] \qquad \text{Eq. 4-7}$$

If the probability variables are c' and r_t, its quotient will be $c_x(-c'/r_t)$, and the probability density function of c_x will be $f_{c_x}(c_x)$, then the failure probability will be shown as Eq. 4-8 and the probability distribution will like Figure 4-5. The shaded area is the probability of failure. Furthermore, if the $tan\emptyset'$ and r_u with the spatial variation were also considered, the probability of failure will be shown as Eq. 4-9. The $f_{Tan\emptyset'}(tan\emptyset')$ and $f_{Ru}(r_u)$ are the probability density functions of $tan\emptyset'$ and r_u.

$$P_F = \int_{\infty}^{g(tan\emptyset', r_u)} f_{c_x}(c_x) dc_x \qquad \text{Eq. 4-8}$$

$$P_F = \int_{\infty}^{\infty} \int_{\infty}^{\infty} \int_{-\infty}^{g(tan\emptyset', r_u)} f_{c_x}(c_x) f_{Tan\emptyset'}(tan\emptyset') f_{Ru}(r_u) \times dc_x dtan\emptyset' dr_u \qquad \text{Eq. 4-9}$$

On the other hand, USACE (U.S. Army Corps of Engineers) also proposed the technical letter and books of the probability and reliability methods for geotechnical engineering. Different with above the literatures of Matsuo and JCSFME, USACE paid more attention to the reliability theory including of the first order second moment methods (FOSM), Taylor's series method, point estimate method, decision tree and so on. Moreover, the probabilistic approach used the capacity-demand model. For example, by FOSM method, the step of the reliability analysis is as followings:

1. Identifying all the variables that affect the stability like the geometry, the weight and strength of materials.

2. Determining the best estimate (usually the mean value) of each variable, and using these to calculate the best estimate of the factor of safety (expected safety factor) by the method of slices.
3. Estimating the uncertainty in each variable and, in particular, its variance, based on the uncertainties in soil properties.
4. Performing sensitivity analyses by calculating the partial derivatives of safety factor with respect to each of the uncertain variables.
5. Using FOSM method to obtain of the variation of safety factor.

Figure 4-6 is a calculated example to calculate the slope stability with different *H* (depth to till). [14]

In summary, the first method is calculating the safety factor with the variation of the soil parameters; the other method is calculating the expected safety factor then considering the variation of the soil parameters and finally obtaining the variation of safety factor.

4.2.3 Safety of levee

In recent years, the safety of levee/ embankment is also considered with the reliability analysis. In America and European countries, there are many methods to calculate the reliability of the levee. Especially the most common is the events tree method. An event tree is a graphical representation of the many chains that might result from some initiating event, a few of which, should they occur, would lead to system failure as shown in Figure 4-7. [14] Figure 4-8 shows the influence diagram for levee failure, and according the diagram, the event tree of levee failure can be built as shown in Figure 4-9. An individual branch probability is typically assigned by one of serval procedures:

1. Statistical (i.e. empirical) estimates: For example, the $P_r = 0.01$ $(100 - years\ storms)$ event, the historical statistical records are usually the basis for estimating exceedance probabilities of external initiating events.
2. Reliability (i.e. engineering) models: They reason from first principles of mechanics or natural science to calculate uncertainties in the performance of specified variables.
3. Fault tree analysis.
4. Expert opinion.

In Netherlands, P.Q. Tu et. al proposed the reliability-based analysis of river dikes during flood waves. [15] There are three levels of reliability calculation:

1. Level I: Semi-probabilistic approach, a characteristic value is used in the analysis, like the load which is not exceeded in 95% of the cases, or the strength which is available for 95% of the material;
2. Level II: Probabilistic approach with statistical distribution of all variables are taken into account. It comprises a number of approximate methods in which the distribution functions are transformed into standard normal or standard Gaussian distributions.
3. Level III: a highest level probabilistic approach and the probability distribution functions of stochastic variables are fully taken into account.

Herein, the flood wave (water level) is calculated by a half harmonic function, piping failure is calculated by time-dependent equation from Sellmeijer, a Dutch man and instability of levee is calculated by using the GeoSlope packages. Furthermore, according to the expert opinions, the failure probability is judged by expert opinions combining with field inspection. Figure 4-10 is the calculation result of the failure probability of a dike section. [15]

On the other hand, in 2015, Kousuke TABATA proposed the failure probability of levee in his Ph.D. thesis. He mainly used seepage calculation and the deviation of soil parameters to obtain the failure probability of levee. The flow chart of calculation is shown as Figure 4-11. [16] First is the calculation of the water level by the flood flow and river bed change analysis. It considered the characteristics of the river channel to calculate the possible the water level. Moreover, the research also collected the boring data of the soil materials of the levees in Japan, and analyzed the variation of the soil parameters including of the cohesion, the friction angle and the permeability coefficient. Finally using the variation of the soil parameters to evaluate the stability of the levee.

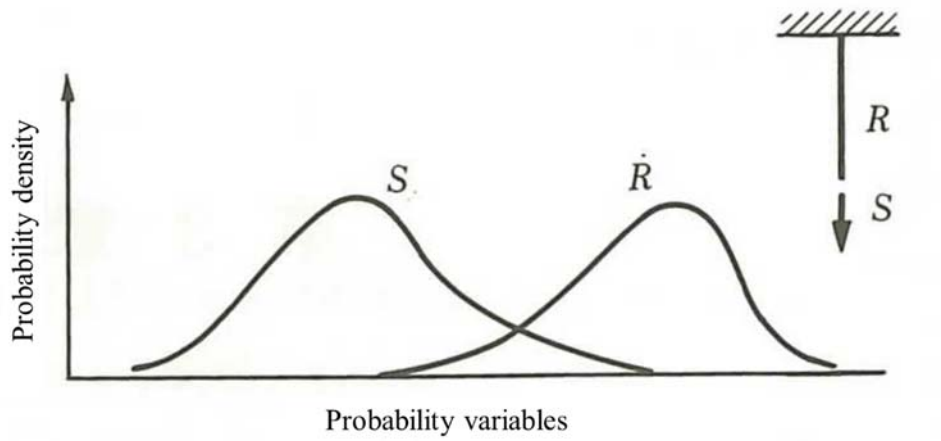

Figure 4-1 the basic model of the reliability analysis [3]

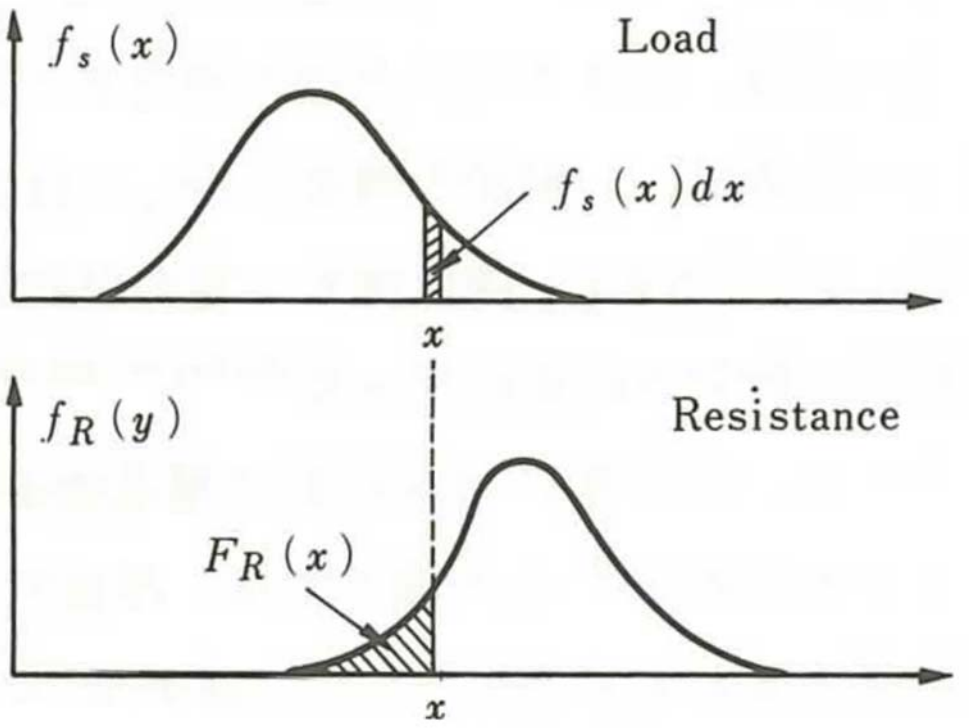

Figure 4-2 the concept of the probability of failure [3]

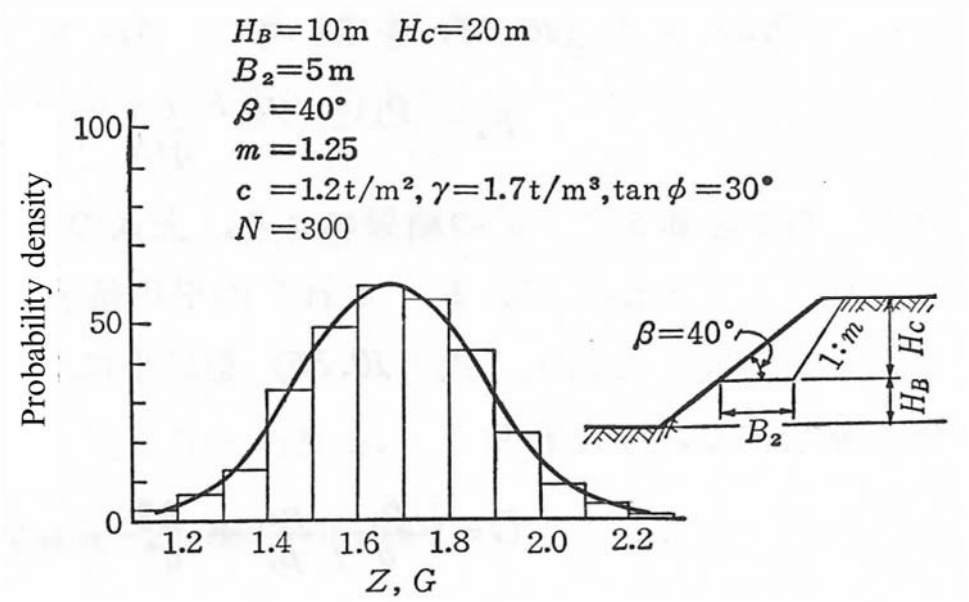

Figure 4-3 the distribution shapes of Z and G

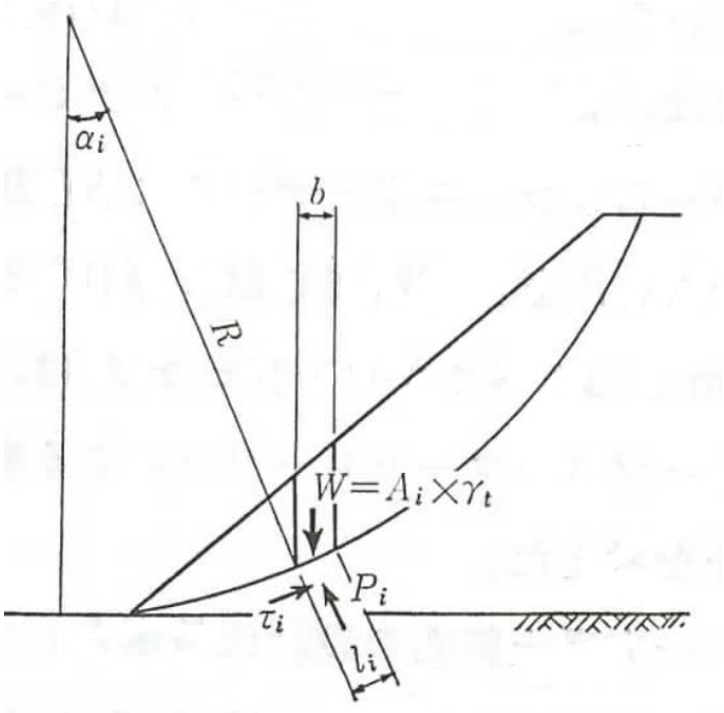

Figure 4-4 the circular slip

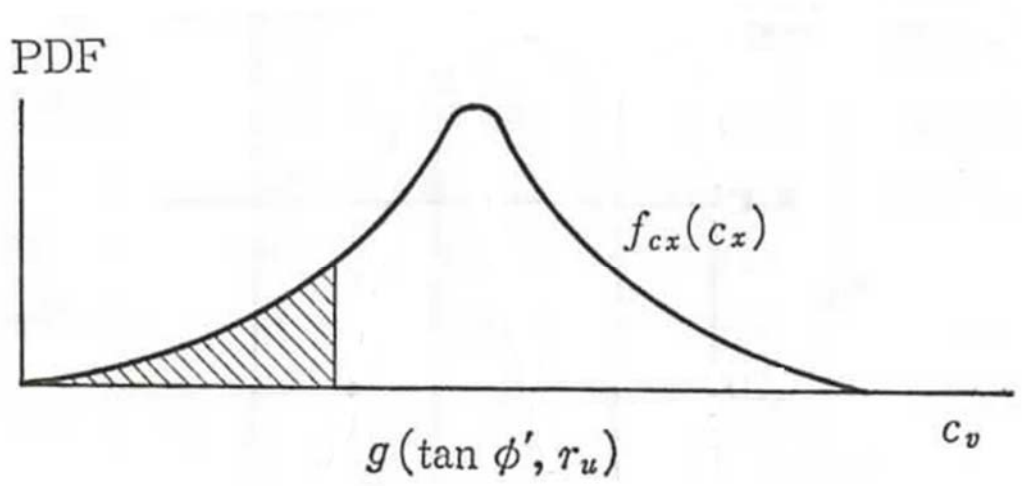

Figure 4-5 the probability of failure (one variable of the probability)

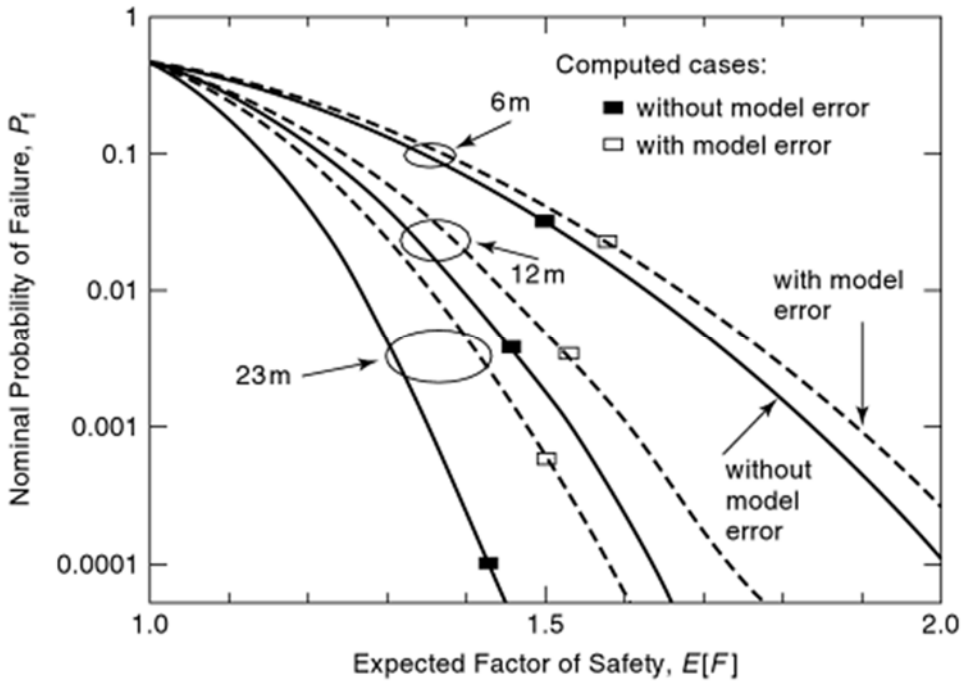

Figure 4-6 Nominal probability of failure versus computed factor safety [14]

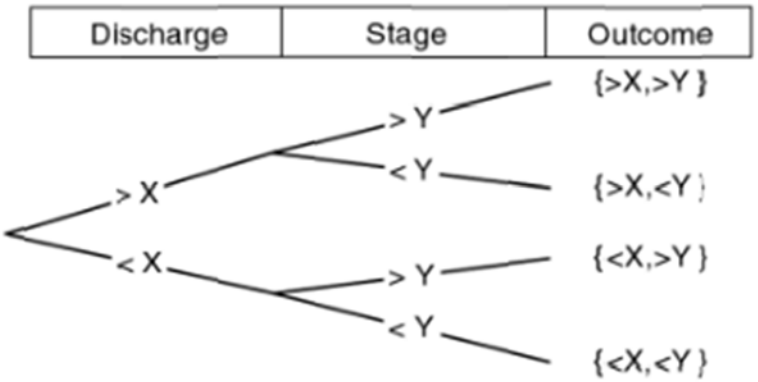

Figure 4-7 A simple event tree for discharge and stage of a river [14]

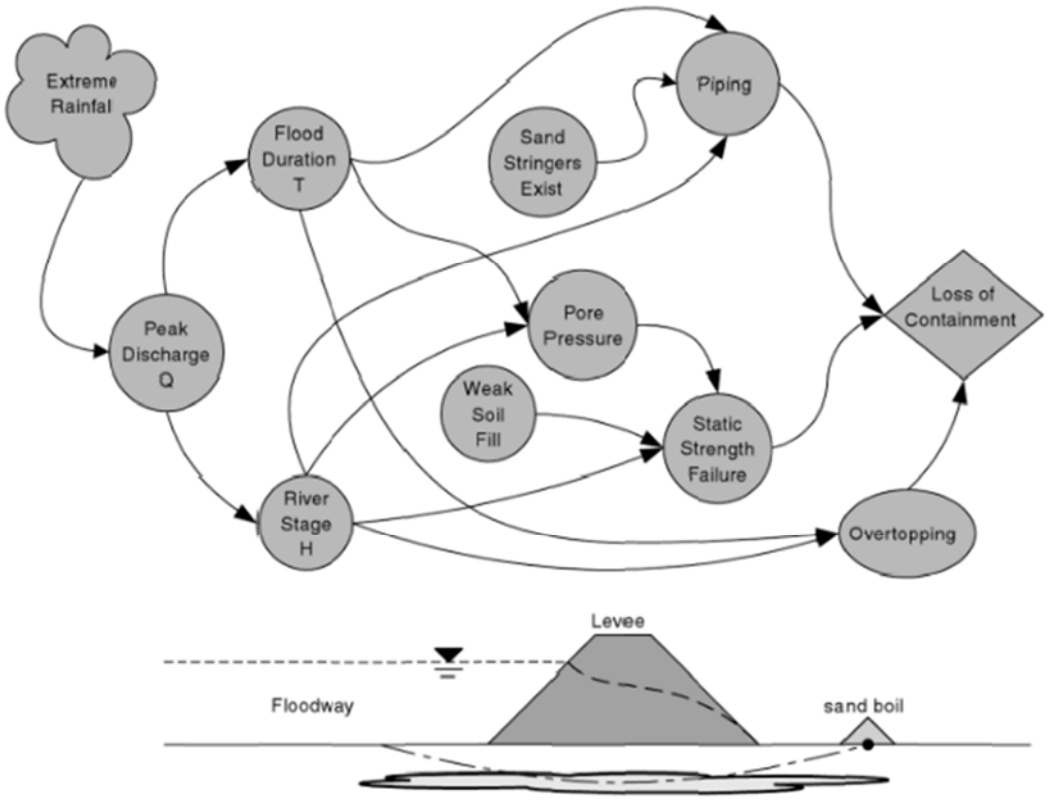

Figure 4-8 Influence diagram for levee failure [14]

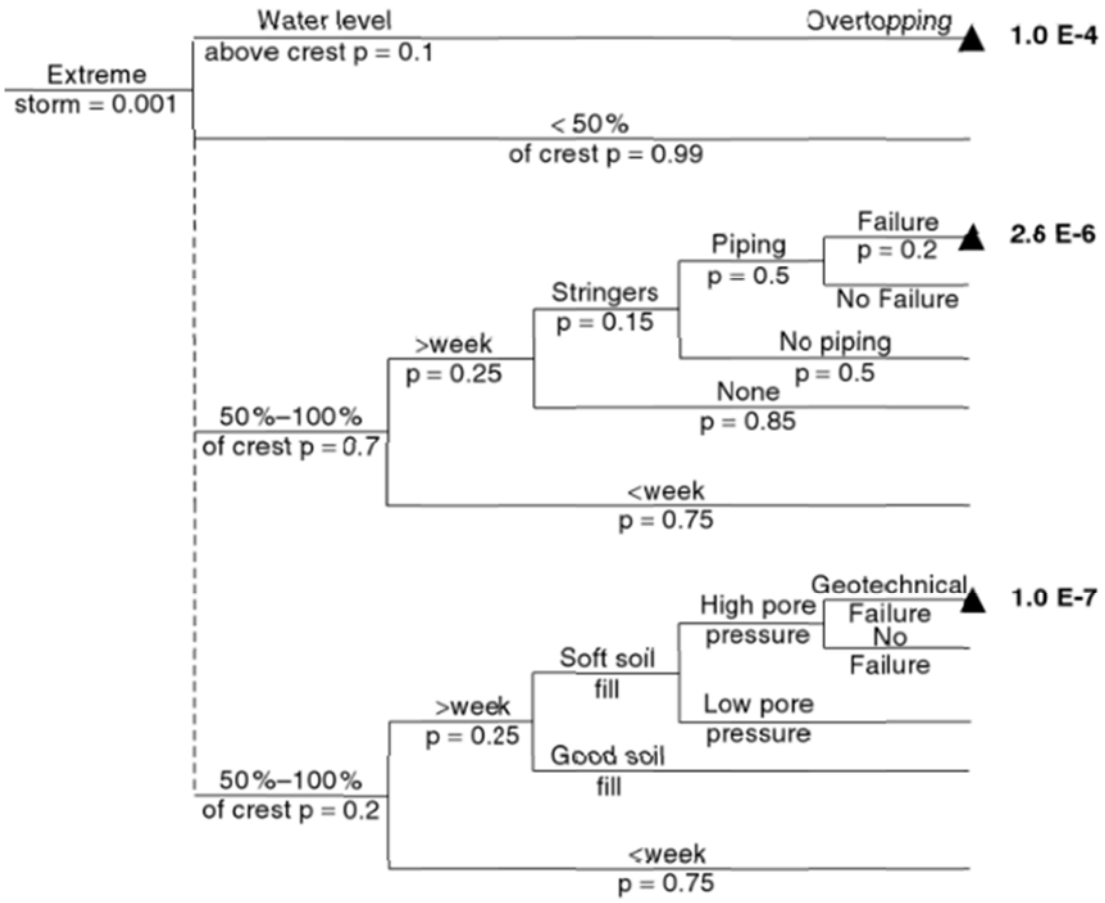

Figure 4-9 Event tree for levee failure during extreme storm [14]

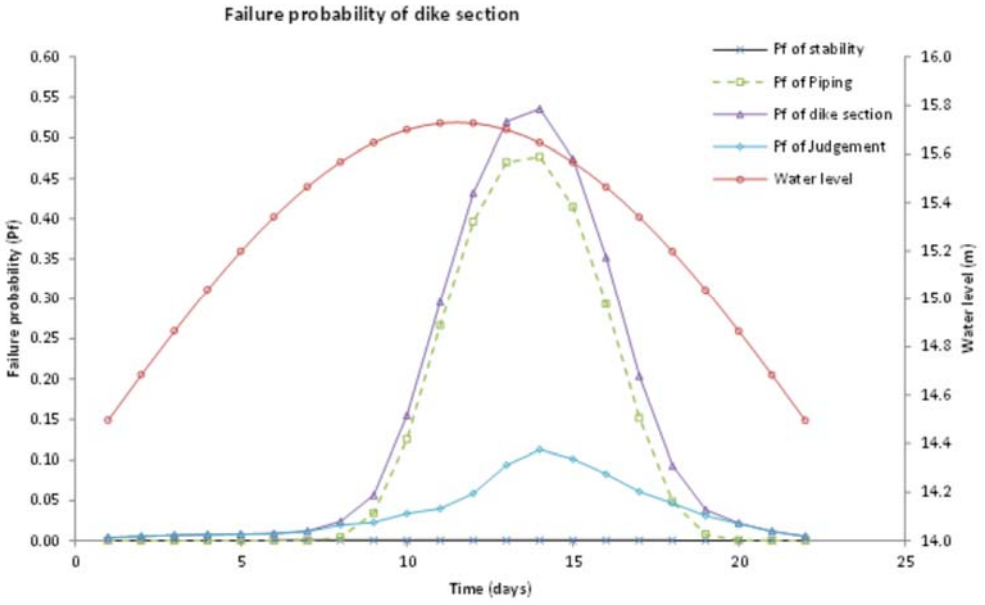

Figure 4-10 failure probability of a dike section

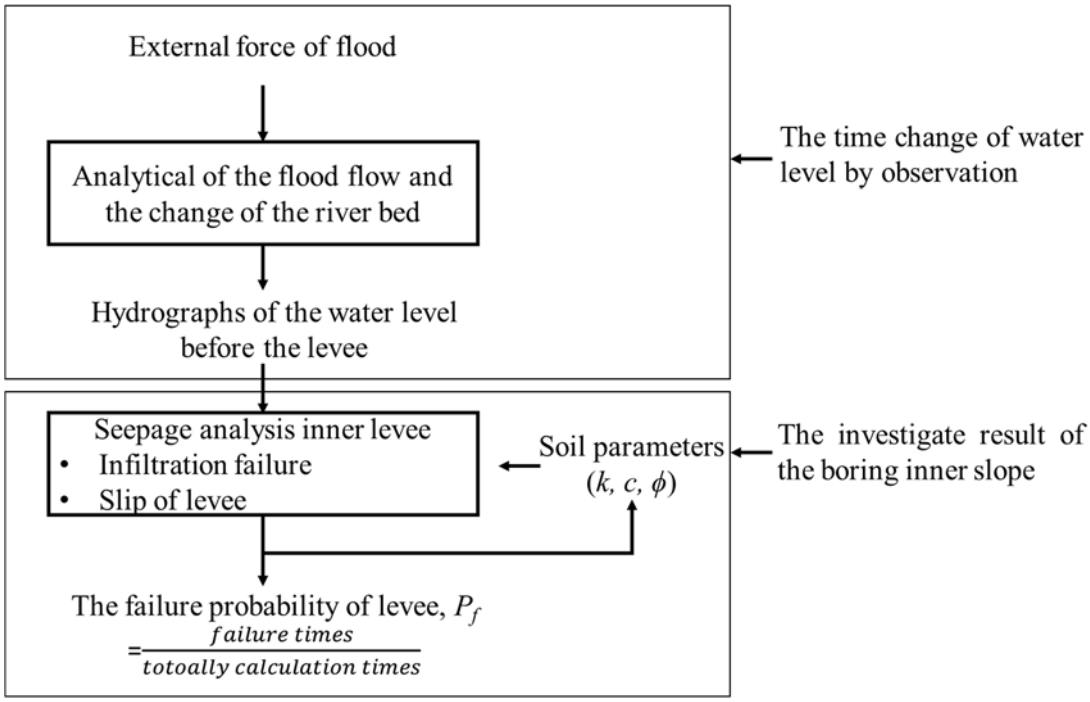

Figure 4-11 the study flowchart by TABATA

4.3 Failure probability analysis of levee

Traditionally in civil engineering assessments of the risk of failure are made on the basis of allowable factors of safety, learned from previous experiences for the considered system in its anticipated environment. Conventionally, the designer forms the ratio of what are assumed to be the nominal values of external force *S* and resistance force *R*, depicted in Figure 4-11.

In general, the demand function is the resultant of many uncertain components of the system under consideration. The external force function will depend on the variability of material parameters, test errors, construction procedures and so on. A schematic representation of the external and resistance forces as probability distributions is shown in Figure 4-12. It is apparent that the nominal values of both the external force $\bar{S}$ and the resistance force $\bar{R}$ cannot be determined with certainty and hence their ratio, the conventional factor of safety, is itself a random variable. As indicated by Figure 4-4 of the external and resistance forces probability distributions $(f_S(s), f_R(r))$, if the maximum external force S_{max} exceeds the minimum resistance force R_{min}, the distribution will overlap and there will be a nonzero probability of failure. A convenient way of assessing this probability is to consider the difference between the resistance and external forces, call safety margin, defined as *R*-*S*. Obviously, the safety margin is itself a random variable (as shown in Figure 4-13). Inadequacy, as measured by the distribution of the safety margin wherein it becomes negative (shown red zone), that is, the portion in which $R - S \leq 0$. Therefore, the red zone is the probability of failure. [17]

In the thesis, the failure of levee can be classified two types, one is overflow and the other is infiltration failure calculated by circular slide method. The overflow failure probability is calculated by the distribution of water level as shown in Figure 4-14①.

The infiltration failure is combined the probability of slip (as Eq. 3-24), $F_R(h)$ is the failure probability with considering the uncertainty of soil parameters in the certain water level *h* as shown in Figure 4-14②.

The safety design is based on the failure probability of the external force. Here according to the design value of H.W.L. the failure probability may be estimated from 0 to ∞ that *s* is external force, f_S is the PDF of external force, *r* is resistance force, f_R is the PDF of resistance force and the failure condition is $R \leq s$. The equation (Eq. 4-10) may be display as follows:

$$P_f = \mathrm{P}[R \leq s] = \int_0^s f_R(r)dr = F_R(s) \qquad \text{Eq. 4-10}$$

As the range of *S* is $s \sim s + ds$, and because the failure probability is independent for *R* and *S* like Eq. 4-11.

$$P[R \leq s, s < S \leq s + ds] = f_S(s)ds \cdot F_R(s) = f_S(s)f_R(s)ds \qquad \text{Eq. 4-11}$$

If the external force *s* is form -∞ (or 0) to ∞, the failure probability of the levee may be shown as Eq. 4-12 and f_R can be shown as Eq. 4-13.

$$P_f = \int_0^\infty f_S(s)\, F_R(s)ds = \int_0^\infty f_S(s)\, ds \int_0^s f_R(r)\, dr \qquad \text{Eq. 4-12}$$

$$f_R = \int_0^\infty \int_0^s f_S(s)\, f_R(r)drds = \int_0^S \int_0^\infty f_S(s) \cdot f_R(r)dsdr \qquad \text{Eq. 4-13}$$

Moreover when *R* is between $r \sim r + dr$, the probability $f_R(r)dr$ is the failure probability of resistance *r* and when *S* is larger than *r, S* is equal $1 - F_S(r)$ that *r* is between 0 ~ ∞.

$$P_f = \int_0^\infty f_S(s)\, F_R(s)ds = \int_0^\infty f_R(r)\, [1 - F_S(r)]dr \qquad \text{Eq. 4-14}$$

Here $f_S(s)F_R(s)$ is the mean value of failure probability when R is $r < s$ and $f_R(r)[1 - F_S(r)]$ is the mean value of failure probability when s is $S < r$.

As described above, the *s* and *R* can be obtained from 0 to ∞ and the failure probability of levee can be considered when the water level is from 0 to an uncertainty water level *H*. Here $f_S(h_S, \sigma_S; h)$ is the PDF of external force h with mean h_s and standard deviation σ_S; $f_R(h_R, \sigma_R; h)$ is the PDF of resistance force h with mean h_R and standard deviation σ_R. Then Eq. 4-14 may be re-written to Eq. 4-15.

$$P_f(H) = \int_{-\infty}^{\infty} f_s(H, \sigma_S; h) F_R(h_r, \sigma_r; h) dh \qquad \text{Eq. 4-15}$$

The summation of failure probability from the water level 0 ~ H is $\overline{P_f}(H)$ and σ_S is assumed and transferred to h_S. In numerical methods, $P_f(H)$ is equal $\overline{P_f}(H)$.

$$\begin{aligned} \overline{P_f}(H) &= \int_0^{\mathrm{H}} dh_S \int_{-\infty}^{\infty} f_s(h_S, \sigma_S; h) \cdot f_R(h_R, \sigma_R; h) dh \\ &= \int_{-\infty}^{\infty} f_R(h_R, \sigma_R; h)[1 - F_S(H, \sigma_S; h)] dh \end{aligned} \qquad \text{Eq. 4-16}$$

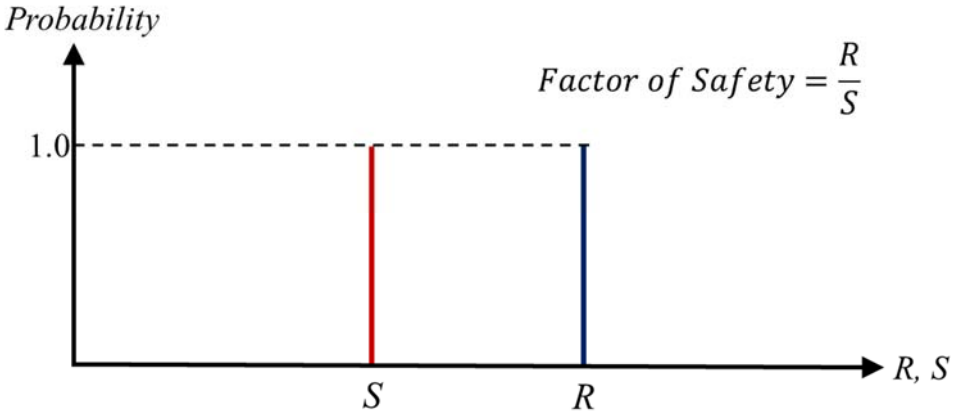

Figure 4-11 the nominal value for safety calculating

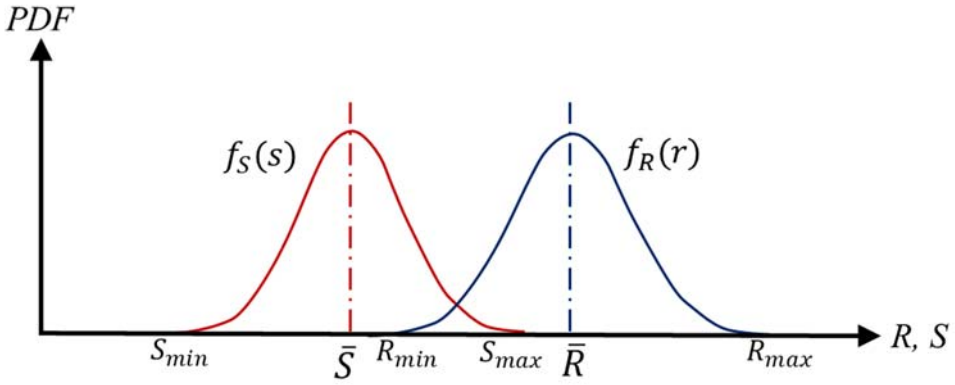

Figure 4-12 the distribution of S and R

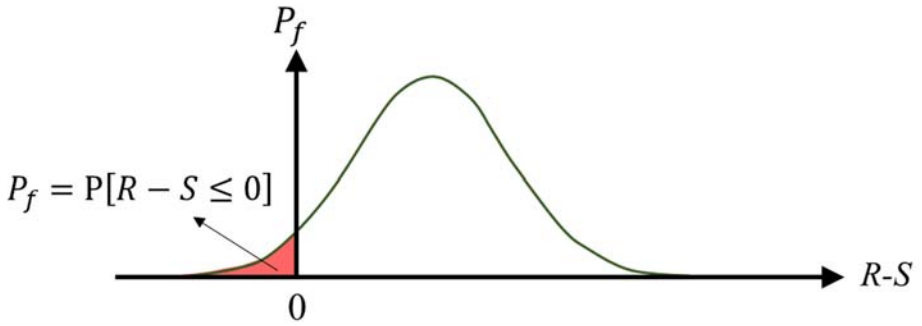

Figure 4-13 the failure probability

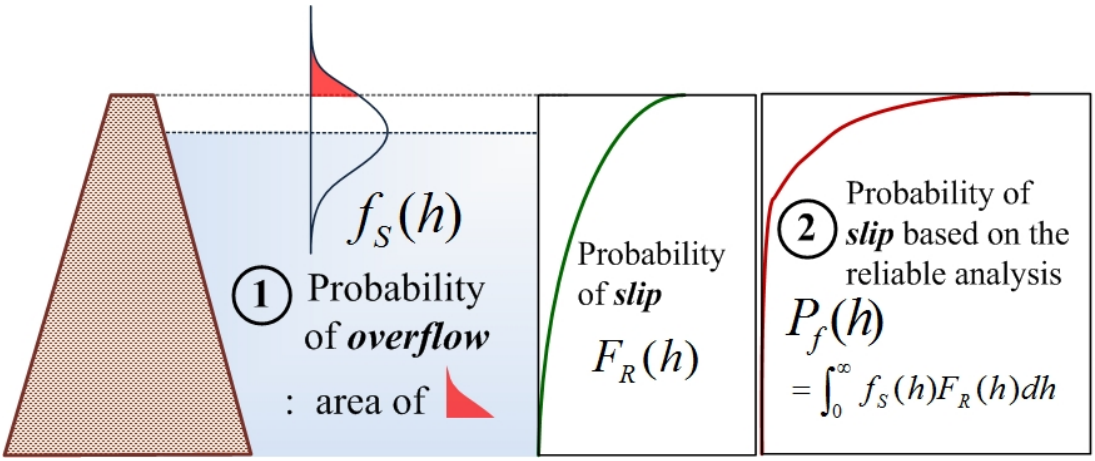

Figure 4-14 the schematic diagram of levee failure probability

4.4 Probability of multi-failure

Probability theory is a branch of algebra with its own axioms and notation. The first notation is the expression for the probability of $f1$, where $f1$ is the first failure type, and the probability can be written as $P_{f1} = P[f1]$. In other words, the safety probability is $1 - P_{f1}$. If the analysis considers only one type, the probability will be shown as Figure 4-15.

When there are two failure types and they are independent, the probability will be shown as Figure 4-16. The associated failure probability is Eq. 4-17.

$$P_f = P[f1] + P[f2] = P_{f1} + P_{f2} \quad \text{Eq. 4-17}$$

If the two failure types are dependent, the probability will be shown as Figure 4-17. The associated failure probability is Eq. 4-18.

$$P_f = P[f1] \cup P[f2] = P_{f1} + P_{f2} - P_{f1} \cdot P_{f2} \quad \text{Eq. 4-18}$$

If the failure types are dependent and more than three types, the probability will be shown as Figure 4-18. The associated failure probability is Eq. 4-19.

$$P_f = \sum_{i=1}^{m} P[f_i] - \sum_{\alpha<i\leq m}^{m} P[f_i \cap f_j] + \sum_{\alpha<i<j<k\leq m}^{m} P[f_i \cap f_j \cap f_k] - \cdots P[f_1 \cap f \cap \ldots \cap f_m] \quad \text{Eq. 4-19}$$

In the thesis, there are main failure types considered, overflow and infiltration failure. Therefore, the detail probability calculated is as Figure 4-19 including the following types:

1. The only overflow failure, P_{fo}, calculated by the distribution of the water level.
2. The only infiltration failure, P_{f1}, calculated by the stability of levee for the probable water level.
3. When one of the two failures occurs, P_{f2}, calculated by Eq. 4-20.
4. When both overflow and infiltration failure occur, P_{f3}, calculated by Eq. 4-21.

$$P_{f2} = P[fo] \cup P[f1] = P_{fo} + P_{f1} - P_{fo} \cdot P_{f1} \quad \text{Eq. 4-20}$$

$$P_{f3} = P[fo] \cap P[f1] = P_{fo} \cdot P_{f1} \quad \text{Eq. 4-21}$$

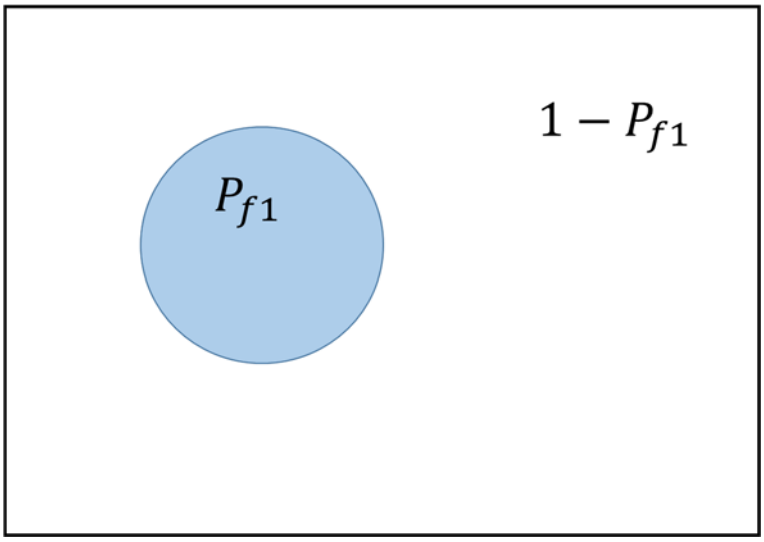

Figure 4-15 the probability of only one failure type

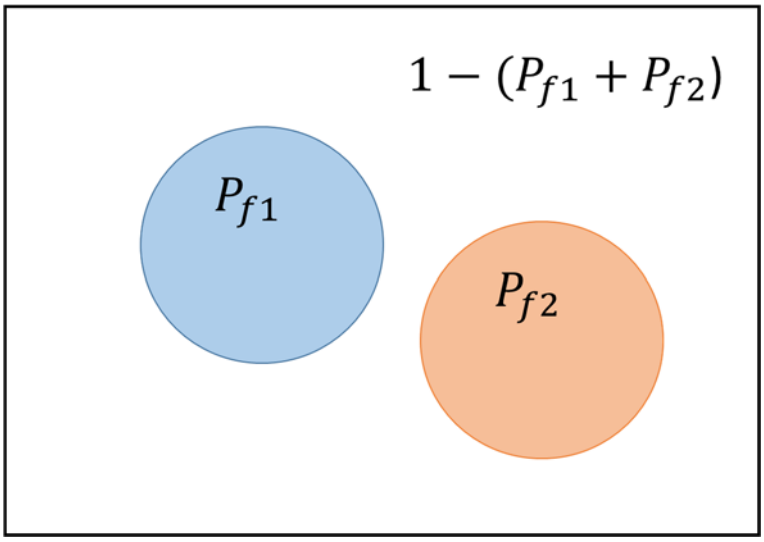

Figure 4-16 the probability of the two independent failure types

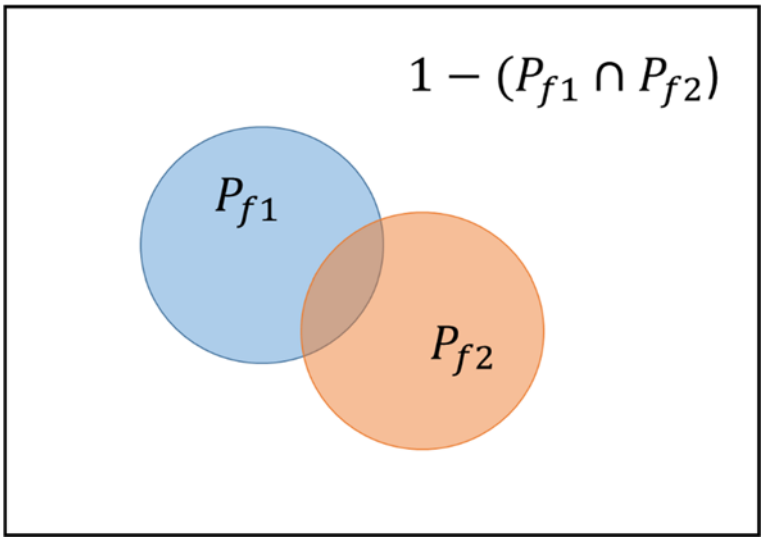

Figure 4-17 the probability of the two dependent failure types

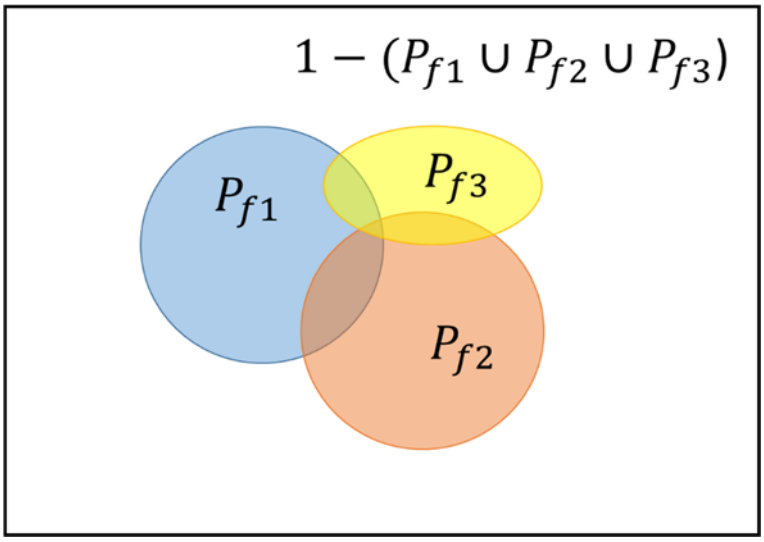

Figure 4-18 the probability of the two dependent failure types

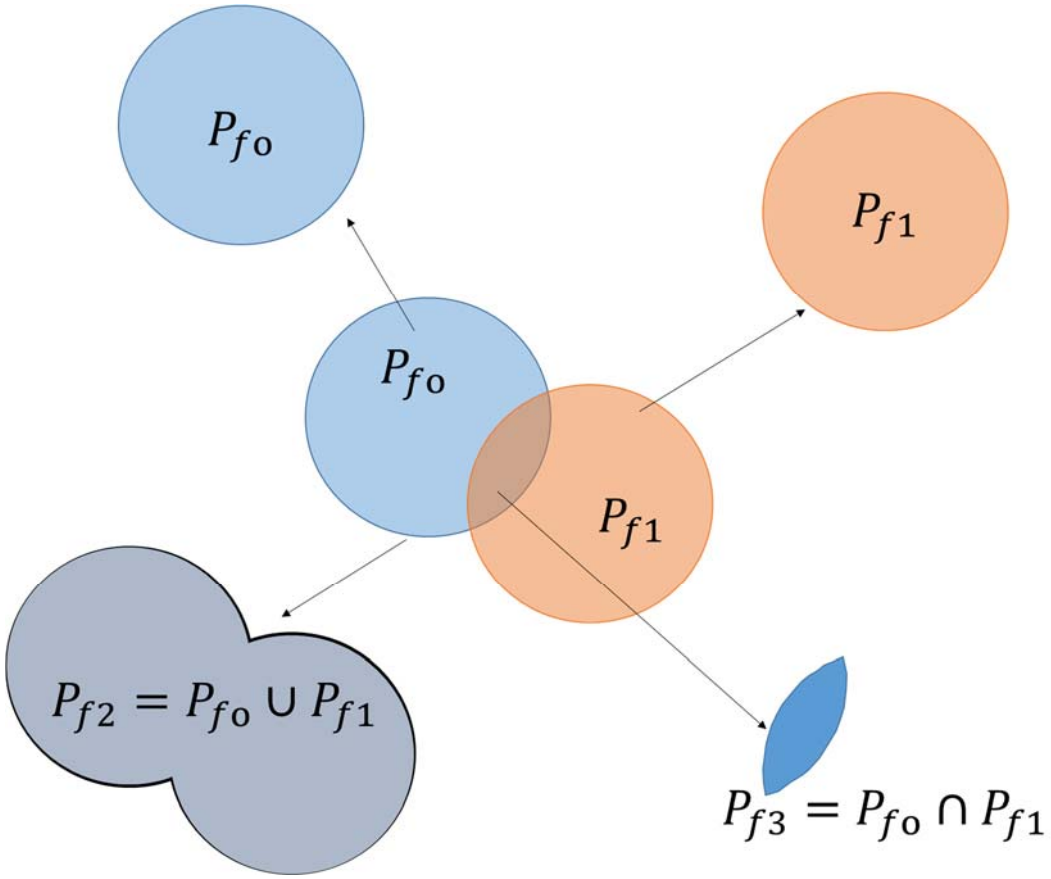

Figure 4-19 the probability relation with the overflow and infiltration failure

Reference

[1] https://en.wikipedia.org/wiki/Reliability_engineering

[2] Matsuo Minaru, (1984). "Geotechnology-With the idea of the reliability design and reality." Gihodo Shuppan Co., Ltd. (in Japanese)

[3] JSCE, (1976). "Safety, Reliability of the Structure." Japan Society of Civil Engineers

[4] Nobuyoshi Takaoka, (1980). "Theory of Reliability Design of Civil Engineering Structures". Maruzen Co., Ltd.

[5] Milton E. Harr, (1987). "Reliability-Based Design in Civil Engineering" McGraw-Hill, Inc.

[6] Motoyuki SUZUKI, (2010). "Reliability-Based Design for Structures". Morikita Publishing Co., Ltd.

[7] Japanese Committee of Soil Mechanics and Foundation Engineering, (1985). "the Reliability design of soil mechanics". (in Japanese)

[8] U.S. Army Corps of Engineers. (1997). ''Engineering and design introduction to probability and reliability methods for use in geotechnical engineering.'' Engr. Tech. Letter No. 1110-2-547, Department of the Army, Washington, D.C.

[9] U.S. Army Corps of Engineers. (1998). ''Risk-based analysis in geotechnical engineering for support of planning studies.'' Engrg. Circular No. 1110-2-554, Department of the Army, Washington, D.C.

[10] U.S. Army Corps of Engineers. (2004). ''Geotechnical Reliability of Dam and Levee Embankments.'' ERDC/GSL CR-04-01, Department of the Army, Washington, D.C.

[11] J. Michael Duncan, (2000). "Factors of safety and reliability in geotechnical engineering." J. Geotech. and Geoenvir. Engrg., ASCE, 126, 307–316.

[12] F.H. Kulhawy, K.K. Phoon, (2002). "Observations on geotechnical reliability-based design development in North America." Foundation Design Codes and Soil Investigation in view of International Harmonization and Performance.

[13] I. Petrovic, (2008) "Probabilistic Stability Analysis of Sanitary Landfill Jakusevec", 1st Middle European Conference on Landfill Technology.

[14] Gregory B. Baecher, John T. Christian, (2005) Reliability and Statistics in Geotechnical Engineering, John Wiley & Sons.

[15] P.Q. Tu et. al., (2012). "Reliability-based analysis of river dikes during flood waves.",11th International Probabilistic Safety Assessment and Management Conference and the Annual European Safety and Reliability Conference 2012 (PSAM11 ESREL 2012)

[16] Kousuke TABATA, (2015). "A Study on Flood Variation of River Bed and Evolution for Probability of Levee Failure in Complicated River Channel" the doctoral thesis, Chuo University.

[17] Milton E. Harr, (1987). "Reliability-Based Design in Civil Engineering" McGraw-Hill, Inc.

CHAPTER 5 SCENARIO TEST

The chapter will assume some scenario conditions to simulate the failure probability of levee. According to the technical report of NILIM, the soil characteristics of all these failure cases can be probably subdivided to clay soil and sandy soil, and the parameters as shown in Table 5-1 and Table 5-2. The cohesion of candy soil is almost 1 kN/m^2 and the range of the friction angle is from 20^o~30^o. The friction angle of clay soil is almost 0^o and the range of the cohesion is from 10 kN/m^2 ~ 60 kN/m^2.

Therefore, in the chapter, the scenario will refer the characteristics of these levee to set the conditions. The following sections will introduce the calculation conditions, assumptions, calculation results and the discussion about the results.

Table 5-1 the soil parameters of sandy soil [1]

Case site	Cohesion[kN/m^2]	Friction angle [^{o}]
Yoneshirogawa L_5K	1	30
Hiikawa R_11.4~11.6K	1	34
Edogawa L_24.5K-1	1	30
Arakawa L_11.3K-2	1	20
Arakawa L_13.7K-1	1	20
Arakawa L_67.6K-1	1	30
Arakawa R_72K-1	1	30
Shounaigawa L_25K-1	1	22
Shounaigawa L_25K-2	1	25
Shounaigawa R_23.8K	1	23
Shounaigawa L_24.4K-1	1	35
Shounaigawa L_24.4K-2	1	26
Aganogawa L_19.2K	1	30
Yoneshirogawa L_7.8K	1	22

Table 5-2 the soil parameters of clay soil [1]

Case site	Cohesion[kN/m^2]	Friction angle [^{o}]
Mogamigawa R_CsNo92~No94)	42.5	0
Abukumagawa L_4K	35	0
Edogawa L_24.5K-2	25	0
Edogawa L_24.5K-3	30	0
Arakawa L_11.3K-1	10	0
Arakawa L_13.7K-2	10	0
Arakawa L_28.2K-1	10	0
Arakawa L_28.2K-2	60	0
Arakawa L_64K	19	0
Arakawa L_67.6K-2	16	0
Arakawa L_69.6K	16	0
Arakawa L_70K	16	0
Arakawa L_70.4K	16	0
Arakawa L_71.2K-1	22	0
Arakawa L_71.2K-2	34	0
Arakawa L_72K	34	0
Arakawa R_72K-2	16	0
Shounaigawa L_24.4K-3	37	0

5.1 Calculation conditions and assumptions

5.1.1 Assumptions

The followings are the assumptions of calculation.

1. The wetting plane is assumed that the same to the water level, the worst situation of infiltration inner levee.
2. The infiltration directly from rainfall is ignored.
3. The failure types are assumed two, one is overflow and the other is slide of levee by using circular slide method.
4. The deviation soil parameters are considered as Table 5-3.
5. The relationship between overflow and slide of levee is shown as Figure 4-19.
6. The soil material is unique and homogeneous inner levee.
7. The underlying material under levee is assumed impermeable layer like Figure 5-1.
8. The slip surface is assumed like Figure 5-2.
9. When the safety smaller than 1.0 is failure.
10. The times of calculation is 10,000 times.
11. The calculation conditions of rainfall-runoff model:
    r=50 [mm/h]; t=5 [h], ks=0.02 [cms]; L=30000 [mm]; m=4; i=15 [^{o}]; D=200 mm ;w=0.42
12. The geometry of levee is shown as Figure 5-3. The height of levee is7.5 m, H.W.L. is

6.5 m (freeboard is 1.0 m).

5.1.2 Scenario conditions

The followings are the scenario conditions of calculation.

1. The soil unit weight is 18 kN/m^2.

2. The scenario cases are shown as Table 5-4.

3. The levee grades are calculated by 1:3, 1:4, 1:5 and 1:6.

The scenario results are subdivided to sandy soil and clay soil. The calculation conditions are as following sections.

Table 5-3 the deviation of soil parameters

	Cohesion c'	Friction angle ϕ'	Correlation coefficient
Coefficient of variation (%)	40	13	-0.72

Table 5-4 the scenario conditions

Soil type	Scenario	Cohesion c' [kN/m^2]	Friction angle ϕ' [º]
Sandy soil	S-1	1	20
	S-2	1	27.5
	S-3	1	35
Clay soil	C-1	10	1
	C-2	35	1
	C-3	60	1

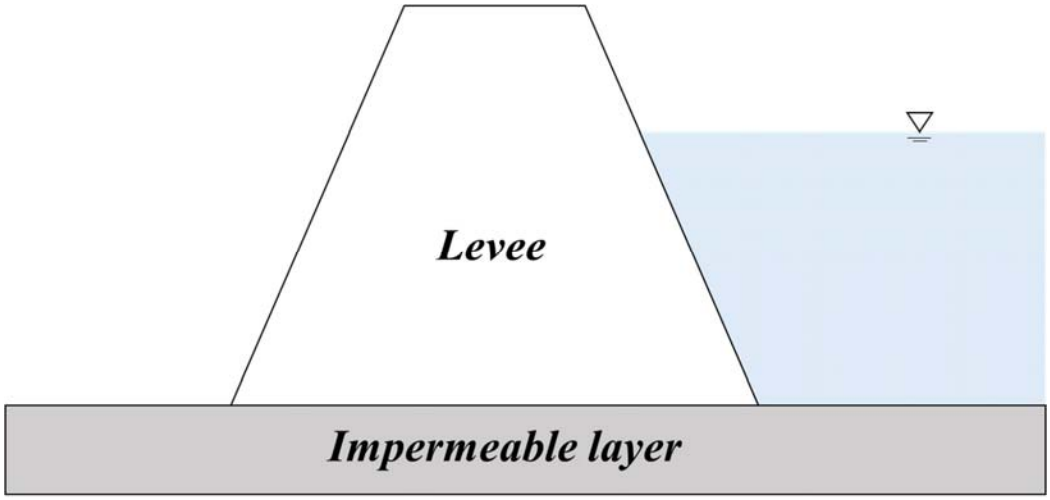

Figure 5-1 The underlying material under levee is assumed impermeable layer

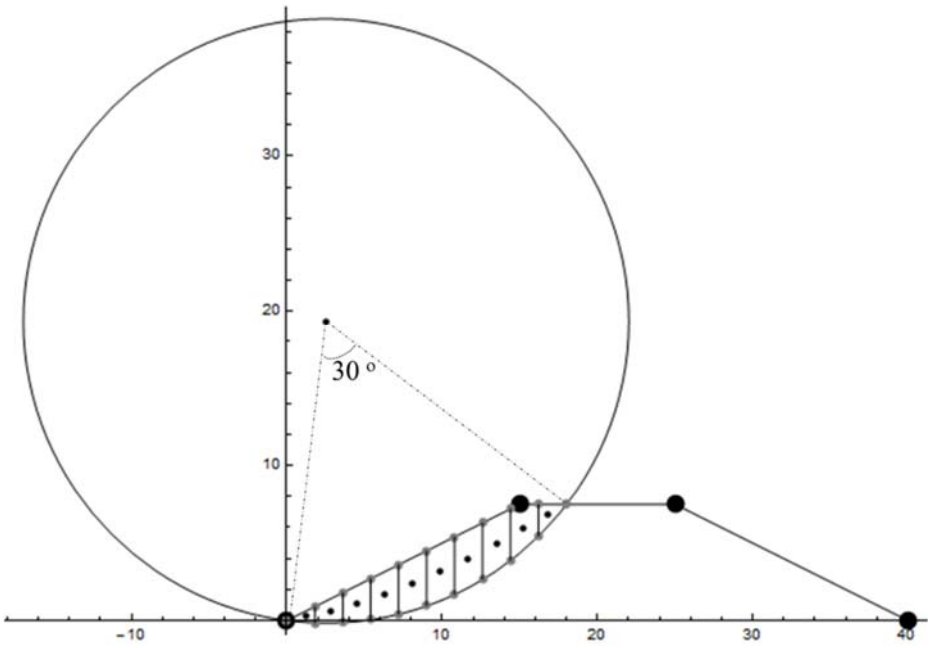

Figure 5-2 The assumed slip surface

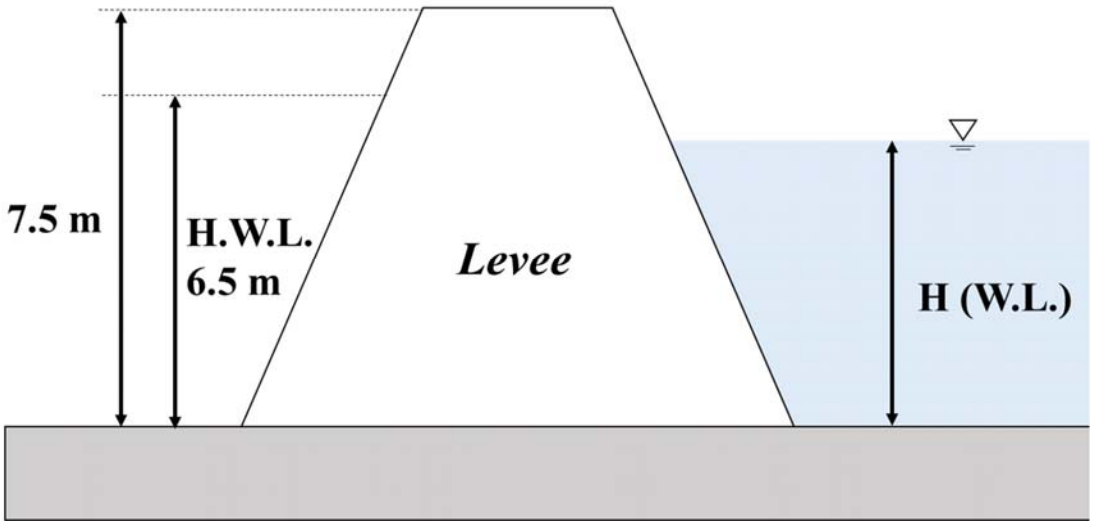

Figure 5-3 the conditions of levee

5.2 Results

5.2.1 the results of sandy soil

The scenario test conditions of sandy soil are assumed the friction angle of soil are 20^o, 27.5^o and 35^o; the cohesion of soil is 1 kN/m^2. Figure 5-4 ~ Figure 5-7 are the S-1 condition results with the different grades. Figure 5-8 ~ Figure 5-11 are the S-2 condition results with the different grades. Figure 5-12 ~ Figure 5-14 are the S-3 condition result with the different grades. The grade of 1:6 of the S-3 conditions didn't calculate because of the infiltration failure is approximate zero in the grades of 1:5.

5.2.2 the results of clay soil

The scenario test conditions of clay soil are assumed the cohesions of soil are 10 kN/m^2, 35 kN/m^2 and 60 kN/m^2; the friction angle of soil is 1^o. Figure 5-15 ~ Figure 5-18 are the C-1 condition results with the different grades. Figure 5-19 ~ Figure 5-22 are the C-2 condition results with the different grades. Figure 5-23 ~ Figure 5-26 are the C-3 condition result with the different grades.

5.2.3 the comparison of sandy soil and clay soil

The Figure 5-27 ~Figure 5-30 are the comparisons of both soil materials in the different levee grade, 1:3 1:4 and 1:5. It shows the very different characteristics of the both soil materials of their failure probability.

The failure probability of the sandy soil is change very significantly when the water level rising. However, the failure probability of the clay soil is not significant in the same rising water level.

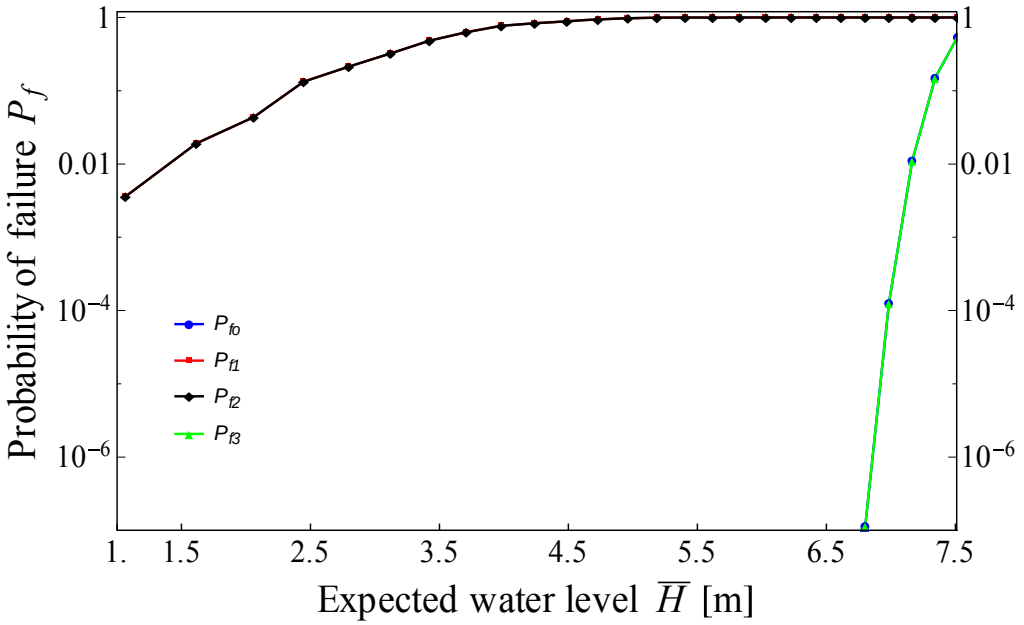

Figure 5-4 the analysis result of S-1 (c'=1 kN/m^2; ϕ'=20°; the grade of levee= 1:3)

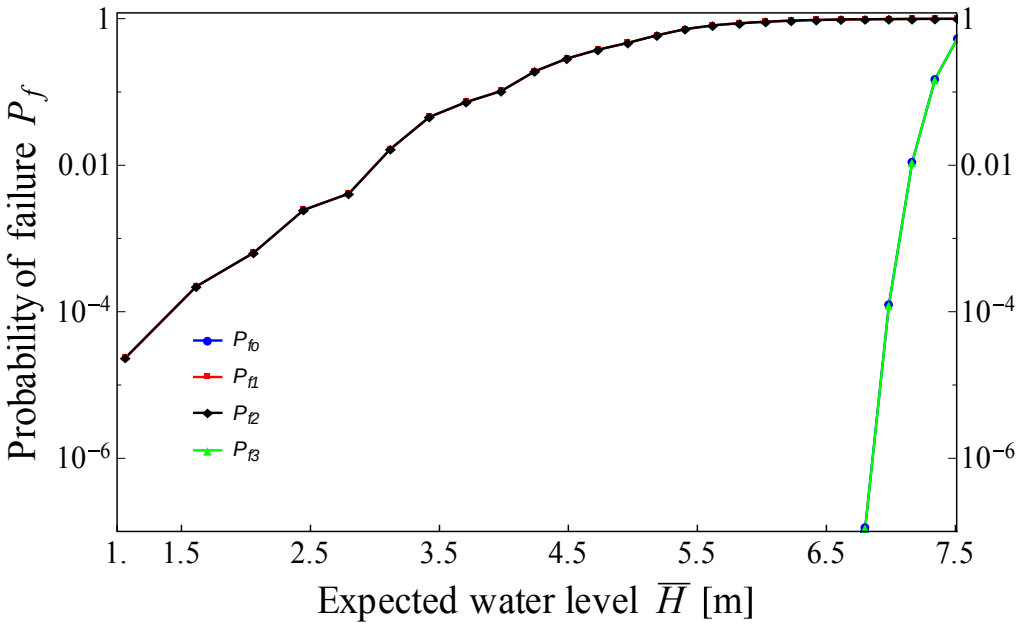

Figure 5-5 the analysis result of S-1 (c'=1 kN/m^2; ϕ'=20°; the grade of levee= 1:4)

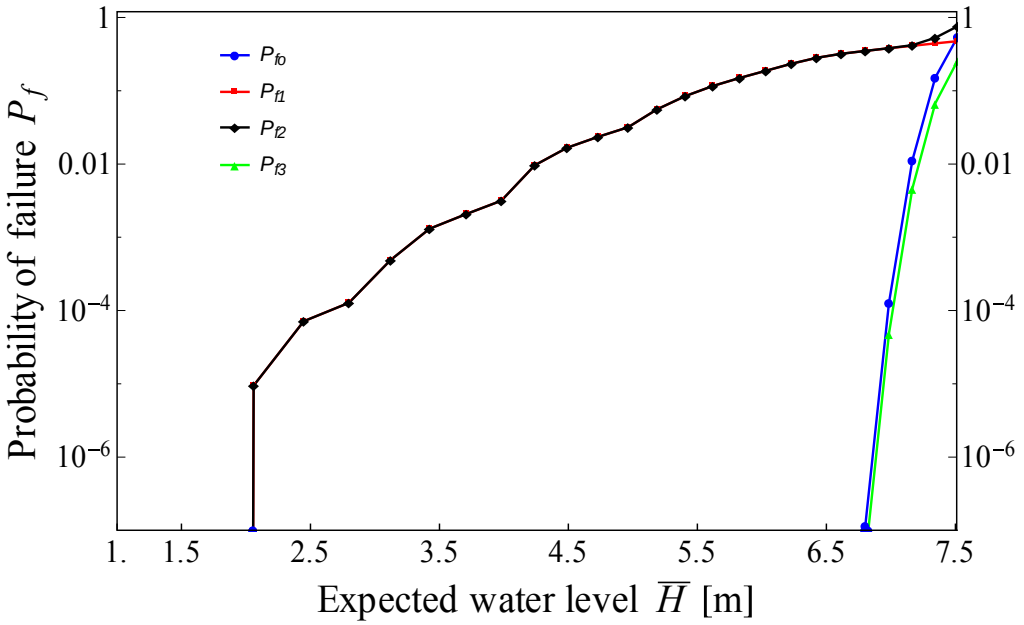

Figure 5-6 the analysis result of S-1 (c'=1 kN/m^2; ϕ'=20°; the grade of levee= 1:5)

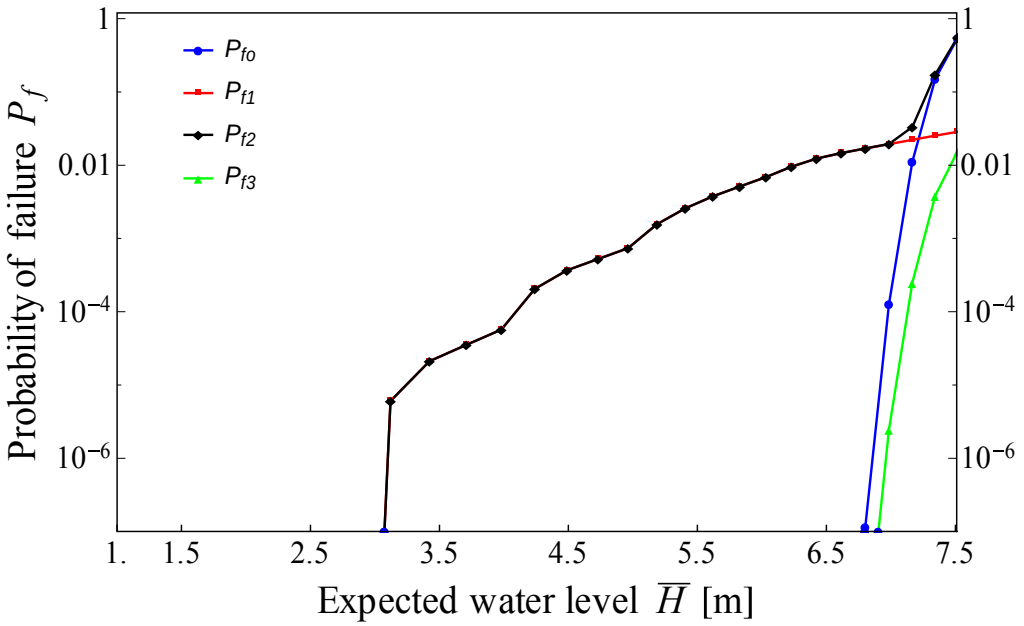

Figure 5-7 the analysis result of S-1 (c'=1 kN/m^2; ϕ'=20°; the grade of levee= 1:6)

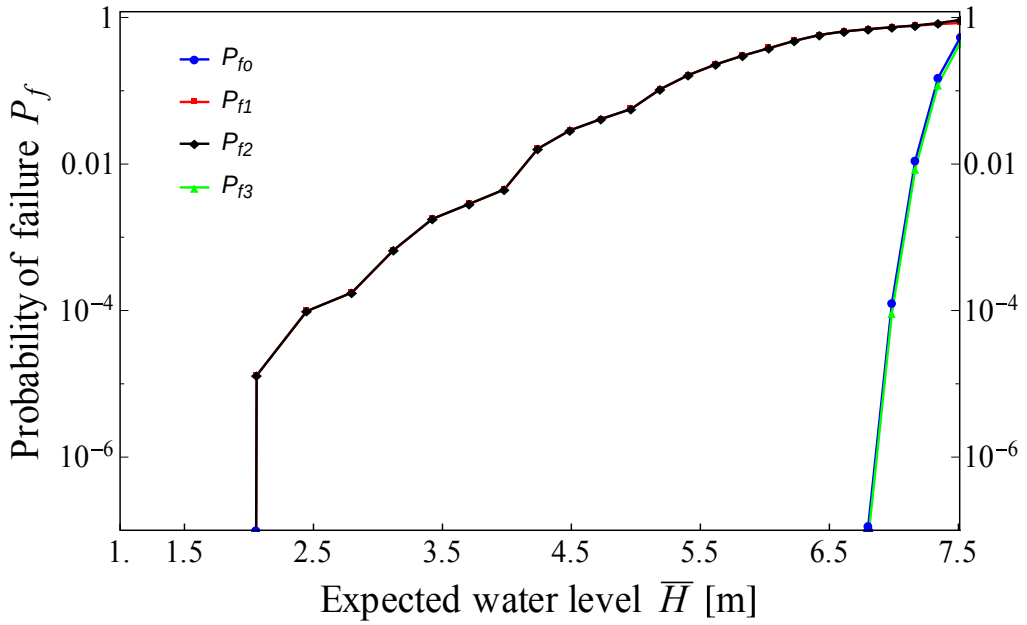

Figure 5-8 the analysis result of S-2 (c'=1 kN/m^2; ϕ'=27.5°; the grade of levee= 1:3)

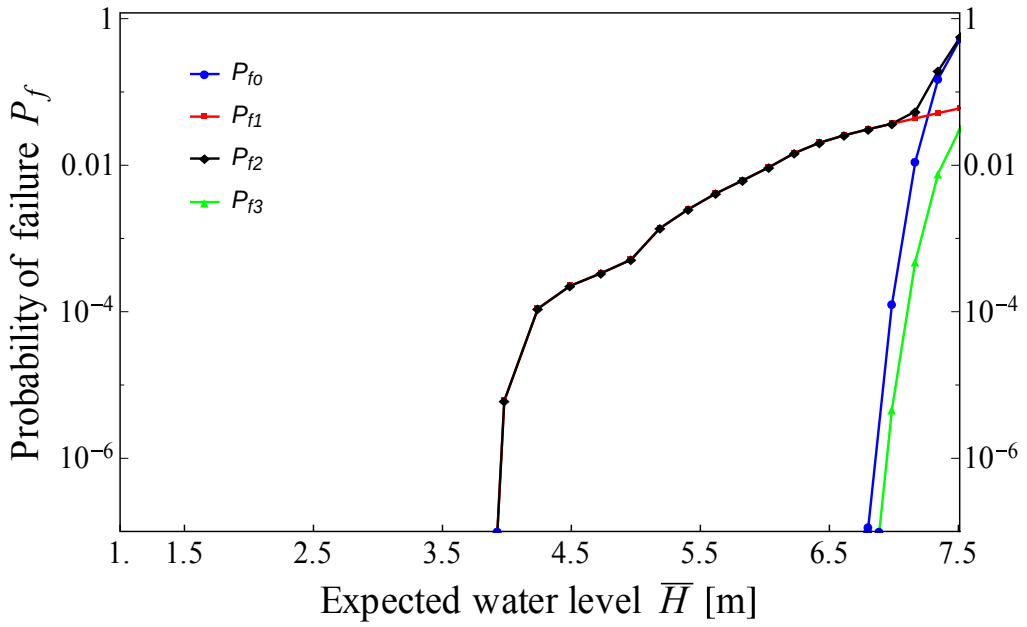

Figure 5-9 the analysis result of S-2 (c'=1 kN/m^2; ϕ'=27.5°; the grade of levee= 1:4)

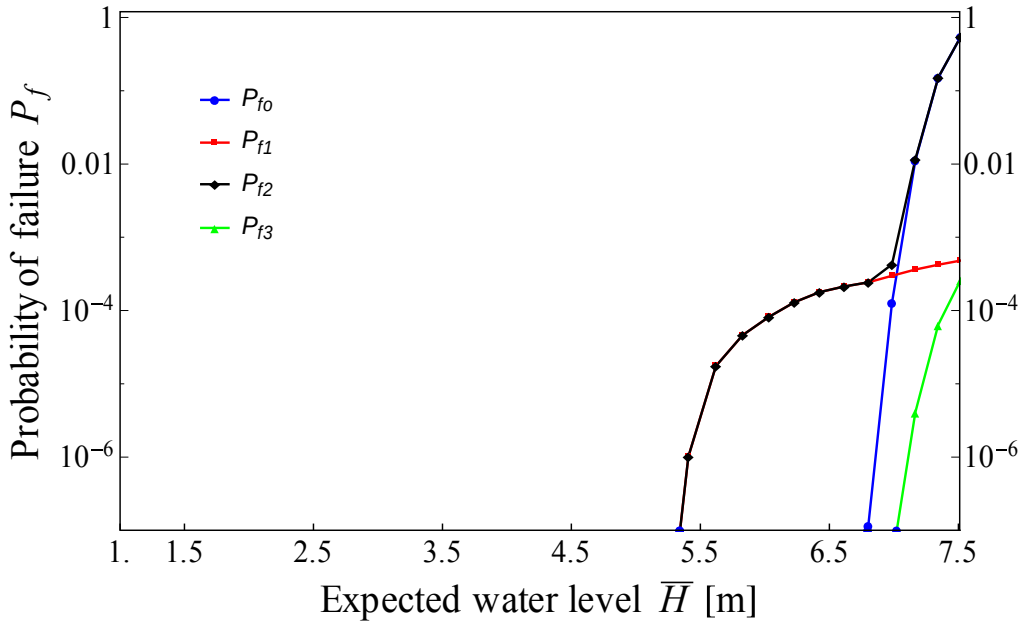

Figure 5-10 the analysis result of S-2 (c'=1 kN/m^2; ϕ'=27.5°; the grade of levee= 1:5)

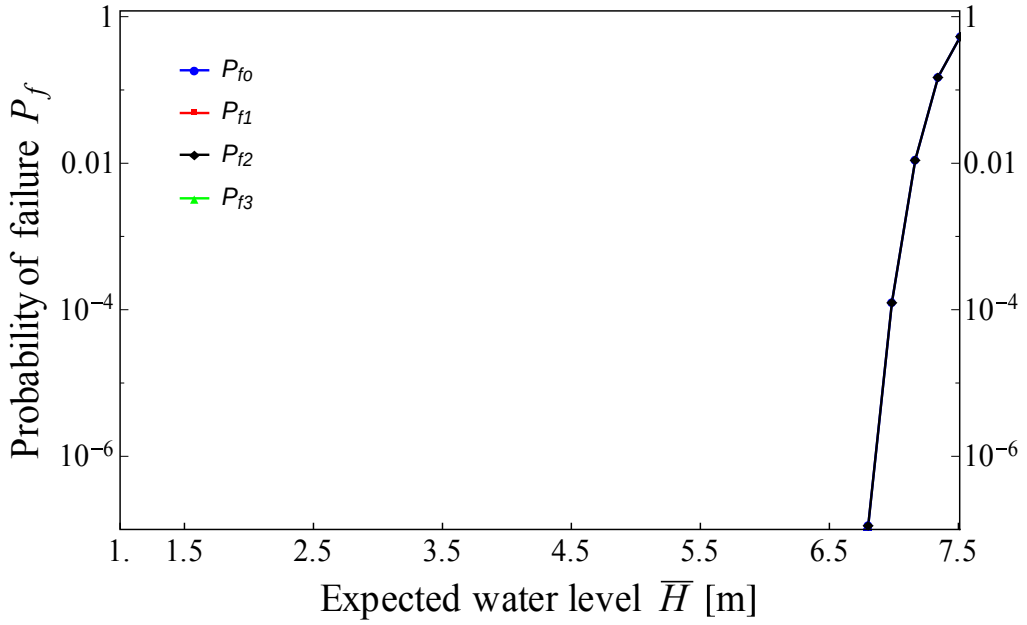

Figure 5-11 the analysis result of S-2 (c'=1 kN/m^2; ϕ'=27.5°; the grade of levee= 1:6)

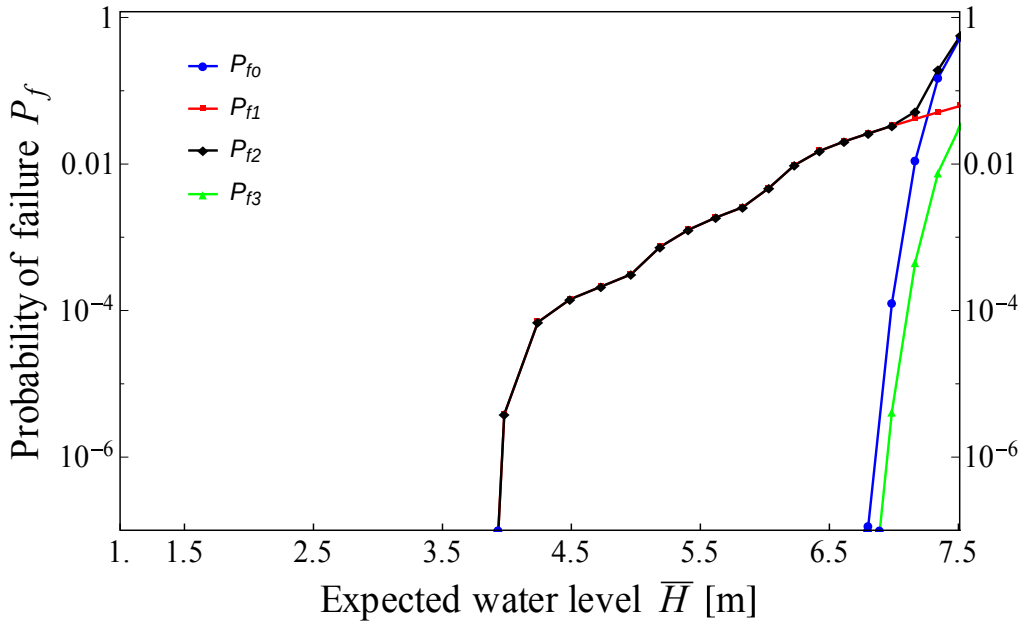

Figure 5-12 the analysis result of S-3 (c'=1 kN/m^2; ϕ'=35°; the grade of levee= 1:3)

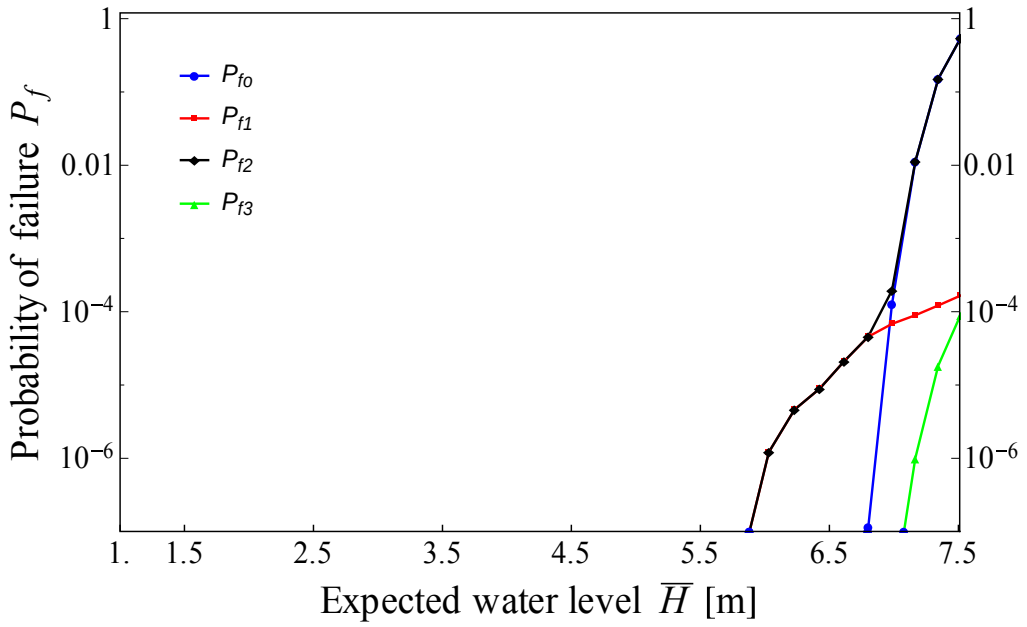

Figure 5-13 the analysis result of S-3 (c'=1 kN/m^2; ϕ'=35°; the grade of levee= 1:4)

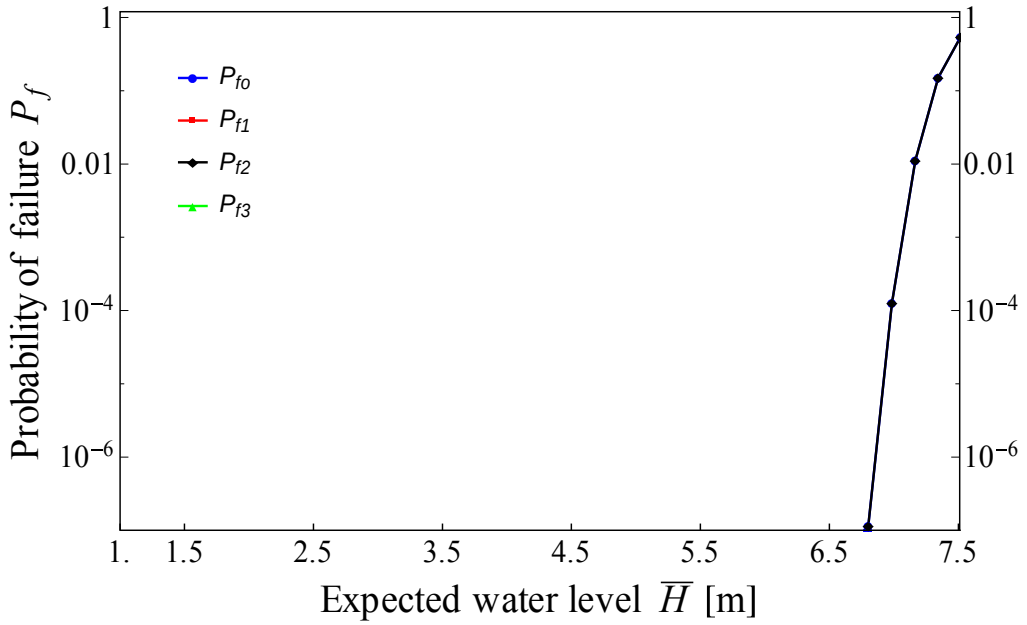

Figure 5-14 the analysis result of S-3 (c'=1 *kN/m2*; ϕ'=35°; the grade of levee= 1:5)

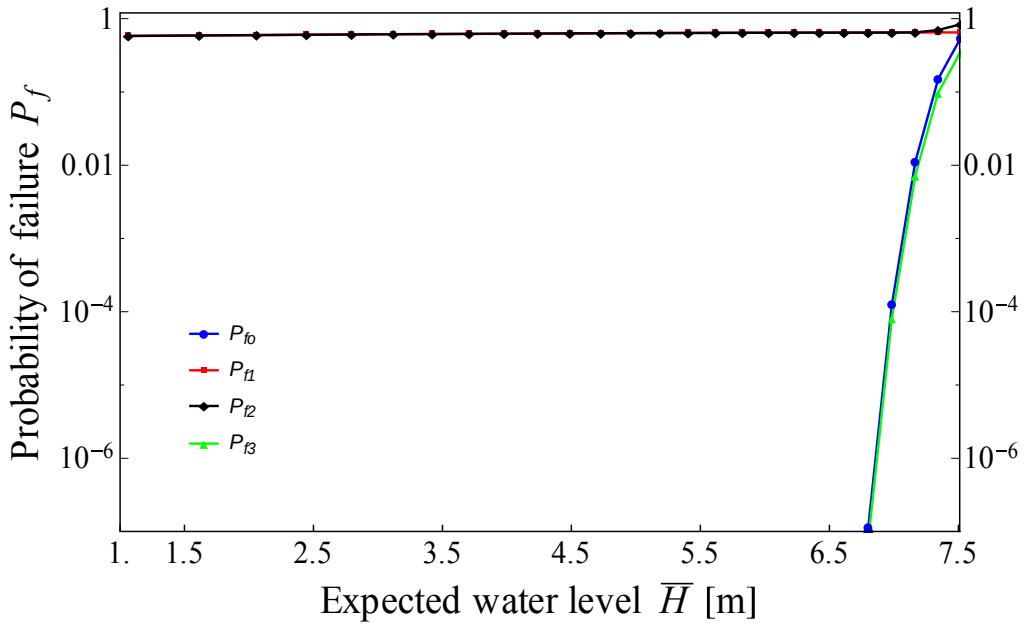

Figure 5-15 the analysis result of C-1 (c'=10 kN/m^2; ϕ'=1°; the grade of levee= 1:3)

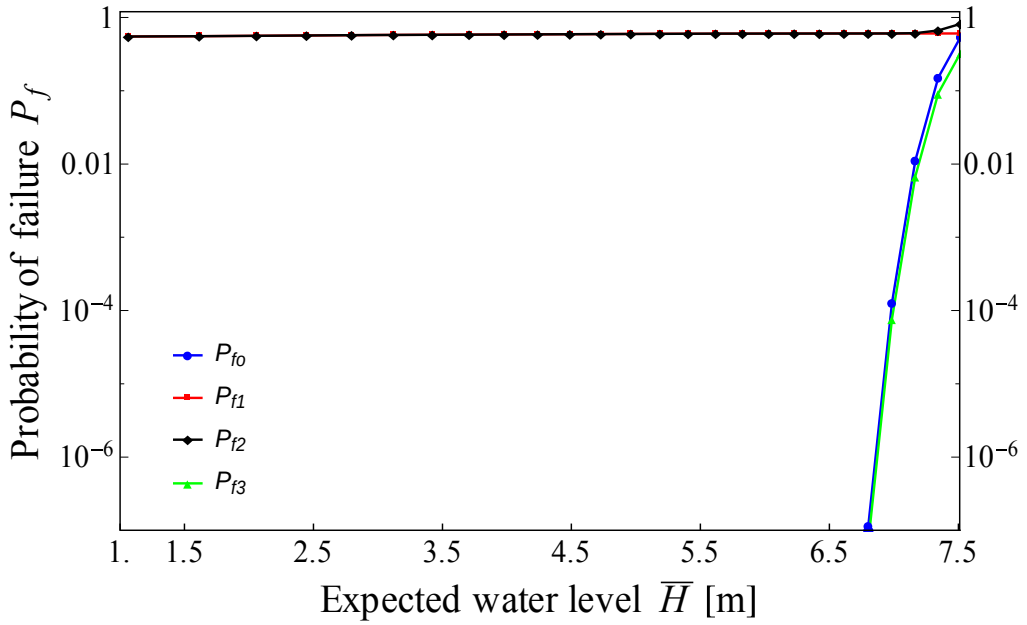

Figure 5-16 the analysis result of C-1 (c'=10 kN/m^2; ϕ'=1°; the grade of levee= 1:4)

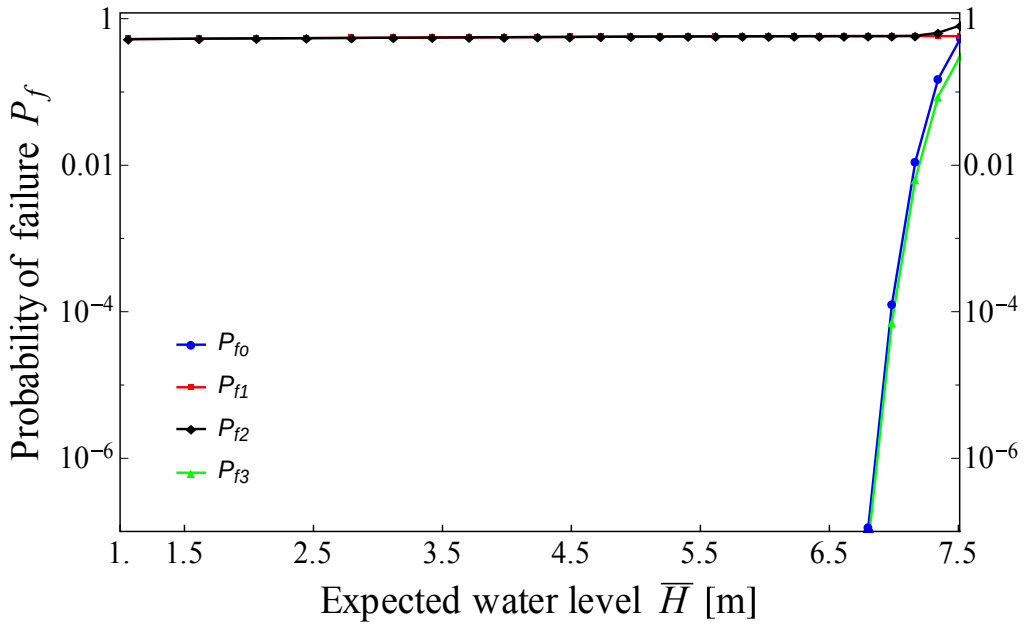

Figure 5-17 the analysis result of C-1 (c'=10 kN/m^2; ϕ'=1°; the grade of levee= 1:5)

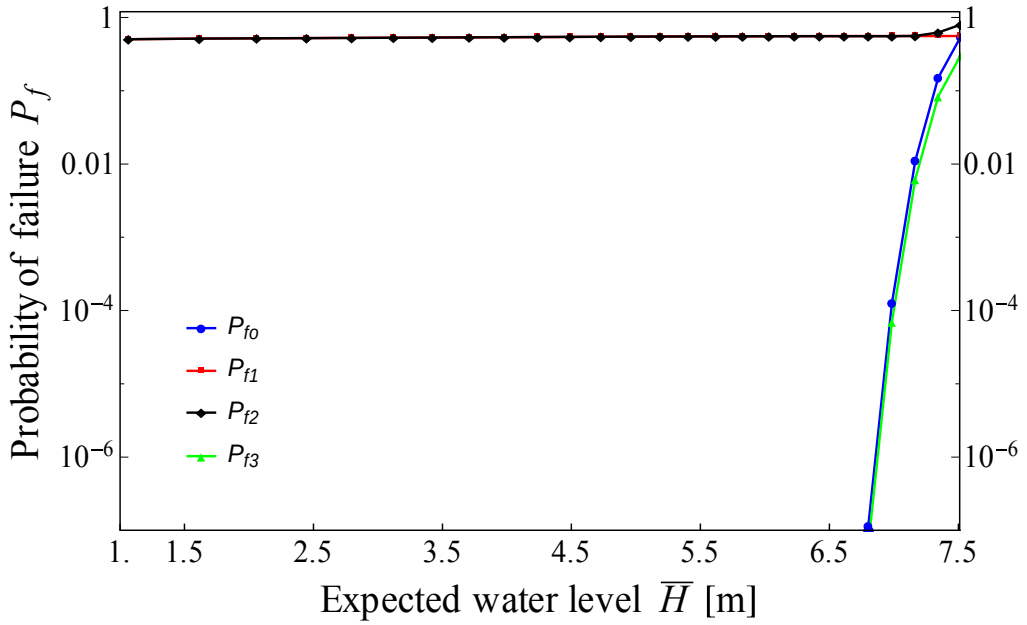

Figure 5-18 the analysis result of C-1 (c'=10 kN/m^2; ϕ'=1°; the grade of levee= 1:6)

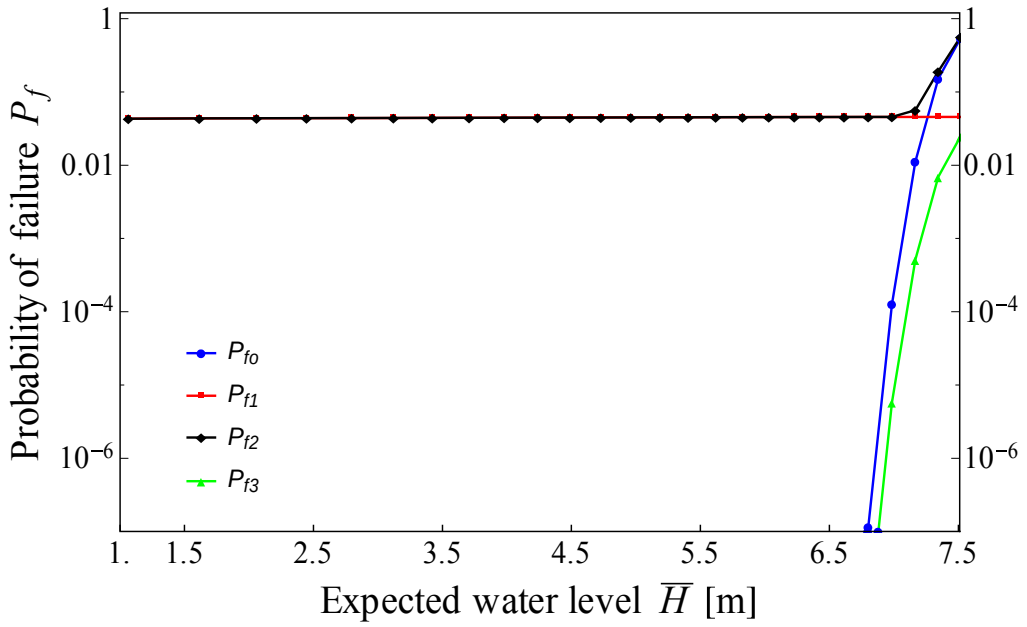

Figure 5-19 the analysis result of C-2 (c'=35 kN/m^2; ϕ'=1°; the grade of levee= 1:3)

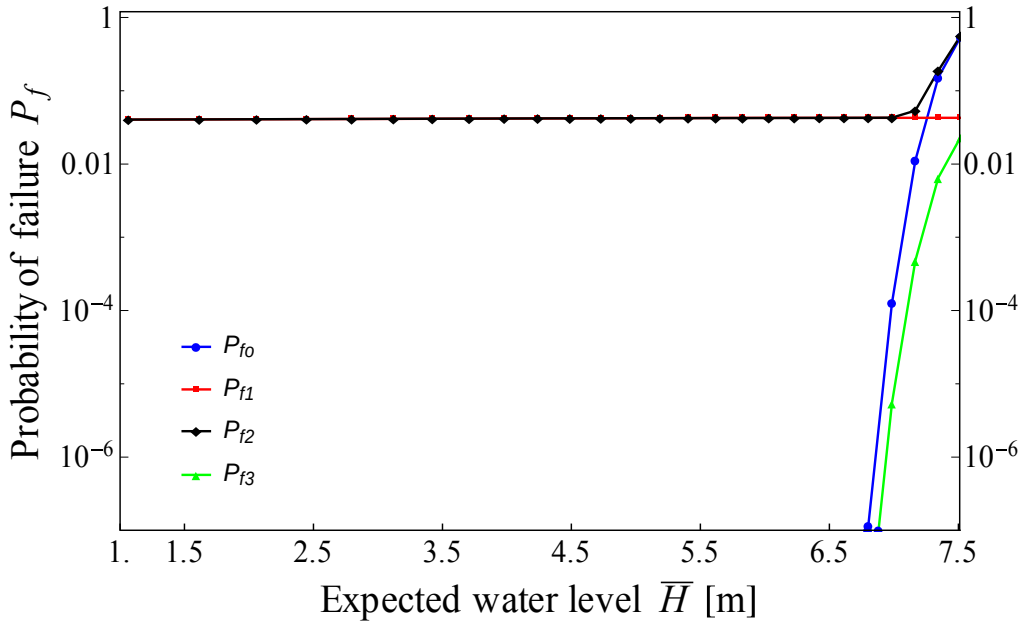

Figure 5-20 the analysis result of C-2 (c'=35 kN/m^2; ϕ'=1°; the grade of levee= 1:4)

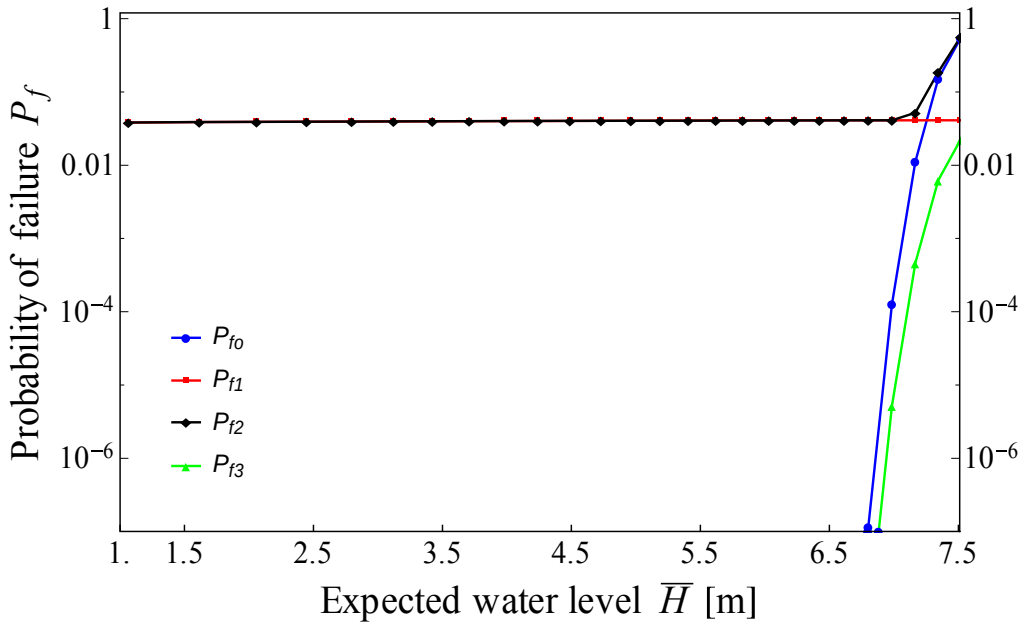

Figure 5-21 the analysis result of C-2 (c'=35 kN/m^2; ϕ'=1°; the grade of levee= 1:5)

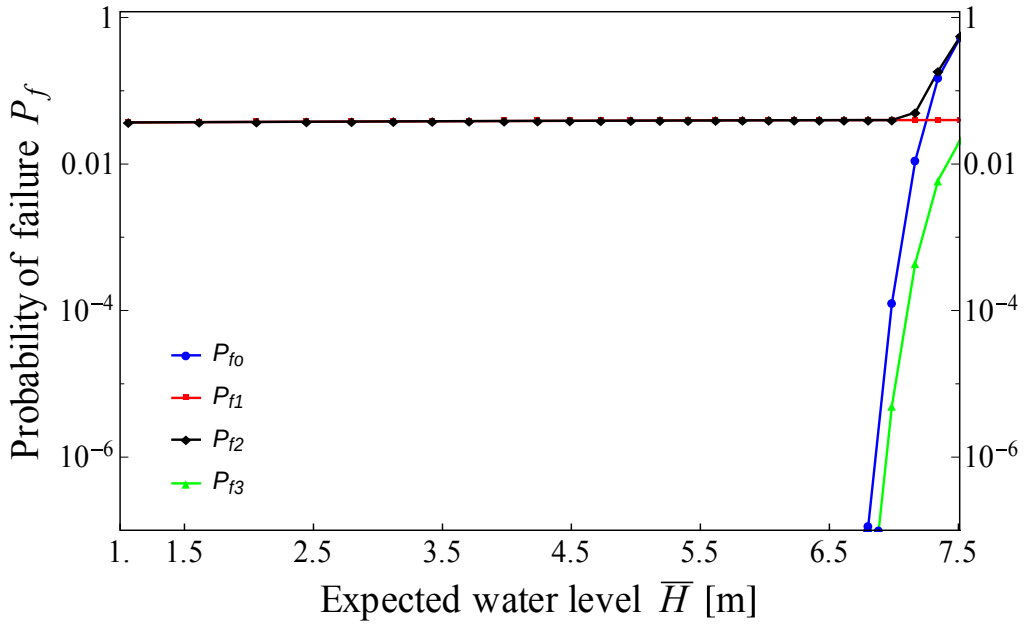

Figure 5-22 the analysis result of C-2 (c'=35 kN/m^2; ϕ'=1°; the grade of levee= 1:6)

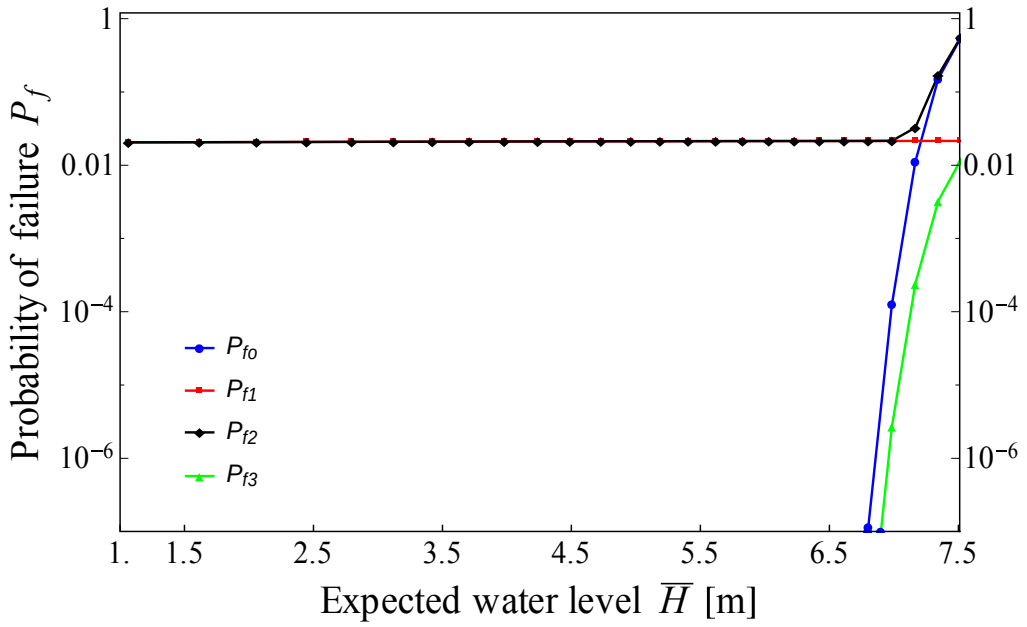

Figure 5-23 the analysis result of C-3 (c'=60 kN/m^2; ϕ'=1°; the grade of levee= 1:3)

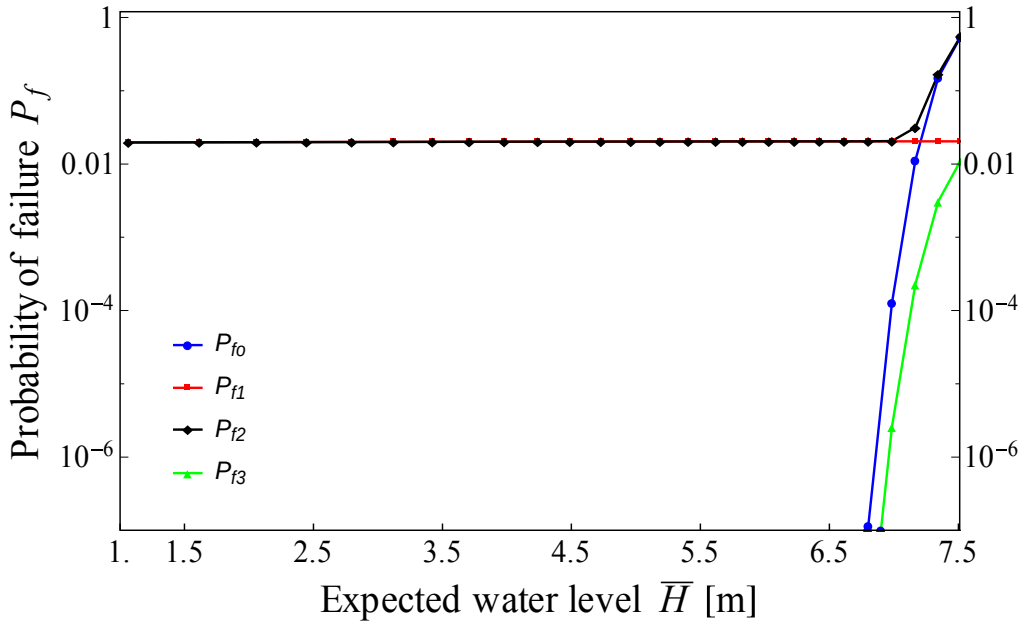

Figure 5-24 the analysis result of C-3 (c'=60 kN/m^2; ϕ'=1°; the grade of levee= 1:4)

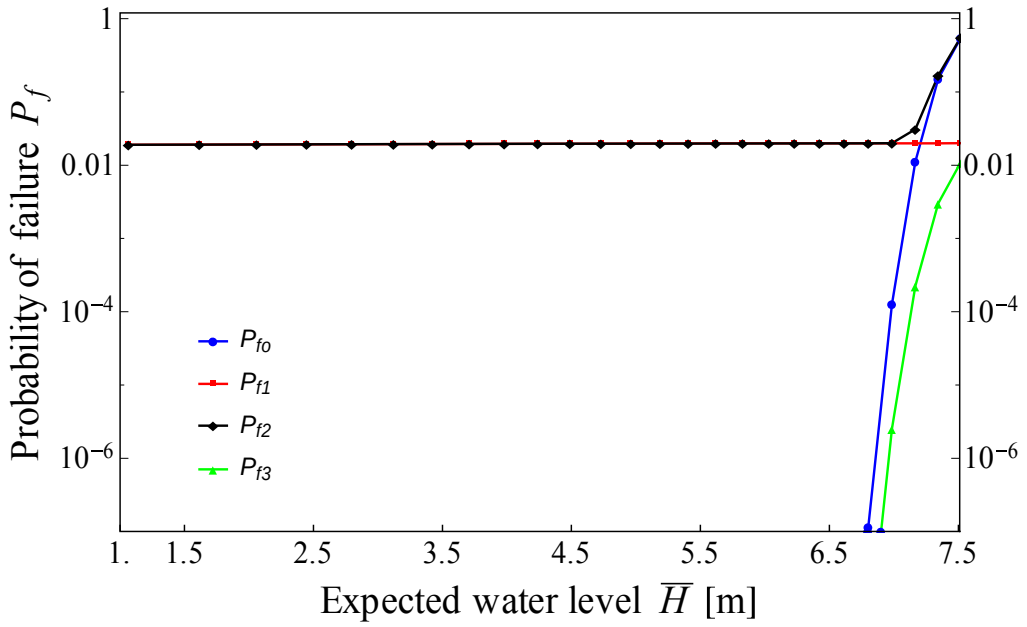

Figure 5-25 the analysis result of C-3 (c'=60 kN/m^2; ϕ'=1°; the grade of levee= 1:5)

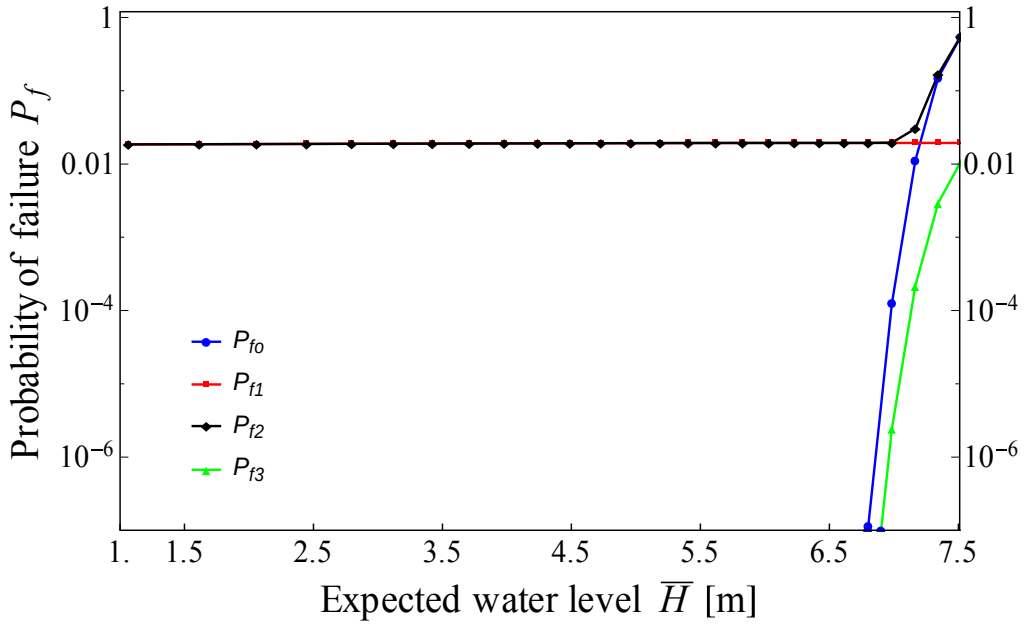

Figure 5-26 the analysis result of C-3 (c'=60 kN/m^2; ϕ'=1°; the grade of levee= 1:6)

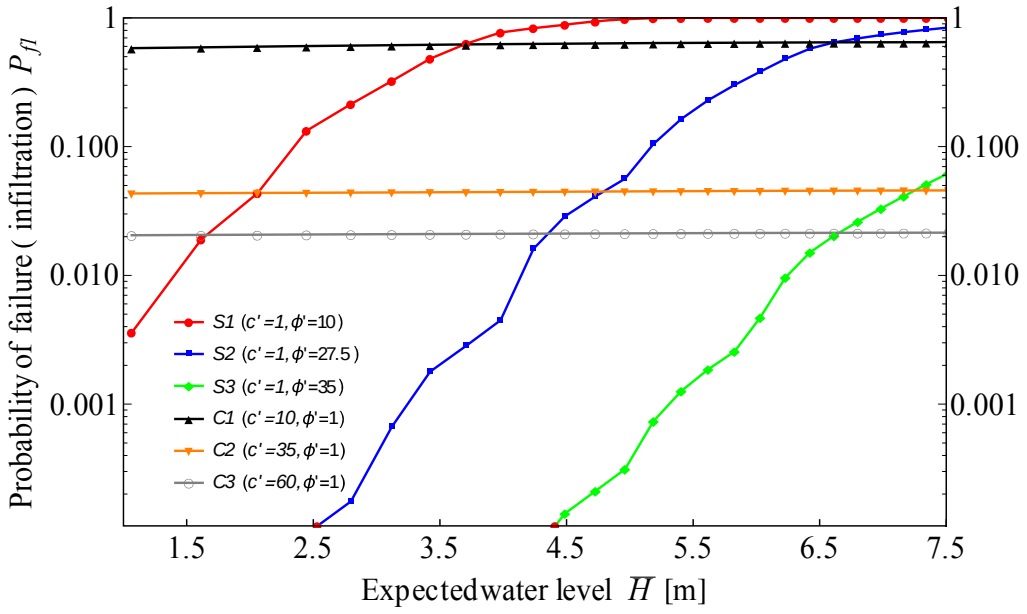

Figure 5-27 the effective of different soil materials (1:3)

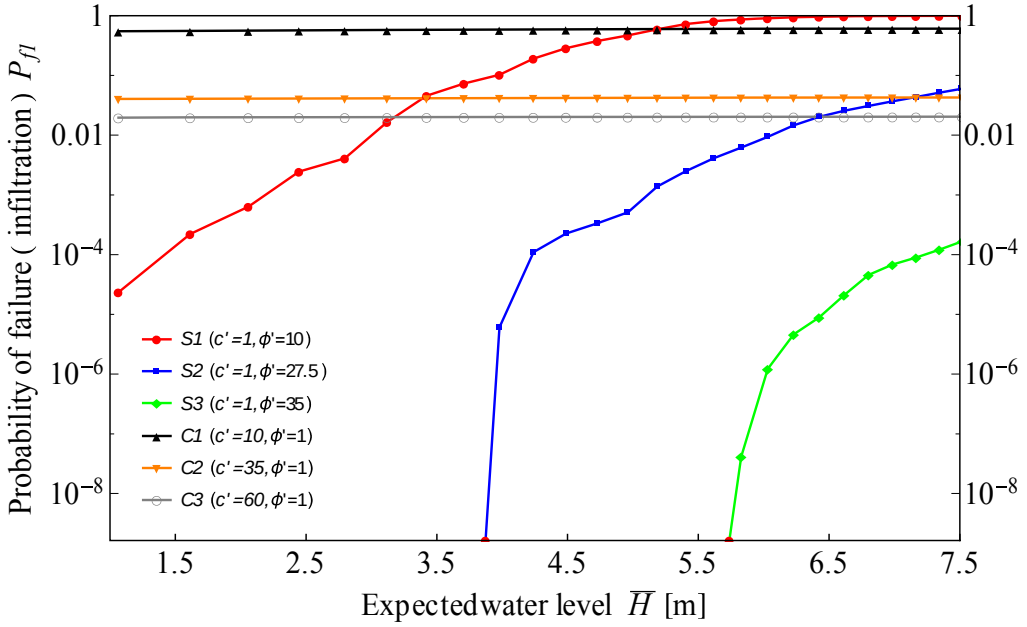

Figure 5-28 the effective of different soil materials (1:4)

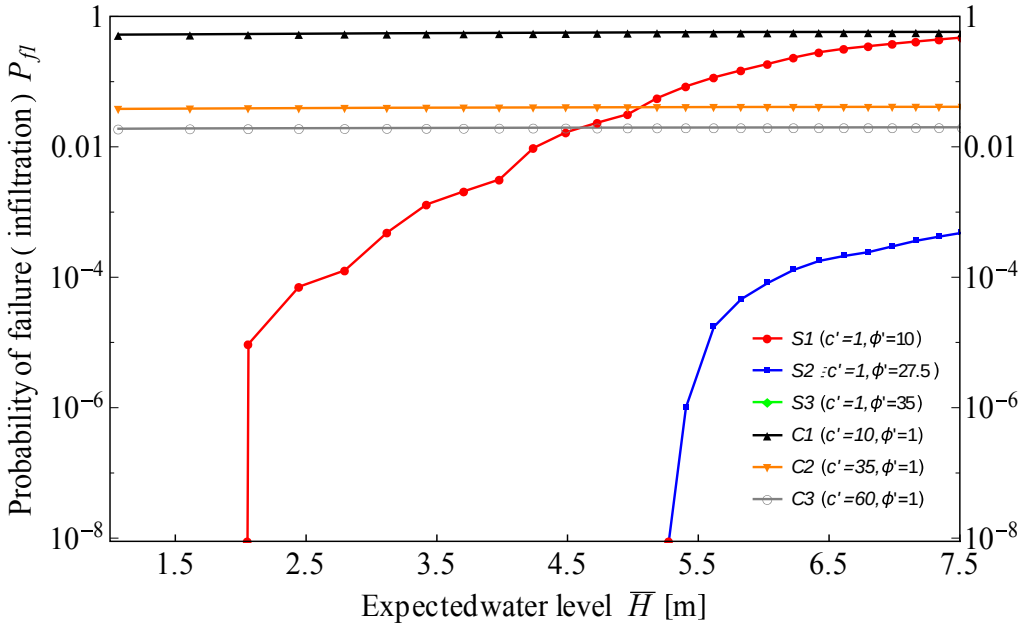

Figure 5-29 the effective of different soil materials (1:5)

5.3 Discussion

The above analysis results show the failure probability of each soil conditions in different levee geometry including of the only overflow failure P_{fo}, the only infiltration failure P_{f1}, when one of the two failures occurrence P_{f2} and both overflow and infiltration failure occurrence P_{f3}. Furthermore, the following will discuss the effective of the design of levee like the freeboard or the levee grade.

5.3.1 the effective of the freeboard

First is the effective discussion of the freeboard. Figure 5-30 shows the effective of the levee freeboard. The calculation condition is S-2 and the grade of levee is 1:4. The water level of the assumption is 6.5 *m* (H.W.L.) and the freeboard is calculated from 0 *m* (the levee height is 6.5 *m*) to 1.0 *m* (the levee height is 7.5 *m*). It shows the effective of the freeboard for the decreasing of the overflow probability and the infiltration probability. By Figure 5-27, when the freeboard is from 0 m to 1.0 m, the infiltration failure probability is not very different. However, it shows a very significant decreasing trend of the overflow probability. Unlike the previous empirical method like Table 1-1, the analysis results can show the real probability trend of overflow in the design of the freeboard.

On the other hand, it also can be applied to as the risk tolerance of the freeboard. It means that risk tolerance of the levee freeboard is a more specific measure of the degree of uncertainty that a decision maker is willing to accept in respect of negative changes to its design. For example, compliance with the design laws or regulations, through the analysis result the levee can consider the necessary strengthen according to the risk of the levee failure and its tolerance of the environment.

5.3.2 the effective the levee grade

Final is the effective of the levee grade. Figure 5-31 shows the effective of the levee grades of S-1 condition and Figure 5-32 shows the effective of C-1 condition. Figure 5-31 is the sandy soil; it shows a very significant decreasing trend when the water level rising from the grade 1:3 to 1:6. Figure 5-32 is the clay soil; it also shows a significant decreasing trend from the grade 1:3 to 1:6. With respect to the clay soil, the smaller grade of sandy soil levee is relatively larger effect for reducing of the infiltration probability. It means even if the soil material is not very good to construct the levee, but through improving the geometry of the levee, the failure probability can also effective to reduce.

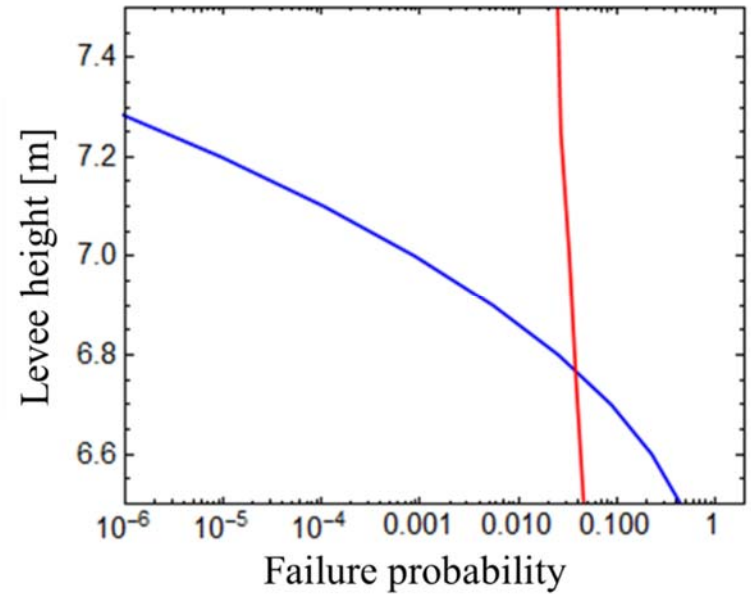

Figure 5-30 the effective of the levee freeboard(S-1)

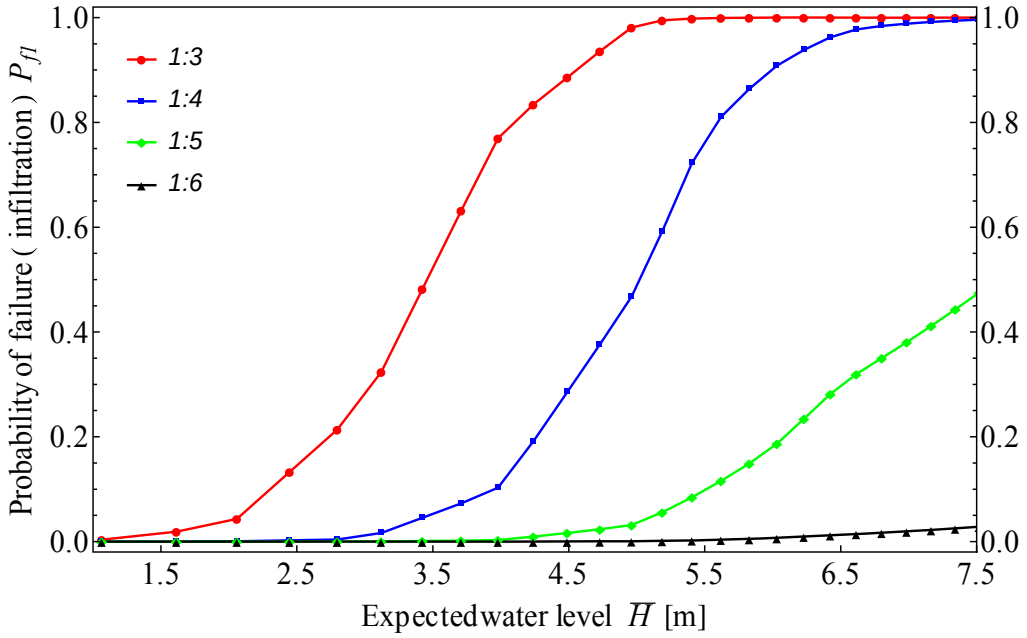

Figure 5-31 the effective of the levee grade (S-1)

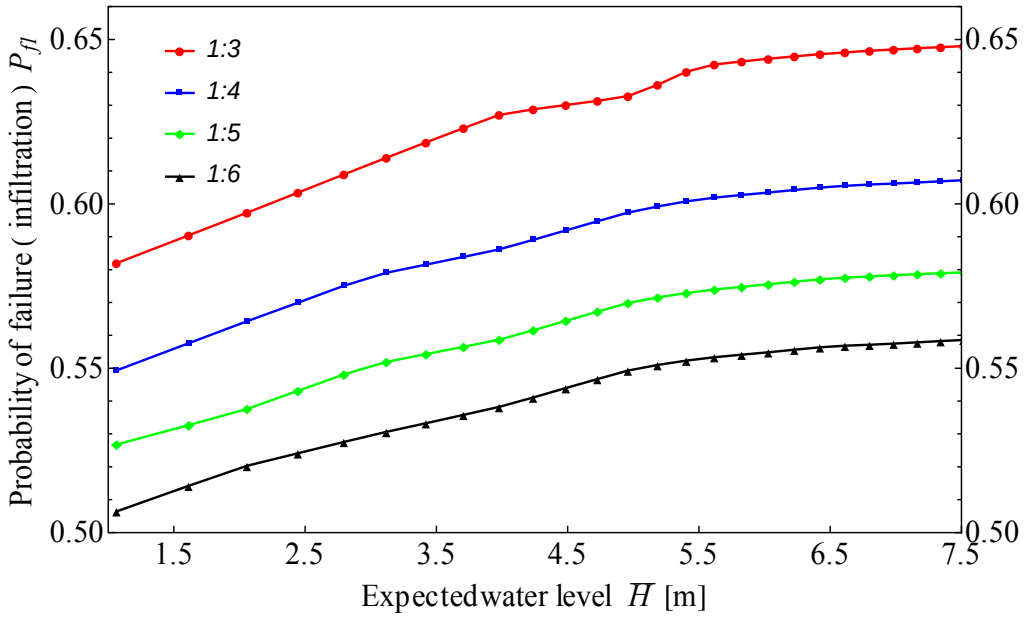

Figure 5-32 the effective of the levee grade (C-1)

Reference

[1] Yoshito Kikumori, 2008. “Study on Accuracy Improvement of Safety Evaluation for Seepage Failure Levees”. Technical Note of NILIM No. 4410 January 2008.

CHAPTER 6 CONCLUSION

Until now, the flood control management and safety of levees are usually evaluated by determinist. That's because many design aspects, the choice of nominal values/parameters are easier to decide. The reasons are:

a) The main source of uncertainty is not explicitly considered.

b) Compared to other scientific area, each case has its own unique characteristic with unrepeatable, therefore the database is difficult to establish. However, few data mean the analysis of uncertainty incomplete.

c) Compared to other scientific area, the civil engineering is more conservatism because that the civil engineering is very nearly the life of people.

In response to these reasons, in the thesis, the main concept is considered the uncertainty of external force- water level and resistance force- stability of levee to evaluate the reliability of the levee. The followings are the conclusions in the thesis.

a) In chapter 2, the hydrology model based on the stochastic process theory has been proposed. Including of the uncertainty of the hydrology phenomenon, the uncertainty of the rainfall to the probability of the water level of the river can be evaluated by the model. The model is based on the relation between the runoff heights of stochastic differential equation and the mathematic equation

of Fokker-Planck to obtain the uncertainty of rainfall and runoff.

b) In chapter 3, the infiltration failure of levees is calculated by the slope stability method. Furthermore, the uncertainty is also considered in the evaluating the probability failure of the levee. The main parameters of the equation are soil cohesion, the soil friction angle, the weight of the soil block, the pore water pressure and the geometric conditions of the circular slip. Among these parameters, the geometric conditions are according to the slip surface to decide, the pore water pressure and the weight are changing with the water level change, and the soil cohesion and the friction angle are usually decided by the lab test or in situ test. Traditionally, the cohesion and the friction angle are the unique value. Herein in order to consider the uncertainty of soil parameters, the variation/ deviation of the parameters will be conducted to evaluate the failure probability of the levee slope.

c) In chapter 4, the reliability analysis of levee failure is proposed. The failure of levee can be classified two types, one is overflow and the other is infiltration failure calculated by the circular slide method. The overflow failure probability is calculated from the distribution of water level. The infiltration failure is combined the probability of slip with considering the uncertainty of soil parameters in the certain water level. Therefore, the detail probability calculated is the following types: the only overflow failure, P_{fo}; the only infiltration failure, P_{f1}; when one of the two failures occurs, P_{f2}; when both overflow and infiltration failure occur, P_{f3}.

d) In chapter 5, the scenario tests have been applied by the method of chapter 2 to chapter 4. It shows the very different result in different conditions of soil parameters. Furthermore, the geometry effects are also reviewed, including of the freeboard and the grade of the levee.

Acknowledgements

Firstly, I would like to express my sincere gratitude to my advisor Prof. Yamada for the continuous support of my Ph.D. study and related research, for his patience, motivation, and immense knowledge. His guidance helped me in all the time of research and writing of this thesis. Furthermore, Prof. Yamada also guided me to learning and enjoying the culture of Japanese. I could not have imagined having a better advisor and mentor for my Ph.D. study. Besides my advisor, I would like to thank the rest of my thesis committee: Prof. Kunio SAITO, Prof. Naotsugu SATO, Prof. Azuma TAGUCHI and Dr. Toru SUEOKA, for their insightful comments and encouragement, but also for the hard question which incented me to widen my research from various perspectives. My sincere thanks also go to Prof. Kenji ISHIHARA and Dr.W.F. LEE, who provided me an opportunity to enter CHUO University, and who gave many suggestions for my research. Without they precious support it would not be possible to conduct this research.

I thank my fellow labmates in for the study discussions, and for all the fun we have had in the three years. In particular, I am grateful to Dr. Chouchou SEN for help me the exercise presentations of my thesis before the public hearing, and to my classmate, Kazuhiro YOSHIMI for help me the learning programming and for the discussions of my research.

Last but not the least, I would like to thank my family: my parents and my sister for supporting me spiritually throughout writing this thesis and my life in general.

最後，我要感謝我的家人：我的爸爸、媽媽及妹妹，謝謝你們在這三年來一直無條件的支持我，不論是在心靈上還是生活上。